ABSTRACT

Title of Document:	Self-Assembly in Polar Organic Solvents
	Niti Agrawal, Doctor of Philosophy, 2019
Directed By:	Professor Srinivasa R. Raghavan, Department of Chemical and Biomolecular Engineering

Self-assembly of amphiphilic molecules occurs extensively in water, and can result in a variety of large, nanoscale aggregates, including long cylindrical chains called wormlike micelles (WLMs), as well as nanoscale containers called vesicles. However, in organic solvents of polarity lower than water, such as formamide, glycerol, and ethylene glycol, self-assembly has been demonstrated only to a limited extent. While there are reports of small micelles in these solvents, there are no reports of large structures such as WLMs and vesicles (with at least one length scale > 100 nm). In this dissertation, we show that both WLMs and vesicles can be formed in these solvents, and thereby our work expands the possibilities for self-assembly to new systems. Applications for the fluids developed here could arise in cosmetics, pharmaceutics, antifreeze agents, and lubricants.

In the first part of this study, we demonstrate the formation of WLMs in polar solvents like glycerol and formamide. WLMs in water are induced by combining a cationic surfactant and a salt, but the combinations that work for water mostly do not work in polar solvents. The combination that does work in the latter involves a cationic surfactant with a very long (erucyl, C_{22}) tail and an aromatic salt such as sodium salicylate. These WLMs display viscoelastic and shear-thinning rheology, as expected.

By using a low-freezing mixture of glycerol and ethylene glycol, we are able to devise formulations in which WLMs remain intact down to sub-zero temperatures (–20°C). Thereby, we have been able to extend the range for WLM existence to much lower temperatures than in previous studies.

Next, in the second part, we focus on the dynamic rheology of WLMs in glycerol, which is shown to be very different from that of WLMs in water. Specifically, WLMs in glycerol exhibit a double-crossover of their elastic (G') and viscous (G'') moduli within the range of frequencies accessible by a rheometer. We believe that the high viscosity of glycerol influences the rheology at high frequencies. We also hypothesize that the WLMs in glycerol are shorter and weakly entangled compared to WLMs in water. Moreover, in terms of their dynamics, we suggest that WLMs in glycerol are similar to polymers – i.e., the chains will remain intact and not break and re-form frequently.

In the last study, we demonstrate the formation of vesicles in polar solvents (glycerol, formamide and ethylene glycol) using the simple phospholipid, lecithin. Lecithin dissolves readily in polar solvents and gives rise to viscous fluids at low concentrations (~ 2 to 4%). At higher concentrations (> 10 wt%), lecithin forms clear gels that are strongly birefringent at rest. Dynamic rheology of the latter reveals an elastic, gel-like response. Images from cryo-scanning electron microscopy (cryo-SEM) indicate that the concentrated samples are ‘vesicle gels’, where multilamellar vesicles (MLVs, also called onions), with sizes between 50 to 600 nm, are close-packed across the sample volume. This structure explains both the rheology and the birefringence.

SELF-ASSEMBLY IN POLAR ORGANIC SOLVENTS

By

Niti Agrawal

Dissertation submitted to the Faculty of the Graduate School of the
University of Maryland, College Park, in partial fulfillment
of the requirements for the degree of
Doctor of Philosophy
2019

Advisory Committee:

Prof. Srinivasa R. Raghavan, Dept. of Chemical and Biomolecular Engineering, Chair
Prof. Mikhail A. Anisimov, Dept. of Chemical and Biomolecular Engineering
Prof. Jeffery B. Klauda, Dept. of Chemical and Biomolecular Engineering
Prof. Silvina Matysiak, Fischell Dept. of Bioengineering
Prof. Robert M. Briber, Dept. of Materials Science and Engineering

Acknowledgements

First and foremost, I would like to extend my deepest appreciation to my advisor, Dr. Srinivasa Raghavan, for his mentorship, encouragement, wisdom and unparalleled support during the entire course of my Ph.D. His knowledge and research acumen have always inspired me to explore different research opportunities and constantly learn new things. I have learned a lot from him both in terms of research as well as meaningful life lessons. I am extremely thankful to him for his constant belief in my abilities and caring about my career. He provides tremendous opportunities to his students for developing independent research ability, presentation and writing skills as well as team collaborations, and I am very grateful for being a part of his group.

I would like to express my sincere thanks to my committee members Dr. Mikhail Anisimov, Dr. Jeffery Klauda, Dr. Silvina Matysiak and Dr. Robert Briber for serving on my PhD proposal and defense committee and providing insightful comments and recommendations which helped me improve my research. I really appreciate the useful insights from Dr. Klauda related to the molecular simulations of self-assembly in polar solvent. I am also grateful to Dr. Anisimov for helping me with dynamic light scattering experiments and for the guidance related to self-assembly of micelles.

I would like to appreciate Dr. Vijay John and Marzhana Omarova from Tulane University for their valuable discussions and assistance with microscopy experiments. I would like to acknowledge Dr. Yun Liu, Dr. Yimin Mao, Dr. Susan Kreuger and Dr. Paul Butler from NIST for teaching me about neutron scattering and guiding me during the

experiments at NCNR, Gaithersburg. I would also like to thank Dr. Wonsoek Hwang at UMD for his assistance with X-ray scattering experiments.

The completion of my dissertation would not have been possible without the support and nurturing of my friends Vivek Nagal, Adyasha Maharana, Sayali Sonawane, Saswathi Natta, Sunandita Patra, Sayanee Adhikari, Shourya Shonkar Roy Burman, Varun Chokshi, Siddharth Mahendran and Sravya Kurapati for always being there for me. I would like to extend my deepest gratitude to my lab members So Hyun Ahn, Dr. Kerry DeMella, Dr. Ankit Gargava and Dr. Brady Zarket for their friendship and continued guidance during my PhD. I'm also extremely grateful to Hema Choudhary, Nikhil Subraveti, Leah Borden, Ben Thompson, Wenhao Xu, and my undergrads Futoon Al-Jirafi, Jane Njihia, Sina Ataei. The visiting researcher in our lab, Dr. Xiu Yue was tremendously helpful in defining the path of my research.

And last but not the least, I want to thank the most important people in my life, my parents Ramesh and Sarita Agrawal and my grandparents. Without their support, I would not be here pursuing my Ph.D. I cannot begin to express my gratitude to my siblings, Anisha, Udhay Prakash, Karan, Swalpa and Kartik Agrawal for their love, motivation and unwavering support throughout these years.

TABLE OF CONTENTS

List of Figures

thinning in steady-shear and a viscoelastic response in dynamic rheology, indicating the presence of WLMs. (c) Visual observations further support this finding. The first photo shows that the sample is viscoelastic and is able to hold its weight in the inverted vial. The second photo, taken under crossed polarizers, shows that the sample is flow-birefringent (streaks of light appear when the sample is shaken).

Figure 3.3. Effects of different salts on the formation of WLMs by EHAC in glycerol at 25°C. The plot shows the relative zero-shear viscosity ($\eta_0/\eta_{solvent}$) as functions of salt concentration for various salts, with the EHAC concentration fixed at 60 mM. WLM formation is reflected by a substantial increase in η_0 and is observed only with NaSal and NaTos.

Figure 3.4. Vial photos showing coacervation of EHAC/NaTos samples in glycerol. Samples of EHAC/NaTos in glycerol show a 2-phase region. Photos of selected samples are shown here. The samples contain 60 mM EHAC and varying NaTos (120, 150, 180, 240 and 300 mM). All samples show two co-existing liquid phases, i.e., coacervation. The phase boundary between the surfactant-rich phase (bluish) and the salt-rich phase (colorless) is indicated in each sample by a line for clarity.

Figure 3.5. Comparison of EHAC and CPyCl for their ability to form WLMs in glycerol at 25°C. The plot shows the relative zero-shear viscosity ($\eta_0/\eta_{solvent}$) as functions of NaSal concentration for the two surfactants, with the surfactant concentration held constant at 60 mM. WLM formation is reflected by a substantial increase in η_0 and is observed only with EHAC.

Figure 3.6. Conditions for WLM formation in polar solvents like glycerol, and a mechanistic picture for the same. WLMs form only when EHAC is combined with binding salts like NaSal or NaTos. For all other cases (EHAC + simple salts; other surfactants + any salts), no WLMs are produced. In the absence of salt, EHAC has a critical packing parameter (CPP) of ~ 1/3 because of strong electrostatic repulsions between its headgroups (and thereby a large area per headgroup a_{hg}). When a binding salt like NaSal is added, its counterions will bind to EHAC micelles. This will occur with the aromatic rings inserting into the hydrophobic core of the micelle. The anionic counterions, in turn, will neutralize the cationic headgroups and thus reduce a_{hg}, which increases the CPP to ~ 1/2. This will induce the spherical micelles to transform into WLMs.

Figure 3.7. Steady-shear rheology of EHAC-NaSal samples in various solvents. The data are for the relative viscosity $\eta/\eta_{solvent}$ as a function of shear-rate. All samples contain 60 mM EHAC. The NaSal concentration is 60 mM in the glycerol sample and 90 mM in the formamide sample. Data are shown for glycerol and ethylene glycol at 25°C and for formamide at 5°C.

Figure 3.8. Steady-shear rheology in formamide at different temperatures. The data are for the relative viscosity $\eta/\eta_{solvent}$ as a function of shear-rate for a sample of 60 mM

EHAC + 90 mM NaSal in formamide at temperatures of 25, 15 and 5°C. The sample remains Newtonian at 15 and 25°C while it is shear-thinning at 5°C.

Figure 3.9. Steady-shear rheology of WLMs in a low-freezing solvent (90-10 mixture of Gly-EG) from ambient to sub-zero temperatures. The data are for the viscosity η as a function of shear-rate. The sample contains 60 mM EHAC and 120 mM NaSal.

Figure 3.10. Arrhenius (semilog) plot of the zero-shear viscosity vs. 1/*T*, using the data from Figure 3.9. The sample contains 60 mM EHAC and 120 mM NaSal in a 90-10 Gly-EG mixture.

Figure 3.11. SANS plots for samples of EHAC/NaSal in deuterated solvents. Each plot shows the scattered intensity I vs. wave vector q. (a) Data for 60/30 and 60/60 mM EHAC/NaSal in glycerol at 25°C. (b) Data for 60/30 EHAC/NaSal in glycerol at 25°C and 65°C. (c) Data for 60/60 EHAC/NaSal in 90-10 Gly-EG at temperatures ranging from –20°C to 80 °C.

Figure 3.12. Model fits to SANS data shown in the paper. Plots of scattered intensity I vs. wave-vector q are shown for sample A (EHAC-NaSal 60-30 mM) and sample B (EHAC-NaSal 60-60 mM) at two different temperatures: 25 and 65°C. In each case, the data (open circles) are fit to a model, and the model fits are shown as continuous lines. The model is discussed in the previous section. Parameters corresponding to the fits are shown in the table 3.2.

Figure 3.13. IFT analysis of SANS data on samples in glycerol. The data for the sample of EHAC-NaSal (60-30 mM) in glycerol at 25°C and 65°C are analyzed by IFT to obtain the corresponding pair distance distribution functions $p(r)$. (a) At 25°C, the $p(r)$ plot is asymmetrical and indicative of elongated micelles (WLMs). The point where $p(r)$ hits the x-axis (~ 150 Å), indicated by the arrow, is an estimate for the micellar length. (b) At 65°C, on the other hand, $p(r)$ is symmetrical, which is indicative of spherical micelles. The point where $p(r)$ hits the x-axis (~ 70 Å), indicated by the arrow, is an estimate for the micellar diameter.

Figure 3.14. Experiment demonstrating the utility of viscoelastic WLMs in Gly-EG mixtures. A Gly-EG (90:10 v/v) mixture has a freezing point below –20°C. It can be rendered viscoelastic (due to the formation of WLMs) by adding EHAC-NaSal (60-60 mM). The bare solvent mixture and its viscoelastic counterpart are compared in a simple visual test. For this, inclined aluminum surfaces were created using glass slides covered with aluminum foil. Red iron oxide pigment (0.1 wt%) was added to the solutions for better visualization. Approximately 1 g of the respective samples were applied onto the surfaces using a paint brush (left top) at time $t = 0$, and the surfaces were then placed in the freezer ($T \sim$ –20°C) for 15 hours. Due to the low freezing point of the solvent, neither sample froze into a solid. Results are shown in (a) for the Gly-EG solvent mixture and in (b) for the viscoelastic sample of WLMs in Gly-EG. In (a), the liquid initially coats the surface (top), but it quickly flows down the surface and collects in a pool below (bottom). The surface is thereby left exposed. Only 28% of the liquid mass was measured to remain

on the surface. In (b), the viscoelastic sample coats the surface as a thin film (top), and this film persists even after 15 hours (bottom). 98% of the sample mass was found to remain on the surface.

Figure 4.1. Comparing the dynamic rheology of WLMs in water and glycerol. In all cases, the elastic modulus G' and the viscous modulus G'' are plotted vs. frequency ω. (a) Typical WLMs in water (60 mM CPyCl + 60 mM NaSal) show the rheology of a single-t_R Maxwell fluid (lines are fits to this model). The data are from rheometry. (b) Data for WLMs of 60 mM CTAB + 100 mM $NaClO_3$ in water are shown over a wide range of ω by combining measurements from rheometry, oscillatory squeeze flow (OSF) and diffusive wave spectroscopy (DWS). In this case, G' and G'' cross twice, indicating three distinct regimes in the data. (c) Typical WLMs in glycerol (60 mM EHAC + 60 mM NaSal) show the same three regimes as in (b), but over a much narrower range of ω. The data are from rheometry. Lines are fits to a 4-mode Maxwell model.

Figure 4.2. Dynamic rheology of WLMs in glycerol at various temperatures. In all cases, the elastic modulus G' and the viscous modulus G'' are plotted vs. frequency ω for a sample of 60 mM EHAC + 60 mM NaSal. (a) Data over a temperature range from 25 to 40°C in increments of 1°C. The moduli at specific temperatures are shown to indicate specific patterns in the data: (b) 15°C; (c) 31°C; and (d) 40°C.

Figure 4.3. Parameters extracted from the temperature-dependent rheology of WLMs in glycerol. The parameters are from Figure 4.2, which shows data at various temperatures for a sample of 60 mM EHAC + 60 mM NaSal in glycerol. (a) Crossover frequencies ω_{c1}, ω_{c2}, and ω_{c3} as a function of temperature. (b) Ratio of ω_{c1}/ω_{c2} as a function of temperature.

Figure 4.4. Cole-Cole plots for WLMs in water and glycerol. A Cole-Cole plot is one of G'' vs. G', with both axes on a linear scale. (a) Comparison via Cole-Cole plots at 25°C of WLMs in water (data from Figure 4.1a) and WLMs in glycerol (data from Figure 4.1c). The aqueous sample is a Maxwell fluid, which corresponds to a semicircle on the Cole-Cole plot. The glycerol sample deviates from the semicircular arc and extends as a straight line. (b) Cole-Cole plots for WLMs in glycerol at various temperatures (data from Figure 4.2a). The plots fan out in a series of straight lines at high moduli. The inset shows the initial portion of the graph, where the order of semicircular arcs is reversed.

Figure 4.5. Dynamic rheology of WLMs in glycerol at various salt concentrations. In all cases, the elastic modulus G' and the viscous modulus G'' are plotted vs. frequency ω. All experiments were done at 25°C. The samples contain 60 mM EHAC and varying concentrations of salt (NaSal): (a) 30 mM; (b) 42 mM; (c) 60 mM; (d) 78 mM.

Figure 5.1. Lecithin self-assembly in water. Lecithin or L-α-phosphatidylcholine consists of two unsaturated non-polar tails (red) and a polar headgroup (blue). In water, lecithin self-assembles to form spherical vesicles with an aqueous core and lipid bilayer.

Figure 5.2. Lecithin self-assembly in water-solvent mixtures. (a) Sample images for lecithin vesicles (2 wt%) in water-glycerol mixtures are shown here. From left to right, the water-glycerol content changes from 50/50 to 0/100. Samples from 50/50 to 30/70 appear bluish and do not show flow birefringence, whereas samples from 20/80 to 0/100 appear clear and exhibit flow birefringence. (b) The optical density and diameter of the lecithin samples are shown here for increasing glycerol content.

Figure 5.3. Steady-shear rheology for lecithin in glycerol solutions. (a) The steady-shear rheology (plots of the relative viscosity $\eta/\eta_{solvent}$ as a function of shear-rate) for lecithin concentrations 2, 4, 8 and 15 wt% in glycerol are shown. The 2 wt% lecithin sample shows Newtonian behavior, whereas 4, 8 and 15wt% lecithin samples are shear thinning. (b) The left image shows the vial inversion test for 15 wt% lecithin in glycerol, indicating that the sample can hold its weight and is gel-like. The right image is taken under cross polarizers and shows that the sample is birefringent at rest (bright streaks of light are visible). The dynamic rheology of (c) 4 wt%, (d) 8 wt% and (e) 15 wt% lecithin samples are shown. The 4 wt% and 8 wt% lecithin samples show viscous response, and 15 wt% lecithin sample is gel-like. In all cases, the elastic modulus G' and the viscous modulus G'' are plotted vs. frequency ω.

Figure 5.4. Birefringence of lecithin samples in ethylene glycol (EG) and formamide. All sample images are taken under cross polarizers. The samples of lecithin in (a) EG and (b) formamide containing 4, 8 and 12 wt% lecithin are shown. All samples are highly birefringent at rest, except for 4 wt% in formamide, which is flow birefringent. The 8 wt% lecithin in EG separates into two phases forming a lipid-rich phase (birefringent).

Figure 5.5. Dynamic rheology of lecithin in formamide. In all cases, the elastic modulus G' and the viscous modulus G'' are plotted vs. frequency ω. The samples contain lecithin in formamide at concentrations of (a) 4 wt%, (b) 8 wt% and (c) 15 wt%. The 4 wt% sample shows viscoelastic response, whereas 8 and 12 wt% samples show gel-like response.

Figure 5.6. Temperature progression for a lecithin in glycerol sample. In all cases, the elastic modulus G' and the viscous modulus G'' are plotted vs. frequency ω. The 15 wt% lecithin in glycerol sample is studied at different temperatures (a) 25 °C, (b) 45°C and 65 °C. The sample remains gel-like at all temperatures. Inset: Vial photo of 15 wt% lecithin in glycerol at 65 °C.

Figure 5.7. Cryo-SEM images of lecithin samples in glycerol. The electron micrographs for (a) 2 wt% and (b) 8 wt% lecithin in glycerol are shown. Both images show spherical structures ranging from 50 nm to 600 nm. The spheres are widely separated for 2 wt% sample but are very densely packed for the 8 wt% sample.

Figure 5.8. SANS and SAXS for lecithin in glycerol. Each plot shows the scattered intensity I vs. wave vector q. (a) SANS data for of 3.2 wt% lecithin in deuterated (d-8) glycerol. (b) SAXS data for 15 wt% lecithin in glycerol. Slope values at different q-regions are included.

Figure 5.9. Schematic of vesicle self-assembly in polar solvents. Vesicle solutions, obtained at low lecithin concentrations (~ 2wt%), are represented by widely separated multilamellar or "onion" vesicles in the left image. The multilamellar structures are represented as concentric vesicles. The vesicle gels are comprised of densely packed multilamellar vesicles which are obtained at high lecithin concentrations (> 10wt%).

Figure 6.1 Phase behavior of WLMs in water-EG mixtures. WLMs were studied for increasing NaSal/EHAC molar ratio at different concentrations of water-EG mixtures ranging from 60/40 to 100/0 water-EG. The EHAC concentration is 60 mM. The blue and red data indicate the single phase (isotropic) and 2-phases (coacervate) of WLMs solutions respectively.

Chapter 1

Introduction and Overview

1.1 Problem Description and Motivation

Self-assembly is a thermodynamically driven process where individual molecules spontaneously aggregate to form assemblies at the nanoscale. The self-assembly of surfactants has been extensively studied in water for more than a century. Surfactants are amphiphilic molecules with polar (hydrophilic) heads and non-polar (hydrophobic) tails. Various structures can be formed by the self-assembly of surfactants in water, including spherical micelles (diameters ~5 nm), cylindrical micelles (diameters ~5 nm and variable length), and vesicles (hollow spherical shells with diameters ~ 100 nm and shell thickness ~5 nm).[1-3] In the case of cylindrical micelles, it is possible in some cases for the cylinders to become very long and flexible (end-to-end lengths > 1 μm) – in that case, they are called wormlike micelles (WLMs)[4-6]. In all these structures, the hydrophilic heads of the surfactants remain in contact with water whereas the hydrophobic tails are shielded from water. The driving force for self-assembly in water is the hydrophobic effect, which results in attractive interactions between molecules having hydrophobic segments.[1,3,7]

To-date, water is the most common solvent in which self-assembly has been studied. In addition to water, self-assembly can also occur in highly non-polar solvents such as alkanes (oils).[8] In such solvents, it is possible to form spherical, cylindrical and wormlike micelles with a 'reverse' structure, i.e., the hydrophilic heads of the surfactants are sequestered from the non-polar solvent whereas the hydrophobic tails are in contact

with the solvent. [3,8] However, not all solvents are capable of supporting self-assembly. Figure 1.1 shows a (schematic) scale of properties that can be used to characterize the cohesive tendency or polarity of a solvent (specific properties may include the cohesive energy density, solubility parameter, surface tension, or dielectric constant). On such a scale, water falls on the blue end while alkanes fall on the red end. In both these extremes, self-assembly readily occurs. Conversely, in solvents of intermediate polarity such as formamide, glycerol, and ethylene glycol, self-assembly occurs to a lesser extent. Previous studies have reported the formation of small spherical micelles in some of these solvents or their mixtures with water.[9-17] However, there are no reports of large structures such as wormlike micelles and vesicles (with at least one length scale > 100 nm) being formed by self-assembly in polar organic solvents. This is the focus of the present dissertation.

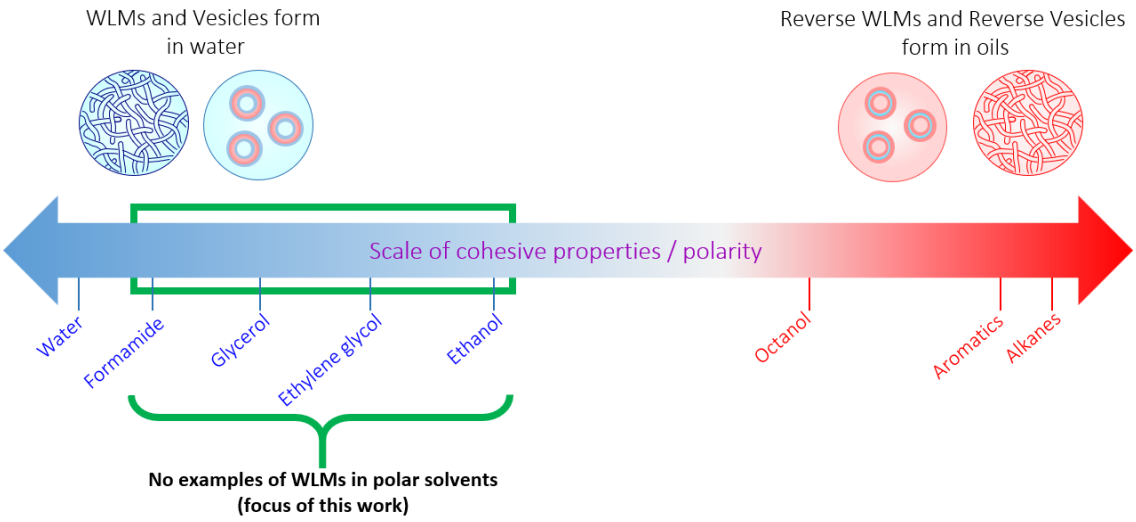

Figure 1.1. Overview of this study. A scale of solvent properties such as their cohesive energy density or polarity is shown schematically. Self-assembly of surfactants into large aggregates such as wormlike micelles (WLMs) and vesicles occurs in solvents at both extremes of this scale: i.e., in water (highly polar) and in oils (highly nonpolar). However, in pure solvents with lower polarity than water, there are no reports of such aggregates thus far, and that is the focus of this dissertation.

1.2 Our Approach

In this dissertation, we report new routes for forming large aggregates (such as wormlike micelles and vesicles) by self-assembly in polar solvents including glycerol, ethylene glycol and formamide. The new routes described here utilize well-known amphiphilic molecules, but they have not been studied before in conjunction with polar solvents. Our studies enable us to identify the 'design rules' that underlie self-assembly in non-aqueous systems. We also show that the resulting fluids exhibit interesting and unusual properties, especially with regard to their rheology.

1.2.1 Wormlike Micelles in Polar Organic Solvents

In Chapter 3, we show, for the first time, that it is indeed possible to form wormlike micelles (WLMs) in polar solvents like glycerol, ethylene glycol and formamide. For this, we combine a long (C_{22})-tailed cationic surfactant with a 'binding' salt, i.e., one with a large organic counterion that is capable of binding to the micelles.[18,19] Examples of such salts include sodium salicylate and sodium tosylate, and we find self-assembly to be maximized when the surfactant and salt concentrations are near-equimolar. The formation of WLMs coincides with a drastic increase in solution viscosity. One feature of polar solvents is that their mixtures can exhibit low freezing points. In a low-freezing mixture of glycerol and ethylene glycol, we show that the above cationic WLMs can persist down to sub-zero temperatures (as low as –20°C). Rheological techniques as well as small-angle neutron scattering (SANS) are used to characterize the WLMs under these conditions.

1.2.2 Rheology of Wormlike Micelles in Polar Solvents

In Chapter 4, we focus on the unique rheology of WLMs in polar solvents such as glycerol. WLMs are long, polymer-like chains that become entangled into a transient network. Thereby, samples containing WLMs exhibit viscoelastic behavior, which can be characterized by dynamic rheology (oscillatory shear). The dynamic rheology of WLMs in water follows a distinctive profile: plots of the elastic modulus G' and viscous modulus G'' as functions of frequency ω can be fit to a 'Maxwell model' with a single relaxation time t_R (correspondingly, G' and G'' intersect at a frequency $\omega_c = 1/t_R$).[6,20] In contrast, we find that WLMs in glycerol exhibit an unusual and very different profile: their moduli G' and G'' intersect twice (at ω_{c1} and ω_{c2}) and the plots cannot be fit by the above Maxwell model. We discuss why these rheological differences arise – our hypothesis is that the WLMs in glycerol are less entangled (due to being shorter in length) and less dynamic than WLMs in water.

1.2.3 Vesicles in Polar Organic Solvents

In Chapter 5, we turn our focus to vesicles. We report the formation of close-packed multilamellar vesicles in a variety of polar solvents including glycerol, formamide and ethylene glycol. The amphiphilic molecule used to create these vesicles is the simple phospholipid, lecithin or soy-phosphatidylcholine. Lecithin is insoluble in water, but in the presence of high shear, vesicles of lecithin can be induced. In polar solvents, we find that lecithin dissolves quite readily at concentrations between 2 and 15 wt%. At the higher concentrations (> 10 wt%), the fluids are clear, colorless, and gel-like. Dynamic

rheology reveals an elastic response, characteristic of a gel. The fluids are also birefringent at rest, which suggests an anisotropic (liquid-crystalline) phase. Images from cryo-scanning electron microscopy (cryo-SEM) indicate that the gel-phase is formed by the close-packing of vesicles with diameters around 100 to 200 nm. This structure is consistent with the rheology. To our knowledge, this is the first report of such a "vesicle-gel" phase in polar solvents.

1.3 Significance of This Work

The significance of this work from a scientific viewpoint is that it extends and enlarges the scope of self-assembly. For the first time, we show that WLMs and 'vesicle gels' can be formed by self-assembly in polar solvents. Both these microstructures are associated with rheological enhancement (thickening and viscoelastic behavior) of the parent solvent. In working with polar solvent mixtures, we have also been able to extend the range of conditions over which WLMs can exist to encompass sub-zero temperatures. Thereby, we have shown a new way to easily form viscoelastic fluids that remain so at low temperatures. We have also elucidated some of the 'design rules' or guidelines for inducing self-assembly of amphiphiles in polar solvents. This knowledge could lead to new fundamental interest in non-aqueous systems as media for self-assembly.

There are also potential applications for some of the new fluids we have created in this study. Specifically, viscoelastic or gel-like fluids in solvents like glycerol (or mixtures of glycerol and other solvents) could be useful as lubricants for use at low temperatures.[21,22] Also, fluids based on glycerol or ethylene glycol are currently sprayed

onto aircraft wings as de-icing fluids, i.e., they prevent the formation of ice when conditions are very cold.[23] These de-icing fluids are generally viscous, but not viscoelastic, and therefore do not stick significantly to aircraft wings. By imparting viscoelasticity to the fluids (via the formation of WLMs), we could significantly improve the retention of the fluid on a coated surface, as shown in Chapter 3. This is an example of a practical application that could be enabled by the new fluids described in this study. We anticipate that many more such possibilities will emerge in the future.

Chapter 2

Background

2.1 Self-Assembly of Amphiphiles in Water

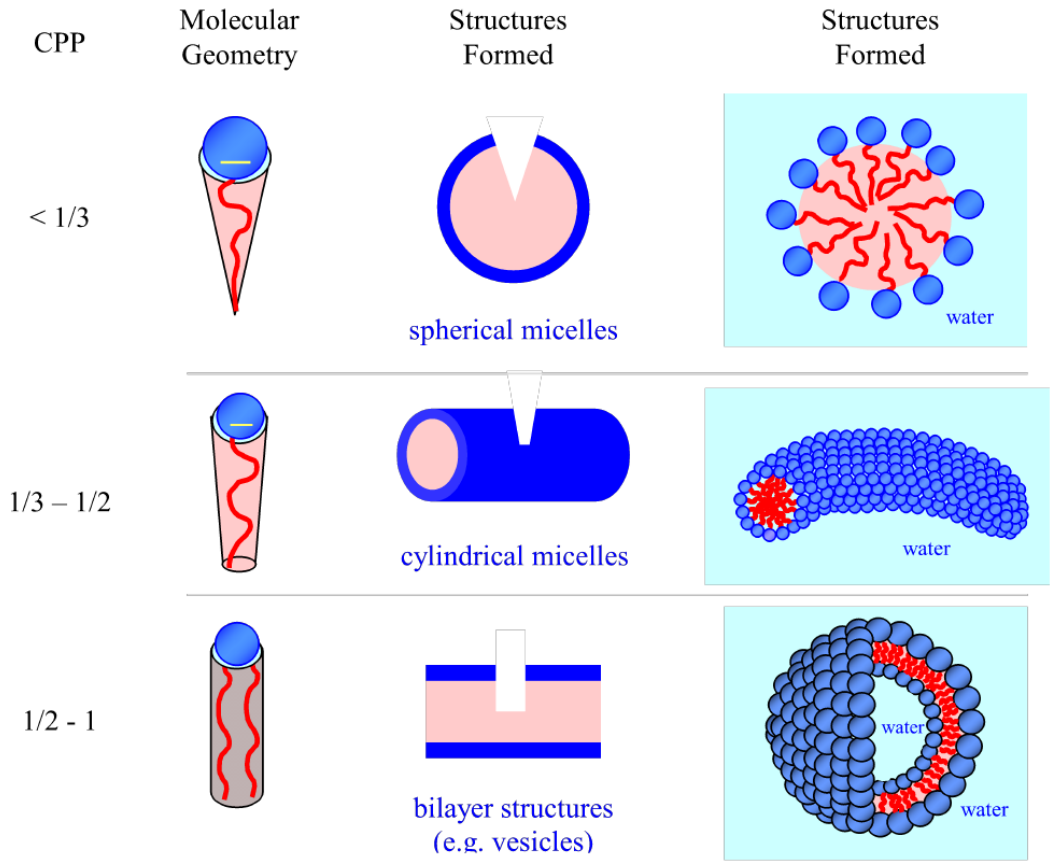

Figure 2.1. Schematics showing how the geometry of amphiphiles dictates the structures formed by self-assembly in water. The hydrophilic heads of the amphiphiles are shown in blue and the hydrophobic tails in red.

Amphiphilic molecules (surfactants or detergents) possess both a polar, hydrophilic moiety (head) and a non-polar, hydrophobic moiety (tail), as shown in Figure 2.1. When added to water, surfactants spontaneously aggregate to form structures of various geometries including spherical micelles, cylindrical micelles, and flat sheets

(bilayers or vesicles), which are all depicted in Figure 2.1. This spontaneous aggregation, which is called 'self-assembly' is a process driven by thermodynamics, i.e., it involves a minimization of the Gibbs free energy of the system. The main attractive interactions between surfactants in water are the hydrophobic interactions, i.e., the gain in entropy of water molecules when the hydrophobic tails of surfactants are removed from water and buried in the core of a structure such as micelle. In turn, the hydrophilic heads of the surfactants in a micelle face outward and remain in contact with the water molecules.

The type (shape) of self-assembled structure formed by a surfactant depends on its molecular geometry. This correlation is described via the critical packing parameter (CPP), which is defined as:[1]

$$\mathrm{CPP} = \frac{a_{\mathrm{tail}}}{a_{\mathrm{hg}}} \tag{2.1}$$

where a_{tail} is the average cross-sectional area of the hydrophobic tail and a_{hg} is the effective cross-sectional area of the hydrophilic headgroup. The larger the CPP, the more curved the aggregate, as depicted in Figure 2.1. In particular, if the CPP ~ ⅓ (i.e., if the surfactant is shaped like a cone), spherical micelles will be formed, whereas if the CPP is between ⅓ and ½ (i.e., if the surfactant resembles a truncated cone), cylindrical micelles are expected to be formed. Finally, if the CPP ~ 1, which implies that the surfactant molecule has nearly equal areas of tail and headgroup ($a_{\mathrm{tail}} \approx a_{\mathrm{hg}}$, shape like a cylinder), then flat bilayer structures are likely to be generated.

A few points are worth noting about the above structures. First, as a surfactant is added to water, the initial structure formed is likely to be spherical micelles (~ 5 nm

diameter), and these will arise when a threshold concentration called the critical micelle concentration (CMC) is crossed. With further addition of surfactant above the CMC, spherical micelles can sometimes transform into cylindrical micelles, which will have the same diameter (~ 5 nm) and variable length. Also, if the surfactant has a charged headgroup, the addition of salt will reduce the area of the headgroup a_{hg} and thereby induce a transition from spherical to cylindrical micelles. A CPP ~ 1 arises when the surfactant has two hydrophobic tails, and such surfactants are called lipids. Cell membranes in our body are composed of such lipids, and the most common class of lipids are the phospholipids, which have a phosphate moiety in their headgroups. When lipids are present at low concentrations (around 1-5 wt%), their bilayers tend to curl and close their ends, resulting in vesicles, i.e., hollow spheres (~ 100 nm diameter) filled with water and enclosed by a bilayer shell of thickness ~ 5 nm.

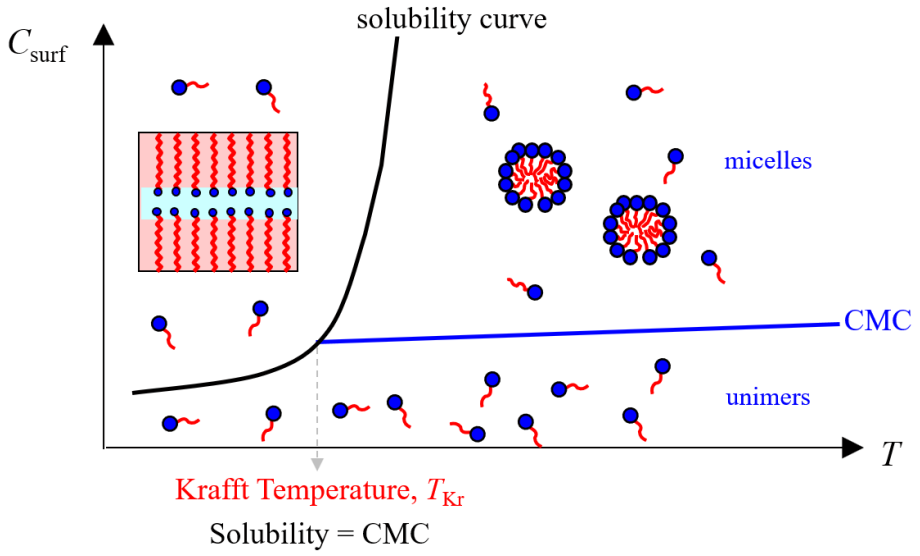

Figure 2.2. Schematic indicating the Krafft temperature (T_K) of a surfactant. The T_K corresponds to the intersection of the solubility curve and the curve of the CMC as a function of temperature. Below T_K, no self-assembly occurs because the surfactant crystallizes out of solution.

With regard to the effect of temperature on self-assembly, the CMC is itself a weak function of temperature, which means that the tendency to form micelles is still very strong at high temperatures. However, long cylindrical micelles (see Section 2.3) will tend to shorten upon heating. An additional key parameter is the Krafft temperature (T_K), which is the minimum temperature above which self-assembly can occur. As shown by Figure 2.2, T_K corresponds to the intersection of the solubility curve and the curve of the CMC as a function of temperature. Below T_K, the surfactant is insoluble in water, i.e., it exists in the form of crystals. For typical surfactants with a C_{16} tail like cetyl trimethylammonium bromide (CTAB), T_K is about 25°C, which means that micelles of CTAB can be studied only above this temperature.[24] One way to lower T_K is by having irregularities in the surfactant tail. For example, a cis-unsaturation in the hydrocarbon tail will mean a 'kink' in the geometry of the tail. Such kinked tails will not be able to pack close to each other in a crystal, and therefore the T_K will be much lower. An example is a surfactant such as erucyl bis(2-hydroxyethyl)methyl ammonium chloride (EHAC), which has an erucyl tail, i.e., a C_{22} tail with a cis-unsaturation in the middle. EHAC has a T_K well below 0°C. We will use EHAC in Chapters 3 and 4.

2.2 Self-Assembly of Amphiphiles in Polar Solvents

Self-assembly has been studied in a variety of solvents in addition to water. A general rule-of-thumb from the literature is that self-assembly can occur only in solvents that are either highly polar or highly non-polar. In highly non-polar 'oils' such as alkanes and aromatics, surfactants will assemble into reverse micelles, which in turn can be

spherical or cylindrical.[8,25,26] The term 'reverse' in the case of a micelle means that the hydrophilic heads of the surfactant are buried in the micellar interior and thus shielded from the oil phase, whereas the hydrophobic tails are extended into the oil. Conversely, self-assembly in polar liquids is similar to that in water and results in 'normal' micelles, much like those in Figure 2.1. Common surfactants such as CTAB can form spherical or short cylindrical micelles in polar liquids such as glycerol, formamide, ethylene glycol, propylene glycol, diethanolamine, 1-amino-2-propanol and diethylene triamine. [9-12,16,27]

The driving force for micelle formation in polar liquids is the 'solvophobic effect' in analogy with the hydrophobic effect in water.[10,12,28-30] That is, the surfactant tails dislike the solvent and therefore prefer to be buried in the core of micelles. However, because of the unique nature of water, i.e., its tendency to form strong hydrogen-bonds, the hydrophobic effect is much stronger than the solvophobic effect in any other polar solvent.[10,12,28-30] As a result, the driving force for micellization is lower in polar solvents than in water. For instance, the CMC of surfactants is much higher in polar solvents as compared to water, i.e., a much higher surfactant concentration is needed to form micelles.[10,29] Moreover, when micelles do form, they tend to be quite small, and there are no examples thus far of large aggregates such as wormlike micelles and vesicles in these solvents.

How polar must a liquid be to support self-assembly? This has been a key question for researchers. A related question is how to characterize the polarity of a solvent. Parameters that have been considered include the dielectric constant ε and the

surface tension γ. The current consensus is that the the parameter that best characterizes the polarity of a liquid is its cohesive energy density (CED).[10] The CED is the energy required to completely separate molecules from their neighbors to infinite separation (ideal gas state). For a given solvent, the CED can be calculated from its heat of vaporization ΔH_{vap} and its molar volume V_s^{mol}. Another measure of the CED that is used to quantify the solvophobic effect in self-assembly is the Gordon parameter G, which is defined below:

$$G = \frac{\gamma}{\left(V_s^{mol}\right)^{1/3}} \tag{2.2}$$

Values of G for some solvents are provided in Table 3.1 in Chapter 3. Water has the highest G of 2.74 $Jmol^{1/3}m^{-3}$.[10] Glycerol, formamide and ethylene glycol – three other solvents that promote self-assembly – all have G values above 1.3 $Jmol^{1/3}m^{-3}$. The above value may be considered a cutoff above which a solvent would promote self-assembly.

2.3 Wormlike Micelles

As discussed in Section 2.1, surfactants self-assemble into cylindrical micelles if the CPP is between ⅓ and ½.[1,4] Under certain conditions, these cylindrical micelles can grow to form very long, flexible chains, and they are then known as wormlike or threadlike micelles (Figure 2.3). Typically, wormlike micelles (WLMs) have a diameter similar to spherical micelles (~ 5 nm) while their end-to-end length (referred to as the contour length) can range from ~ 100 nm to a few microns (i.e. > 1000 nm).[2,31,32] Similar to a solution of flexible polymers, WLMs tend to become entangled in solution. Such entanglement results in a transient network of chains (as shown in Figure 2.3) and in turn,

the solution becomes highly viscous and displays viscoelastic properties.[4,32-34] The term viscoelastic implies that the solution exhibits both viscous (or liquid-like) and elastic (or solid-like) characters. In water, WLMs are expected to be in dynamic equilibrium and constantly exchange surfactant "unimers" between the micelles. Thereby, individual WLMs can break into pieces while other pieces recombine to form different WLMs. This process of breaking and recombination differentiates WLMs from chains of polymers, which never break because monomers are connected by covalent bonds. WLMs are therefore termed as 'living' or 'equilibrium' polymers.[2,6,32,34,35]

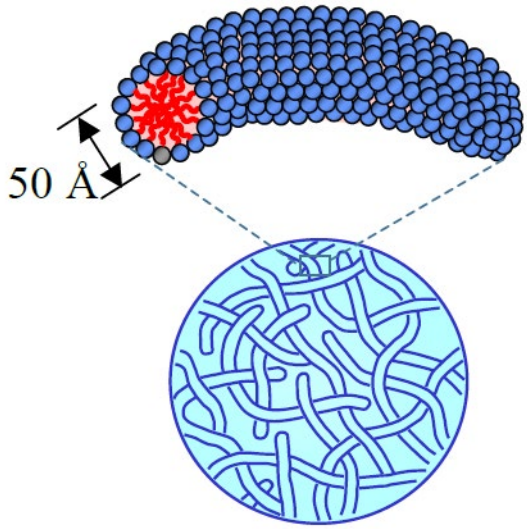

Figure 2.3. Schematic of wormlike micelles (WLMs). The structure of an individual WLM as well as the entanglement of micellar chains into a transient network are both shown.

Another characteristic property of WLMs is flow-birefringence i.e., when a vial containing a WLM solution is shaken and observed under crossed-polarizers, bright streaks of light are observed.[32,35] Birefringence (also known as double refraction) is an optical property referring to a difference in refractive indices along mutually

perpendicular directions. It is a characteristic property of optically anisotropic materials such as liquid crystals. In the case of WLMs, flow or shear causes the chains to align along the direction of shear, thus making the sample temporarily anisotropic. It is also important to note that WLMs are not birefringent when the solution is at rest because the chains are randomly oriented.

WLMs can be formed by cationic, anionic, or nonionic surfactants in water. In particular, WLMs of cationic surfactants like CTAB and EHAC have been extensively studied.[18,31,36-40] When these surfactants are added to water, the electrostatic repulsions between the headgroups will lead to a large area per headgroup a_{hg} and therefore the result will be spherical micelles. To form WLMs, salt must be added to the solution, which will reduce a_{hg} and thereby alter the CPP from ½ to ⅓. In this context, two kinds of salts can be distinguished: 'simple' salts and 'binding' salts. Simple salts are those like sodium chloride (NaCl) are added at a concentration around 100 mM or higher, the ions from the salt screen the electrostatic repulsions between the headgroups, leading to a lower a_{hg}. Conversely, 'binding' salts are those like sodium salicylate (NaSal), where the counterion (Sal^-) is aromatic and thereby hydrophobic. Thus, Sal^- counterions embed their aromatic part in the core of the micelle while the anionic portion binds to the cationic headgroup of the surfactant.[38,41] The net result is a reduction in the overall charge of the micelle due to the binding of the counterions. Binding salts can thus induce WLMs at lower concentrations compared to simple salts, and their effectiveness is often maximized at a concentration that is equimolar to the surfactant. Finally, we reiterate that, while WLMs have been extensively studied in water, there are no reports of WLMs in

polar solvents like glycerol and formamide. The latter will be the focus of this dissertation.

2.4 Characterization Technique – I: Rheology

Rheology is the study of deformation and flow in materials.[42,43] Rheological measurements help to correlate the microstructure in fluids to the flow properties.[35] Measurements can be performed under steady or dynamic shear. In the case of steady shear, the sample is subjected to a constant shear-rate $\dot{\gamma}$ and the response is measured as a shear-stress σ. The (apparent) viscosity $\eta = \sigma / \dot{\gamma}$ and a plot of η vs. $\dot{\gamma}$ is called the flow curve of the material. Pure solvents including water and glycerol are Newtonian fluids, indicated by a constant viscosity independent of the shear-rate. Several fluids, including WLMs show a 'Newtonian plateau' in their flow curve at low shear-rates. In this regime, the viscosity is independent of shear-rate and is called the zero-shear viscosity η_0. At shear-rates beyond the Newtonian plateau, the viscosity of WLMs will decrease with increasing shear rate, which is called a 'shear-thinning' response. [43]

Rheological experiments can also be conducted in dynamic or oscillatory shear, where the sample is subjected to a strain $\gamma = \gamma_0 \sin(\omega t)$. Here γ_0 is the strain-amplitude and ω the frequency of the oscillations. The sample response will be in the form of a sinusoidal stress $\sigma = \sigma_0 \sin(\omega t + \delta)$, which is shifted by a phase angle δ relative to the strain. The stress can be decomposed into two components, the first being in-phase with the strain, and the second being out-of-phase by 90°:

$$\sigma = \gamma_0 \left[G'(\omega) \sin(\omega t) + G''(\omega) \cos(\omega t) \right] \tag{2.3}$$

where G' is the **Elastic** or **Storage Modulus** and G'' is the **Viscous** or **Loss Modulus**. The dynamic experiment ultimately yields plots of G' and G'' as functions of ω (usually plotted on a log-log scale), which are collectively called the frequency spectrum of the material. Such a plot is useful because it shows how the viscoelasticity of the material varies with timescale, which in turn is a signature of the microstructure.[35]

The physical interpretation of G' and G'' are as follows. The elastic modulus G' reflects the elastic nature of the material and is also called the storage modulus since elastic behavior implies the storage of deformational energy. The viscous modulus G'' characterizes the viscous nature of the material and is also known as the loss modulus since viscous deformation results in the dissipation of energy. G' and G'' are meaningful only if the dynamic rheological measurements are taken in the "linear viscoelastic" or LVE regime. The LVE regime corresponds to low imposed strains, such that the stress response is linearly proportional to the strain.[43] In that case, G' and G'' will be independent of strain amplitude and will be functions only of the frequency ω – the moduli will then be true material properties.

An important advantage of dynamic rheology is that the material is characterized with its microstructure intact. Since only small-amplitude strains (within the LVE regime) are used, the net deformation imposed on the sample is minimal. Thus, G' and G'' correlate with the microstructure present at rest. In contrast, steady-shear rheology measures material properties under continuous flow conditions, which correspond to

large deformations. Therefore, dynamic rheological parameters can be correlated with static microstructures and steady-shear rheological measurements correspond to flow-induced changes in the microstructure.

2.5 Characterization Technique – II: SANS

Scattering techniques are very useful for probing structure at the nanoscale.[44] The basic principle behind these techniques is that the intensity of scattered radiation from a structured fluid is a function of the size, shape, and interactions of the "particles" present. We will use small-angle neutron scattering (SANS) to study our samples as it is useful in probing structure over size scales ~ few nm. In SANS, the contrast between the solvent and the "particles" is achieved by differences in their scattering length densities (SLDs). This is achieved by switching the hydrogen in the solvent molecules with deuterium, for example using D_2O instead of H_2O. We perform SANS experiments at one of the premier facilities in the USA, which is located nearby at the National Institute of Standards and Technology (NIST) in Gaithersburg, MD.

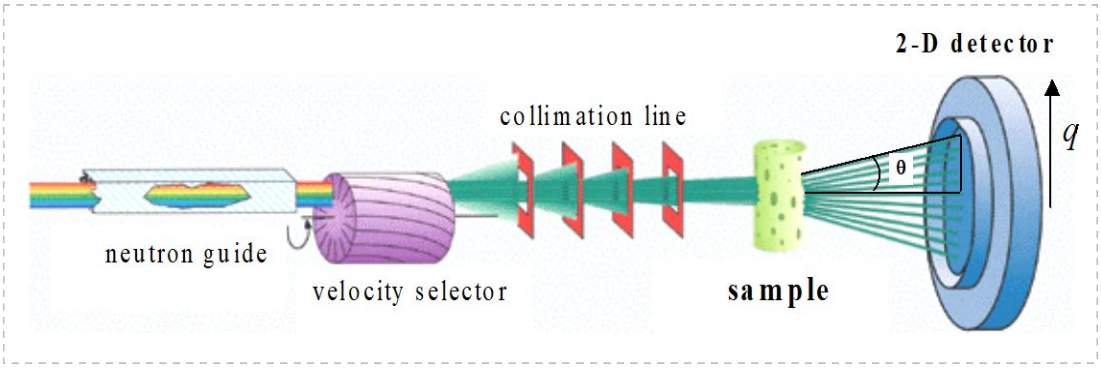

Figure 2.4. Schematic of a SANS experiment (adapted from www.gkss.de).

The basic geometry of a SANS experiment is illustrated in Figure 2.4. A nuclear reactor emits neutrons, which then pass through a velocity selector set for a particular wavelength and wavelength spread. These neutrons then pass through several collimating lenses and into the sample placed in the sample chamber. Finally, a 2-D detector collects the neutrons scattered by the sample. Using calibration standards, the collected 2-D data is corrected and placed on an absolute scale. This data is then spherically averaged to give a plot of the scattered intensity I vs. wave vector q.[44] The wave vector is defined as:

$$q = \frac{4\pi}{\lambda}\sin\left(\frac{\theta}{2}\right) \tag{2.4}$$

Here, λ is the wavelength of the incident radiation and θ is the scattering angle. q can be considered an inverse length scale, with high q corresponding to small structures, and low q to large structures in the sample.

For a structured fluid containing n_p particles per unit volume, the intensity $I(q)$ can be expressed as follows:[44]

$$I(q) = n_p \cdot P(q) \cdot S(q) \tag{2.5}$$

where $P(q)$ is referred to as the form factor and $S(q)$ as the structure factor. $S(q)$ is the scattering that arises from *interparticle* interactions and thus reflects the spatial arrangement of the particles. $P(q)$ is the scattering that arises from *intraparticle* interferences, and thus is a function of the particle size and shape. When the particles are in dilute solution (i.e., n_p is small), the interparticle interactions become negligible and therefore the structure factor $S(q) \rightarrow 1$. The SANS intensity $I(q)$ can then be modeled purely in terms of the form factor $P(q)$. Form factors for different particle geometries are

known, which can be fit to the data to extract structural information about the particles. However, one has to make an *a priori* assumptions about the type of particles present to select a particular form factor. Thus, a good fit to the data does not necessarily mean the model is correct, i.e., many models may fit the same data, especially if they have a large number of adjustable parameters.

The shortcomings with the "straight modeling" approach have led to the development of an alternate method of analysis that requires no *a priori* knowledge about the scatterers. This is the Indirect Fourier Transform (IFT) method, and here a Fourier transformation is done on the scattering intensity $I(q)$ to give the pair distance distribution function $p(r)$ in real space. $I(q)$ and $p(r)$ are related by the following equation: [7,44,45]

$$I(q) = 4\pi \int_0^\infty p(r) \frac{\sin(qr)}{qr} dr \tag{2.6}$$

The $p(r)$ function provides structural information about the scatterers in the sample. In particular, the largest dimension of the scattering entities can be estimated. The simplest form of the IFT technique is valid only for non-interacting scatterers. Before implementing the IFT methodology, it is useful to first subtract the incoherent background from the scattering data. This background can be estimated from the asymptotic slope of a Porod plot ($I(q)\cdot q^4$ vs q^4). In Chapter 3, we will use both the "straight modeling" and the IFT approaches to analyze the SANS data of our samples.

Chapter 3

Wormlike Micelles in Polar Organic Solvents

The results presented in this chapter have been published in the following journal article: N. R. Agrawal, X. Yue, Y. Feng and S. R. Raghavan, "*Wormlike Micelles of a Cationic Surfactant in Polar Organic Solvents: Extending Surfactant Self-Assembly to New Systems and Sub-Zero Temperatures*" Langmuir, 35, 12782−12791 (**2019**).

3.1 Introduction

Surfactants, *i.e.*, amphiphilic molecules with a polar headgroup and a non-polar tail, can self-assemble into various nanoscale structures, the most common of which are micelles (Figure 3.1A).[1-3] A particularly interesting class of micelles are the wormlike micelles (WLMs), also called threadlike micelles.[4-6,31,34] WLMs are long, flexible cylindrical chains, with diameters around 5 nm and contour (end-to-end) lengths L ranging from 100 to 5000 nm. They are formed at relatively low surfactant concentrations (2 to 5 wt% or 20 to 100 mM). Much like chains of polymers, WLM chains become entangled in solution (Figure 3.1A), thereby imparting high viscosity and viscoelasticity to the solution. This ability to modulate the rheological properties has led to numerous applications for WLMs, including in oil recovery, home-care and personal care products, and as drag-reducing agents.[4,46,47] Most studies on WLMs have been conducted in water, and aqueous WLMs have been formed using cationic,[6,18,31,34,36,37,40,48] anionic,[49] and zwitterionic[50-52] surfactants. Reverse WLMs, with their tails facing outward to the solvent, have also been reported in nonpolar liquids (oils).[8,25,26] Lastly, some studies have

been conducted on WLMs in mixtures of water and polar organic solvents (such as alcohols or diols).[23,53-56] To our knowledge, however, there have been no reports of WLMs in pure solvents of intermediate polarity.

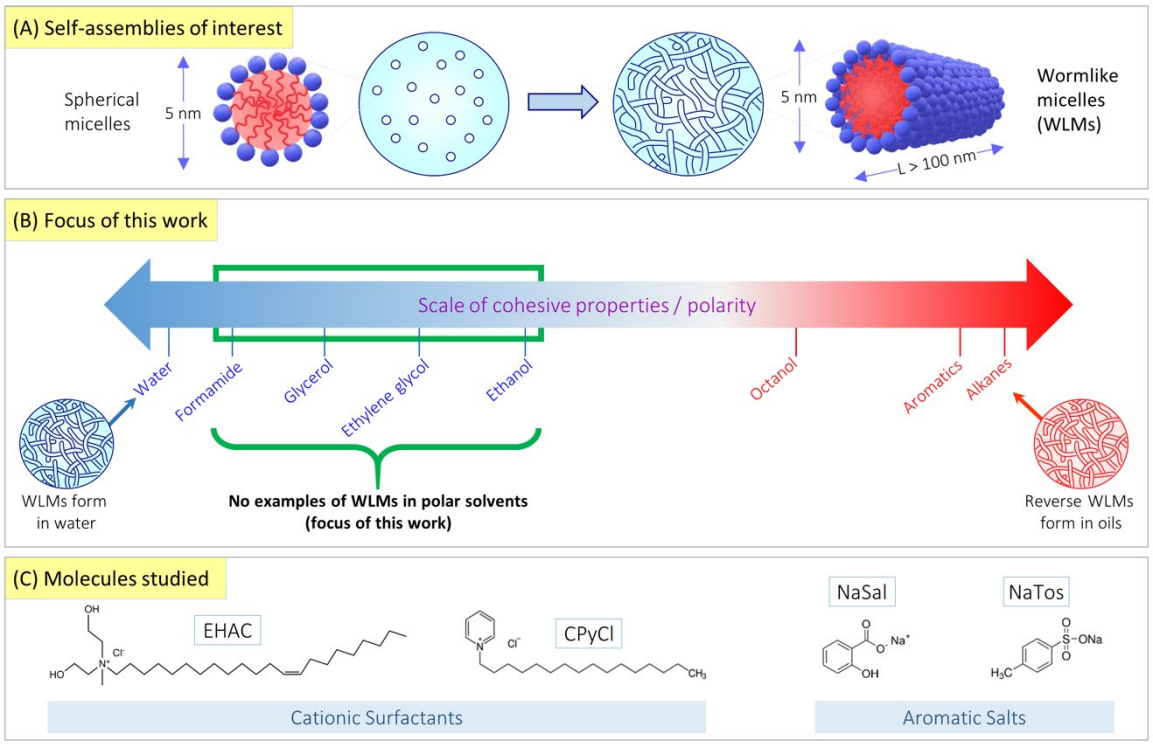

Figure 3.1. Overview of this study. (A) Surfactants (with their hydrophilic heads in blue and their hydrophobic tails in red) can self-assemble into micelles, which can be discrete spheres (5 nm in diameter), or wormlike chains (diameter of 5 nm and length L > 100 nm). The latter, termed WLMs, are the main structures of interest here. Their formation results in the solution becoming viscoelastic. (B) Scale of solvent properties such as the cohesive energy density or polarity. WLMs have been formed in solvents at both extremes of this scale: i.e., in water (highly polar) and in oils (highly nonpolar). However, in solvents with lower polarity than water, there are no reports of WLMs thus far, and that is the focus of this work. (C) Structures of molecules used in this study. These include the cationic surfactants erucyl bis(hydroxyethyl) methyl ammonium chloride (EHAC) and cetyl pyridinium chloride (CPyCl), and the aromatic salts sodium salicylate (NaSal) and sodium tosylate (NaTos).

With regard to solvent polarity, it can be quantified using parameters such as the dielectric constant or the Gordon parameter, as illustrated by Figure 3.1B. On one extreme of such a scale is water (highly polar), while on the other extreme are oils such as *n*-alkanes (highly non-polar). As the figure shows, in pure organic solvents with lower polarity than water, such as glycerol, formamide, and ethylene glycol, there have been no reports of WLMs thus far. Self-assembly has been shown to occur in some of these polar solvents,[9-15,27,57] but it only results in small micelles with an aggregation number N_{agg} (*i.e.*, the number of molecules associated into a micelle) less than about 100. The driving force for self-assembly in polar solvents is the 'solvophobic effect', analogous to the hydrophobic effect,[28,29,58,59] and it too involves the non-polar portions of surfactants segregating into the core of the micelles while the polar portions remain in contact with the solvent. But the solvophobic effect is generally weaker than the hydrophobic effect, which is why large aggregates like WLMs (having $N_{agg} > 1000$) are usually not formed in polar solvents. In recent years, there has been renewed interest in studying self-assembly in non-aqueous media, including ionic liquids. One motivation to study polar solvents is that they can have freezing points (T_f) well below 0°C. Recently, WLMs of a zwitterionic surfactant in water-ethylene glycol mixtures were reported to exist at sub-zero temperatures.[23,56] However, self-assembly into WLMs under such extremely cold conditions has not been achieved in pure non-aqueous solvents, to our knowledge.

Here, we show that WLMs can indeed be formed in polar solvents like glycerol and formamide if the surfactant and salt are carefully selected. Our surfactant of choice is a cationic surfactant with a long (C_{22}, unsaturated) tail (Figure 3.1C).[18,36,37,40,48] To form

WLMs in solvents like glycerol, this surfactant has to be combined with a salt having an organic counterion like sodium salicylate (NaSal) (Figure 3.1C). In addition to pure non-polar solvents, we have also studied solvent mixtures, and in particular, mixtures of glycerol and ethylene glycol that have freezing points far below 0°C. We have formed WLMs in these mixtures and find that the WLMs are preserved down to temperatures as low as –20°C. The rheology of these WLMs under both steady and dynamic shear over a range of low temperatures extending into the sub-zero range are reported. In addition, the technique of small-angle neutron scattering (SANS) is used to probe the nanostructure of the WLMs at these temperatures. Our studies provide insight into the design rules for self-assembly in polar solvents as opposed to water. Apart from fundamental insights, our findings may also have technological importance. The ability to form WLMs and thereby convert a solvent into a viscoelastic fluid could be useful in a variety of scenarios. One possibility is as lubricants that can be stable under extremely low temperatures. Another possibility is as anti-freeze liquids, which when sprayed onto airplane wings (or cars or wind turbines) would remain in place for a longer time due to their higher viscosity.[23]

3.2 Experimental Section

Materials. The following chemicals were obtained from Sigma-Aldrich: the surfactants cetyl pyridinium chloride (CPyCl), cetyl trimethylammonium bromide (CTAB) and cetyl trimethyl ammonium *p*-toluene sulfonate (CTAT); the salts sodium salicylate (NaSal), sodium tosylate (NaTos), sodium chloride (NaCl), potassium chloride (KCl); and the solvents glycerol (Gly), ethylene glycol (EG), formamide and propylene glycol (PG). The surfactant erucyl bis(hydroxyethyl)methyl ammonium chloride (EHAC) was obtained from Akzo Nobel. For SANS experiments, deuterated glycerol (d_8) was purchased from Cambridge Isotope Laboratories, and deuterated ethylene glycol (d_4) was purchased from Polymer Source, Inc. The molecular structures of key surfactants and salts used in this study are shown in Figure 1C.

Sample Preparation. Stock solutions of the surfactants and salts were prepared by adding weighed amounts of each into the solvent of interest and heating to ~ 60°C on a hot plate under constant stirring for 4–5 h. After clear solutions were obtained, they were cooled and stored at room temperature. To prepare a sample with desired molar concentrations of surfactant and salt, the respective stock solutions were combined and diluted with the solvent. After vortex mixing, the sample was heated to 60°C for 10–15 min and then cooled to room temperature. Samples were left at room temperature for at least a day before any measurements.

Rheology. Rheological experiments were conducted on an AR2000 stress-controlled rheometer (TA Instruments). A cone-and-plate geometry (2° cone) was used to perform

the steady-shear and oscillatory-shear experiments. The temperature was controlled by a Peltier assembly on the rheometer, which employed a circulating fluid that was fed from a chiller. A 50-50 mixture of ethanol-water (with a T_f < –30°C) was used as the circulating fluid. Rheological experiments were conducted at temperatures ranging from –5 to 65°C. Dynamic rheology experiments were conducted in the linear viscoelastic regime for each sample, which was determined from strain-sweep experiments. For rheological experiments at temperatures below 0°C, a crucial issue was the formation of ice on the cone-and-plate. To minimize ice formation, the plates were coated with the above EG-water mixture, then wiped dry. This allowed experiments to be conducted down to –5°C.

Small-Angle Neutron Scattering (SANS). SANS experiments were performed at the National Institute of Standards and Technology (NIST), Gaithersburg, MD on the NG-B (30 m) beamline. Neutrons with a wavelength λ of 6 Å were selected and the range of wave-vector q accessed was from 0.004 to 0.4 $Å^{-1}$. The sample holders were 1 mm titanium cells with quartz windows. The scattering data was reduced using IGOR-Pro software and were corrected to obtain an absolute scale of scattering intensity using NIST calibration standards. SANS fitting was done using the SasView software.

SANS Modeling. SANS data were fit using the SasView software package provided by NIST. Data were modeled in two ways: in one case by the Indirect Fourier Transform (IFT) method (Secion 2.5), and in the other case by fitting a model to the data. In the latter case, the structures in the sample were modeled as cylinders interacting via hard-

sphere interactions. The cylinders are modeled as being polydisperse in their radius, but monodisperse in their length. The form factor $P(q)$ for cylinders of radius r and length L is given by the following equations:[45,60]

$$P(q) = \frac{\text{scale}}{V_{cyl}} \int_0^{\pi/2} F^2(q,\alpha) \sin\alpha \, d\alpha \tag{3.1}$$

where the scattering amplitude F is given by:

$$F(q,\alpha) = 2V_{cyl}(\rho_{cyl} - \rho_{solv}) j_0\left(\frac{qL}{2}\cos\alpha\right)\left[\frac{J_1(qr\sin\alpha)}{qr\sin\alpha}\right] \tag{3.2}$$

Here, 'scale' is the volume fraction of cylinders, $V_{cyl} = \pi r^2 L$ is the volume of each cylinder, $j_0(x) = \sin(x)/x$, J_1 is the first-order Bessel function, and α is the angle between the cylinder axis and the scattering vector q. ρ_{cyl} and ρ_{solv} are the scattering length densities of the cylinder and the solvent. To account for polydispersity in the radius, $P(q)$ was averaged over a Schulz distribution of the cylinder radius. The size-averaged $P(q)$ is given by the following, where $f(r)$ is the normalized Schulz distribution of the radius r and V_{poly} is the volume of the polydisperse object.

$$\overline{P}(q) = \frac{1}{V_{poly}} \int_0^{x} P(q) f(r) dr \tag{3.3}$$

Next, the structure factor $S(q)$ accounts for interactions between the cylinders:

$$S(q) = 1 + 4\pi n_p \int_0^{\infty} [g(r) - 1] \frac{\sin qr}{qr} r^2 dr \tag{3.4}$$

Here $g(r)$ represents the pair correlation function and n_p is the number of particles (scatterers) per unit volume. From the models for $S(q)$ available in SasView, the one used here assumes that the particles are 'hard spheres', i.e., that they have no interaction at long distances and an infinite repulsion upon contact.

3.3 Results and Discussion

3.3.1 Formation of WLMs in Glycerol

We first describe the formation of WLMs in glycerol at 25°C. Glycerol is a polar solvent that has high cohesive energy density and strong hydrogen-bonding capability.[1,13] Therefore, glycerol can allow the self-assembly of micelles; however, previous reports of micelles in glycerol have been confined to small micelles with low aggregation numbers.[13] We first attempted to form WLMs in glycerol using the same precursors used previously to form WLMs in water. The vast majority of the studies on aqueous WLMs have been done with cationic surfactants, especially those with a C_{16} tail like CPyCl and CTAB.[6,31,34] To form WLMs, these surfactants are usually combined with either simple, inorganic salts (such as NaCl and KCl) or organic 'binding' salts (such as NaSal and NaTos). We studied if any of these surfactant/salt combinations could result in WLMs in glycerol. To initially assess the presence of WLMs, we resorted to visual inspection, looking for samples with high viscosities (as indicated by gradual flow out of a vial or the persistence of bubbles). However, none of the above combinations yielded WLMs. CTAB was found to be insoluble in glycerol at all concentrations, consistent with previous studies.[29] CPyCl was soluble, but did not form WLMs with the salts tested (data on the viscosities of CPyCl/NaSal mixtures are presented later).

Next, we tried EHAC, a cationic surfactant with a longer C_{22} tail (see Figure 3.1C for structure). Due to its longer tail, EHAC is a much stronger surfactant than CTAB or CPyCl; for example, the critical micelle concentration (CMC) of EHAC is about 50 times lower than that of the others.[18,36] WLMs of EHAC have been studied in water and can be

induced both by simple and binding salts.[18,36,37,40,48] In glycerol, though, we find that EHAC forms WLMs only when mixed with binding salts like NaSal. Figure 3.2 shows visual observations and rheological data at 25°C for a sample containing 60 mM EHAC + 60 mM NaSal. This sample is highly viscous (Figure 3.2a) and viscoelastic (Figure 3.2b). Visual observations show that the sample flows slowly out of a tilted or inverted vial and that bubbles are trapped in the sample after it is shaken (Figure 3.2c).

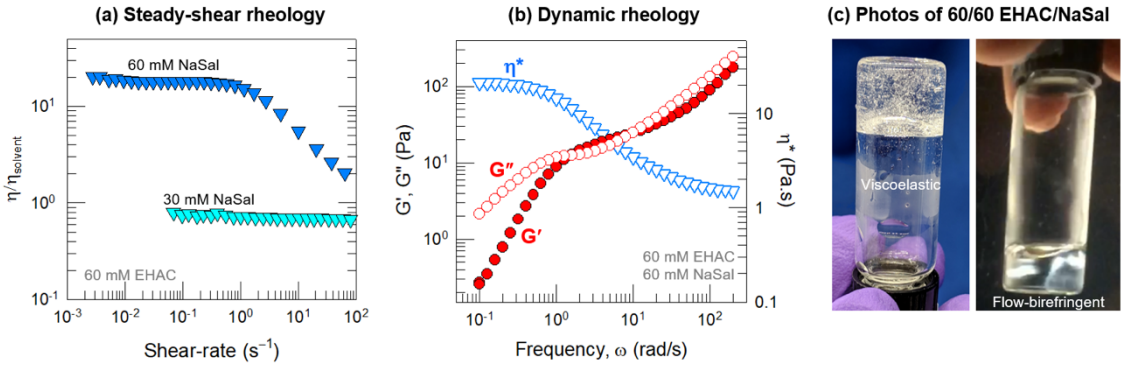

Figure 3.2. Wormlike micelles (WLMs) of EHAC-NaSal in glycerol at 25°C. (a) Steady shear rheology (plots of the relative viscosity $\eta/\eta_{solvent}$ as a function of shear-rate) for 60 mM EHAC samples containing 30 or 60 mM NaSal. (b) Dynamic rheology (plots of the elastic modulus G', viscous modulus G'', and complex viscosity η^* as functions of frequency ω) for the 60 mM EHAC + 60 mM NaSal sample. This sample shows shear-thinning in steady-shear and a viscoelastic response in dynamic rheology, indicating the presence of WLMs. (c) Visual observations further support this finding. The first photo shows that the sample is viscoelastic and is able to hold its weight in the inverted vial. The second photo, taken under crossed polarizers, shows that the sample is flow-birefringent (streaks of light appear when the sample is shaken).

The sample in Figure 3.2c also exhibits flow-birefringence, which is a phenomenon associated with WLMs.[34] When a sample of WLMs is sheared (*e.g.*, by shaking), the WLM chains align along the direction of shear, and as a result, the sample shows birefringence, *i.e.*, it has different refractive indices along perpendicular directions.

A simple way to see birefringence is by viewing the sample under crossed polarizer plates, whereupon streaks of light become visible in the sample when shaken (as can be noted in Figure 3.2c); these indicate aligned domains of WLMs. Note that there is no birefringence in the sample at rest because the WLM chains will not be aligned; rather they will be entangled into an isotropic network.[34]

The rheology of the 60 mM EHAC + 60 mM NaSal sample in glycerol at 25°C is consistent with the presence of WLMs. The steady-shear rheological data (Figure 3.2a) are shown as plots of the relative viscosity, *i.e.*, the ratio of sample viscosity with respect to the solvent viscosity ($\eta/\eta_{solvent}$), as a function of shear-rate. The 60 mM NaSal sample shows a constant and high viscosity at low shear-rates (in the Newtonian plateau), with its zero-shear viscosity η_0 being about 20 times that of the solvent. The high η_0 indicates the presence of long, entangled WLMs.[31,34] Above a critical shear-rate, η drops with increasing shear, indicating a shear-thinning response. Shear-thinning arises because the WLM chains tend to align with the flow.[31] For comparison, data are also shown in Figure 3.2a for a sample of 60 mM EHAC + 30 mM NaSal. This sample has the same viscosity as that of the solvent, i.e., there is no thickening, which implies that the micelles in it are not WLMs, but short cylinders. Long WLMs are only seen around an equimolar ratio of EHAC to NaSal, as will be further clarified by Figure 3.3.

The dynamic rheology of the 60 mM EHAC + 60 mM NaSal sample also reveals interesting features (Figure 3.2b). The elastic modulus G' and the viscous modulus G'' are both strong functions of the frequency ω, and the data overall reflect a viscoelastic

response, consistent with the presence of a WLM network.[31,34] However, typical WLMs in water show a single intersection of G' and G'' at a crossover frequency ω_c.[6,34] The relaxation time t_R of the WLMs is then given by $1/\omega_c$. Here, the glycerol-based WLMs show *two* intersection points of G' and G'' over the frequency range. At low ω, a 'terminal' region occurs, as expected, where $G'' > G'$, indicative of viscous behavior. Thereafter, at intermediate ω (1 to 10 rad/s), G' overtakes G'', indicating a transition to an elastic response at short timescales. Usually, G' will then become ω-independent and reach a plateau value, termed the plateau modulus G_p, which correlates with the mesh size of the entangled WLM network.[6] Here, instead, G' shows an upturn at $\omega > 10$ rad/s and at these short timescales, we again find that $G'' > G'$, indicating viscous dissipation. To our knowledge, such a rheological response has never been reported before for WLMs!

We have also plotted the complex viscosity η^* as a function of ω in Figure 3.2b. $\eta^*$is a quantity derived from G' and G'', as per eq 3.5:[35,42]

$$\eta^* = \frac{\sqrt{G'^2 + G''^2}}{\omega} \tag{3.5}$$

While the complex viscosity η^* is comparable to the viscosity η from steady-shear, we note that the η^* curve in Figure 3.2b shows two plateaus, one at low ω and the other at high ω. In contrast η shows one plateau at low shear-rates and then a monotonic decrease at higher shear-rates. The presence of two plateaus in the η^* vs. ω is again unusual for WLMs, and it also has never been reported previously.[31,34] Why is the rheology different for WLMs in glycerol compared to those in water? This is a complex topic, which is

addressed in detail in Chapter 4. Briefly, we believe there are two reasons for the differences: first, the structure of the WLMs in the two solvents, and second, the differences between the solvents themselves (i.e., the fact that water has a low viscosity compared to glycerol). For the rest of this paper, we will focus on the physical chemistry of the WLMs in glycerol as a function of salt, surfactant, and temperature.

3.3.2 Effects of Salt Concentration and Type

Figure 3.3 shows the relative zero-shear viscosity $\eta_0/\eta_{solvent}$ of glycerol solutions with 60 mM EHAC and increasing concentrations (C_{salt}) of different salts. The η_0 for each sample is obtained from the Newtonian plateau at low shear-rates in the steady-shear data (similar to the curves shown in Figure 3.2a). In the case of NaSal, there is no increase in viscosity until C_{NaSal} = 36 mM (*i.e.*, a molar ratio C_{NaSal}:C_{EHAC} = 0.6), indicating that there is no growth of WLMs up to this point. Thereafter, the viscosity increases with increasing C_{NaSal} and reaches a peak at C_{NaSal} = 48 mM (C_{NaSal}:C_{EHAC} = 0.8). The viscosity peak occurs close to the equimolar ratio of salt:surfactant, which suggests that there is molecular binding of the two species. Beyond the equimolar ratio, further addition of NaSal causes the viscosity to decrease and finally reach a plateau. Note that the peak value of η_0 is 34 Pa.s, which is comparable to the η_0 values exhibited by aqueous WLMs at similar surfactant and salt concentrations.[31,34] However, since glycerol is a viscous solvent, the peak enhancement in glycerol viscosity due to the WLMs is only a factor of about 40.

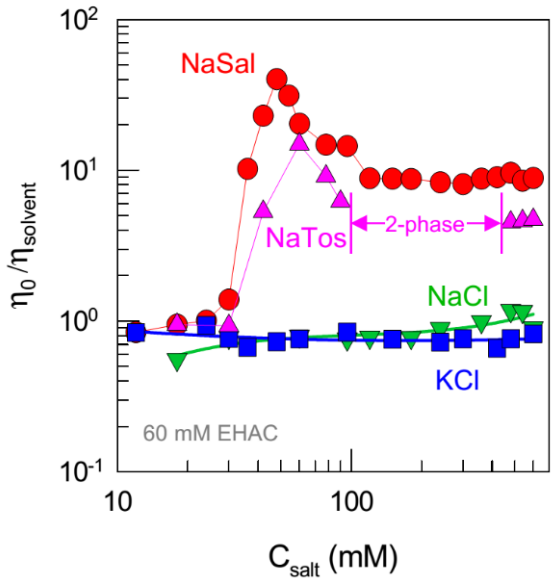

Figure 3.3. Effects of different salts on the formation of WLMs by EHAC in glycerol at 25°C. The plot shows the relative zero-shear viscosity ($\eta_0/\eta_{solvent}$) as functions of salt concentration for various salts, with the EHAC concentration fixed at 60 mM. WLM formation is reflected by a substantial increase in η_0 and is observed only with NaSal and NaTos.

Similar results as those for NaSal are shown in Figure 3.3 for a second binding salt, sodium tosylate (NaTos) (structure in Figure 3.1B). Again, there is a sharp increase in viscosity of 60 mM EHAC solutions around C_{NaTos} = 36 mM, indicating growth of WLMs. The peak in η_0 is reached at C_{NaTos} = 60 mM (C_{NaTos}:C_{EHAC} = 1) and the value of η_0 at this peak is 13 Pa.s. With further increase in C_{NaTos}, the viscosity drops to a plateau. Note that, between 90 and 480 mM NaTos, EHAC/NaTos samples in glycerol at 25°C separate into two co-existing liquid phases, which is why no data are shown for the viscosities over this concentration range. The two phases are a coacervate phase that contains most of the surfactant and a thin salt solution. Photos of selected samples are shown in Figure 3.4. Such 'coacervation' is unusual for surfactant solutions, but interestingly, it also occurs for EHAC/NaTos mixtures in water at 25°C.[36] In contrast to

NaSal and NaTos, simple salts such as NaCl and KCl do not induce any appreciable change in solution viscosity, regardless of the salt concentration (Figure 3.3). We conclude that simple salts are incapable of inducing WLMs of cationic surfactants in glycerol (and the same is true in other polar solvents).

Figure 3.4. Vial photos showing coacervation of EHAC/NaTos samples in glycerol. Samples of EHAC/NaTos in glycerol show a 2-phase region. Photos of selected samples are shown here. The samples contain 60 mM EHAC and varying NaTos (120, 150, 180, 240 and 300 mM). All samples show two co-existing liquid phases, i.e., coacervation. The phase boundary between the surfactant-rich phase (bluish) and the salt-rich phase (colorless) is indicated in each sample by a line for clarity.

We have also evaluated a variety of surfactants for their ability to form WLMs in glycerol. As mentioned, CTAB has limited solubility in glycerol, and this is also the case for other alkyl trimethyl-ammonium bromides with C_{14} or C_{12} tails.[13] Another widely used cationic surfactant in WLM studies is cetyl trimethylammonium tosylate (CTAT),[61] but this is also insoluble in glycerol. The one other cationic surfactant that was reasonably soluble in glycerol was CPyCl. Figure 3.5 shows the viscosities of 60 mM CPyCl solutions in glycerol as a function of NaSal. Negligible increases in viscosity are seen up to 600 mM NaSal, indicating a lack of WLMs. Thus, CPyCl/NaSal mixtures do not form WLMs in glycerol, although they do so in water. In contrast, EHAC/NaSal mixtures give rise to WLMs in both glycerol and water. The inability of CPyCl to form

WLMs in glycerol suggests that its shorter tail (C_{16}) is insufficient to induce extensive self-assembly in non-aqueous systems.

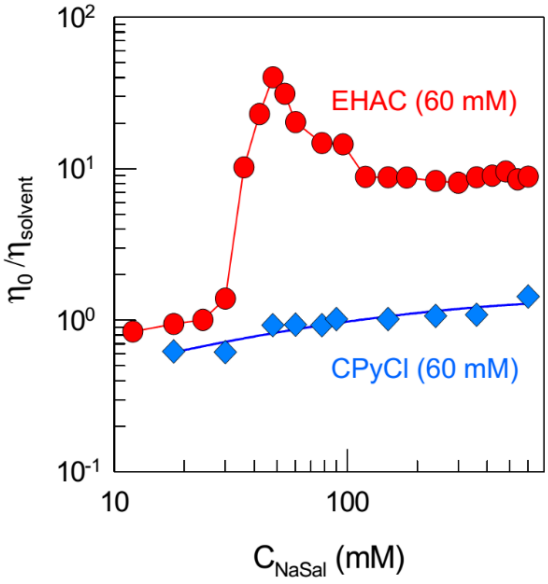

Figure 3.5. Comparison of EHAC and CPyCl for their ability to form WLMs in glycerol at 25°C. The plot shows the relative zero-shear viscosity ($\eta_0/\eta_{solvent}$) as functions of NaSal concentration for the two surfactants, with the surfactant concentration held constant at 60 mM. WLM formation is reflected by a substantial increase in η_0 and is observed only with EHAC.

A summary of the results thus far is sketched in Figure 3.6. To form WLMs in glycerol, both a long-tailed surfactant like EHAC as well as a binding salt like NaSal or NaTos are required. All other combinations of surfactants and salts failed to produce WLMs. Why are there differences between simple and binding salts in glycerol? In water, both kinds of salts induce WLMs, but by different mechanisms. It is helpful to relate salt effects to the critical packing parameter CPP = a_{tail}/a_{hg} where a_{tail} and a_{hg} refer to the average cross-sectional areas of the tail and the headgroup, respectively.[1,3] For a cationic surfactant in water, the CPP will be ~ 1/3 and the molecule will have a cone

shape (Figure 3.6). This is because the headgroups, when ionized, will experience significant electrostatic repulsions with each other, and thus the *effective* a_{hg} will be large relative to a_{tail}.[1,3] Molecules with a CPP of 1/3 will tend to form spherical micelles.

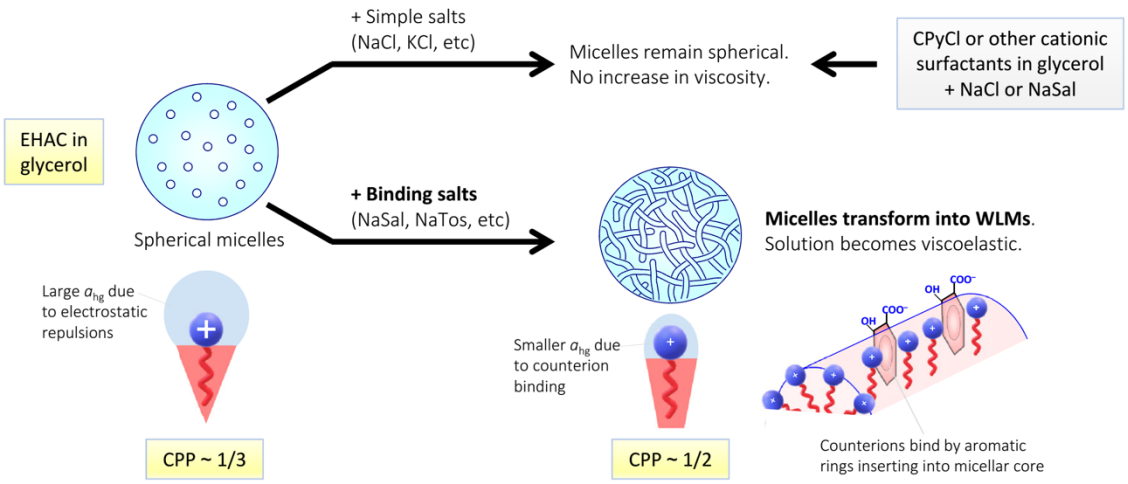

Figure 3.6. Conditions for WLM formation in polar solvents like glycerol, and a mechanistic picture for the same. WLMs form only when EHAC is combined with binding salts like NaSal or NaTos. For all other cases (EHAC + simple salts; other surfactants + any salts), no WLMs are produced. In the absence of salt, EHAC has a critical packing parameter (CPP) of ~ 1/3 because of strong electrostatic repulsions between its headgroups (and thereby a large area per headgroup a_{hg}). When a binding salt like NaSal is added, its counterions will bind to EHAC micelles. This will occur with the aromatic rings inserting into the hydrophobic core of the micelle. The anionic counterions, in turn, will neutralize the cationic headgroups and thus reduce a_{hg}, which increases the CPP to ~ 1/2. This will induce the spherical micelles to transform into WLMs.

When a salt like NaCl is added to the water, the ions will screen the electrostatic repulsions, reducing a_{hg} and thereby increasing the CPP from 1/3 to 1/2. This change in CPP causes a transition from spherical to cylindrical micelles (and thereby, eventually, to WLMs). Thus simple salts induce micellar growth, not by binding to micelles, but by

screening the micellar charge.[18,31] Binding salts like NaSal, on the other hand, have aromatic counterions that are significantly hydrophobic.[31,62] These counterions will penetrate the palisade layer of the micelles and embed in the hydrophobic core (Figure 5).[62] At the same time, the anionic (e.g., carboxylate) moiety of the counterion will bind to the cationic headgroups. Due to this binding, the micellar charge will be appreciably reduced, and in turn, the repulsions will be lowered. Thus, once again, an increase in CPP from 1/3 to 1/2 will occur, causing a sphere-to-cylinder (WLM) transition.[31,34] If all the counterions were to bind to the micelles, the net charge on the micelles would be lowest at an equimolar ratio of salt:surfactant.

Our results suggest that the binding of counterions like salicylate and tosylate to EHAC micelles occurs quite readily in a polar solvent like glycerol, which explains the growth of WLMs. This is illustrated in Figure 3.6. Presumably, the solvophobic effect with glycerol is sufficiently strong to allow the counterions to insert their aromatic ring into the micellar core. One indication of such binding is the fact that the viscosity maxima occur at or near the equimolar ratio of salt:surfactant. However, simple salts like NaCl seem ineffective at screening the electrostatic repulsions between EHAC headgroups in glycerol. The reason for this is not completely clear at the moment. It is possible that these salts do not completely dissociate into ions in glycerol due to its lower dielectric constant compared to that of water (see Table 3.1). Alternately, electrostatic screening by ions may not be as effective in glycerol compared to water. This aspect requires further study.

3.3.3 WLMs in Other Polar Solvents

Having identified the EHAC/NaSal system as one that results in WLMs in glycerol, we proceeded to study if WLMs could be formed by the same surfactant/salt combination in other polar solvents. For a polar solvent to allow self-assembly through the solvophobic effect, it must have a high cohesive energy density (CED), *i.e.*, there must be strong interactions between the solvent molecules. Solvents with high CED tend to be highly polar (as quantified by their dielectric constant ε) and also have strong hydrogen-bonding ability.[28,29,58,59] One way to quantify the CED is by the Gordon parameter G, which is given by eq 2.2 (see Section 2.2). Table 3.1 lists ε, γ, G and also the freezing point T_f for a few solvents in which self-assembly has been studied previously. Water has the highest values of G and γ and is thus the most favorable solvent for self-assembly. Glycerol, formamide and ethylene glycol (EG) are three other solvents with high G. Note that formamide also has the highest ε. Although glycerol has lower G and ε than formamide, it has high γ and strong hydrogen-bonding capability through its three hydroxyl groups. We have already demonstrated the formation of WLMs in glycerol. Thus, we proceeded to try the other solvents in this table.

Table 3.1. Selected properties of various polar solvents compared to those of water

Solvent	**Dielectric constant** ε (at 20°C)	**Surface Tension** γ (mN/m) (at 20°C)	**Freezing Point** T_f (°C)	**Gordon Parameter** G ($Jmol^{1/3}m^{-3}$)
Water	80	72.8	0	2.74
Glycerol	47	64.0	18	1.52
Formamide	109	58.2	3	1.73
Ethylene glycol	37	47.7	–13	1.36

One further aspect to consider at this stage is the effect of temperature on self-assembly. Generally, self-assembly becomes stronger at lower temperatures,[2,3] and WLMs are a case in point. The contour (end-to-end) length L of WLMs increases exponentially with decreasing absolute temperature T, as per the following equation:[6,18]

$$L \sim \sqrt{\phi} \cdot \exp\left(E_c / 2k_B T\right) \tag{3.6}$$

where k_B is Boltzmann's constant, ϕ is the volume fraction of the WLMs, and E_c is their end-cap energy. The key parameter here is E_c, which is the energy penalty associated with surfactant molecules that are stuck in the hemispherical end-caps of the WLMs rather than in their cylindrical bodies. The higher the E_c, the longer the WLMs will grow (to avoid forming end-caps).[6,18] As T is decreased, the exchange of surfactants between micelles is slowed down; this mitigates the influence of the end-caps and thereby allows the chains to grow longer. Longer WLMs will take a longer time to relax, and in turn, the solution will become more viscous. Based on eq 3.6, even if the WLMs are not very long at room temperature, they could become much longer upon cooling. For this reason, we have extended our studies on WLM formation in the solvents from Table 3.1 to temperatures well below room temperature.

It should be noted that studies on WLMs in water have rarely been conducted at temperatures much below 25°C. The reason for this lies in a key characteristic of surfactants called their Krafft temperature T_K.[2] This is the temperature below which the surfactant crystallizes out of solution, and hence, no micelles can be formed below T_K. Generally, T_K increases with surfactant tail length:[2,51] it is ~ 20°C for surfactants with saturated C_{16} tails, such as CTAB and CPyCl, and it is above room temperature if the tail

is saturated-C_{18} or longer. Thus, the relatively high T_K of CTAB and CPyCl has posed a limitation to studying their WLMs at low temperatures. In the case of EHAC, the erucyl tail has a *cis*-unsaturation in its middle (Figure 3.1B), and this represents a kink or bend in the tail. Due to this kink, EHAC molecules cannot pack tightly into a crystal, which is why EHAC has a very low T_K (< –20°C).[18,36] Thus, our choice of EHAC as the surfactant allows us to investigate WLMs down to low temperatures.

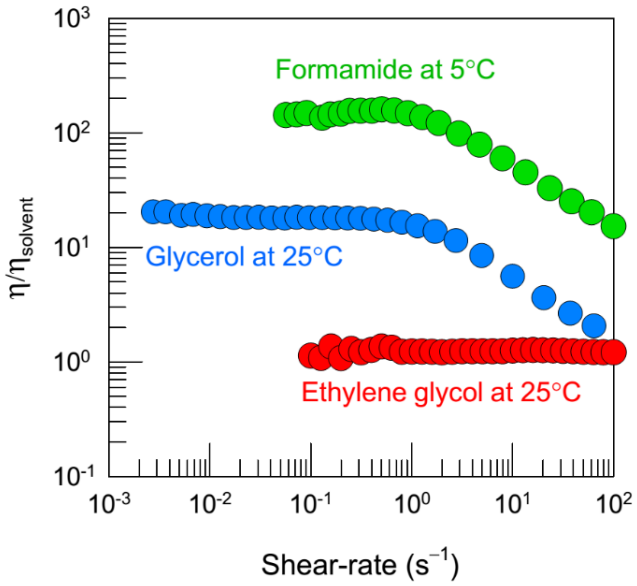

Figure 3.7. Steady-shear rheology of EHAC-NaSal samples in various solvents. The data are for the relative viscosity $\eta/\eta_{solvent}$ as a function of shear-rate. All samples contain 60 mM EHAC. The NaSal concentration is 60 mM in the glycerol sample and 90 mM in the formamide sample. Data are shown for glycerol and ethylene glycol at 25°C and for formamide at 5°C.

Figure 3.7 shows representative data from steady-shear rheology on samples in different solvents. All samples have 60 mM EHAC while the NaSal is 60 or 90 mM. The data are for the relative viscosity ($\eta/\eta_{solvent}$) as a function of shear-rate. In EG at 25°C,

there is no increase in viscosity and the sample shows Newtonian behavior, indicating a lack of WLMs. Similar data were obtained in EG at lower temperatures, regardless of the EHAC or NaSal content. In formamide at 25°C, the sample exhibited $\eta/\eta_{solvent}$ close to 1 and the behavior was Newtonian. However, at lower temperatures, the rheology became characteristic of WLMs. Data at 5°C are provided in Figure 3.7 and data at different temperatures are included in Figure 3.8. The plot in Figure 3.7 clearly shows a profile similar to that for glycerol: i.e., there is a high η_0 at low shear-rates and shear-thinning at higher shear-rates. This implies the presence of long, entangled WLMs of EHAC/NaSal in formamide. Note that η_0 for this sample is about 200 times that of the solvent at 5°C, which is a substantial enhancement in viscosity.

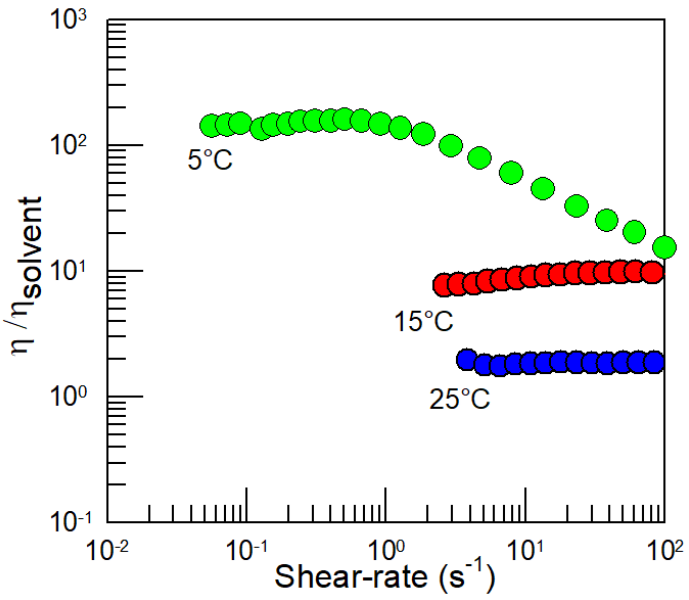

Figure 3.8. Steady-shear rheology in formamide at different temperatures. The data are for the relative viscosity $\eta/\eta_{solvent}$ as a function of shear-rate for a sample of 60 mM EHAC + 90 mM NaSal in formamide at temperatures of 25, 15 and 5°C. The sample remains Newtonian at 15 and 25°C while it is shear-thinning at 5°C.

3.3.4 WLMs at Low and Sub-Zero Temperatures

Next, we attempted to push the limits of WLM formation to temperatures below 0°C. One way to obtain a liquid with a low freezing temperature T_f is by mixing pure solvents. For example, it is well-known that mixtures of glycerol and water have lower T_f than either of the pure liquids.[63] In a similar vein, we studied mixtures of glycerol (Gly) and EG. As shown by Table 3.1, the T_f for Gly is 18°C and that for EG is –13°C. We confirmed that Gly-EG mixtures over a vast composition range have lower T_f than those of the individual solvents. For our studies, we used a 90-10 mixture of Gly-EG, which has a T_f < –5°C. To form WLMs in this mixed solvent, we added 60 mM EHAC + 120 mM NaSal. Although WLMs did not form in pure EG at this composition, they did so in the 90-10 Gly-EG mixture. Through visual observations, we confirmed that the sample remained clear and viscoelastic even when cooled to temperatures as low as –20°C.

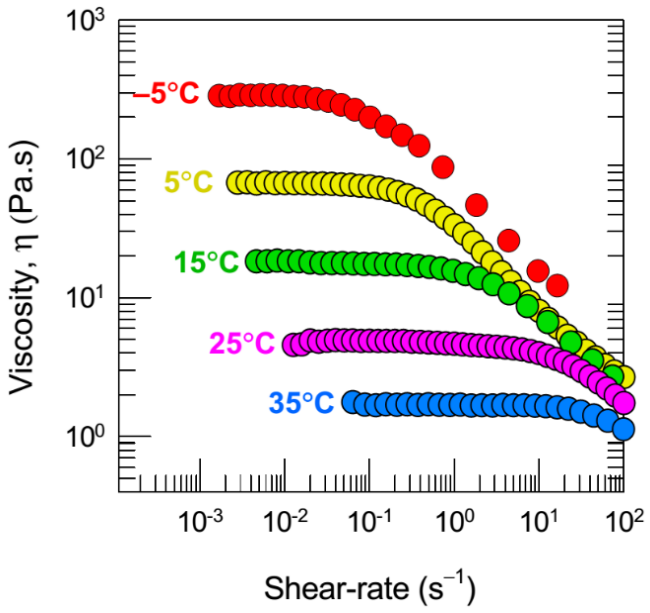

Figure 3.9. Steady-shear rheology of WLMs in a low-freezing solvent (90-10 mixture of Gly-EG) from ambient to sub-zero temperatures. The data are for the viscosity η as a function of shear-rate. The sample contains 60 mM EHAC and 120 mM NaSal.

Figure 3.9 shows steady-shear rheological data on the above sample over a temperature range from –5 to 35°C. At all temperatures, the sample shows a shear-thinning response similar to that in Figure 3.2a; thus the data reflect the presence of WLMs over the temperature range. The zero-shear viscosity η_0 increases significantly with decreasing temperature: η_0 is 1.7 Pa.s at 35°C and 285 Pa.s at –5°C, i.e., there is a 150-fold increase in η_0 over a 40°C span. At even lower temperatures, the viscosity increases further and the sample becomes almost gel-like, but we could not perform accurate measurements due to experimental limitations; hence, data are not shown. Still, Figure 3.9 is significant because it shows systematic rheological data on WLMs at temperatures below 0°C.

The rise in the zero-shear viscosity η_0 of WLMs with decreasing temperature is expected to follow an exponential relation:[6,18]

$$\eta_0 = A \cdot \exp\left(E_a / RT\right) \tag{3.7}$$

where A is a pre-exponential factor, T the absolute temperature, and E_a the flow activation energy. This relation arises from the exponential rise in WLM contour length L with decreasing T, as given by eq 3.8. That is, the longer the WLMs, the higher the η_0. To verify if eq 3.9 holds for our system, we construct a semilog (Arrhenius) plot of η_0 vs. $1/T$. This is shown by Figure 3.10, and the data fall on a straight line, as expected. From the slope, we calculate the flow activation energy E_a to be 88 kJ/mol for this sample. For comparison, WLMs of 60 mM EHAC + 30 mM NaSal in water had a much higher E_a of 198 kJ/mol. At first glance, this suggests that E_a may be higher for WLMs in water.

However, WLMs based on other surfactant/salt combinations in water have been reported to show similar E_a values to those determined here.[40,48,49]

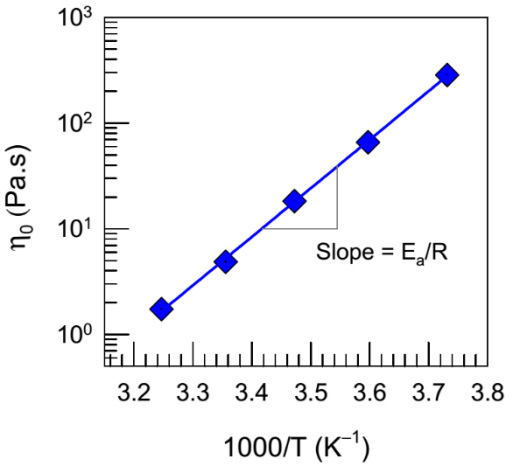

Figure 3.10. Arrhenius (semilog) plot of the zero-shear viscosity vs. 1/*T*, using the data from Figure 3.9. The sample contains 60 mM EHAC and 120 mM NaSal in a 90-10 Gly-EG mixture.

3.3.5 Nanostructure from SANS

Thus far, we have provided evidence from rheology and visual observations for the presence of WLMs in polar liquids. To further confirm the nanostructure, we resorted to SANS. Samples for SANS were prepared using deuterated solvents to ensure that there was sufficient contrast between the scattering objects and the continuous phase. SANS data are provided in Figure 3.11 as plots of the scattering intensity I vs. wave vector q. In Figure 3.11a, data are shown at 25°C for samples containing 60/30 and 60/60 EHAC/NaSal in glycerol. There is an upturn (higher slope) for I at low q for the 60/60 sample compared to the 60/30 one. This is consistent with the presence of longer micelles (WLMs) in the former, and it also tallies with the higher viscosities of the former from Figure 3.3. For comparison purposes, a slope of –1 on the log-log plot is marked on all

the plots; this corresponds to the scaling relationship expected for scattering from long, noninteracting cylinders ($I \sim q^{-1}$).[64,65] The slope of I in the low-q limit for the 60/60 sample is –0.7, which is close to –1. Both samples show nearly identical data at intermediate and high q, which suggests that both contain cylindrical micelles with similar radii (estimated to be around 2.4 nm; see below), but different lengths.

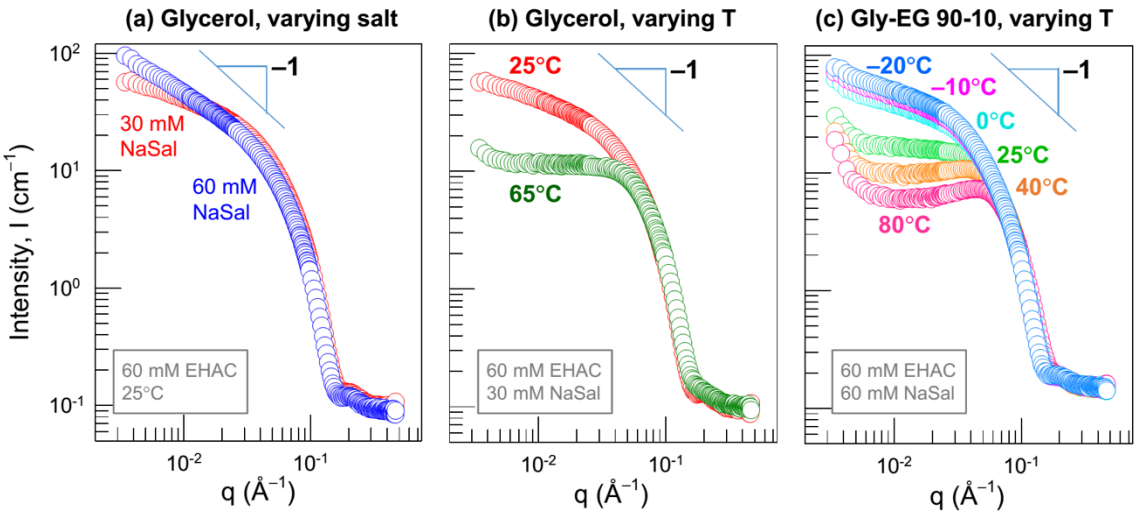

Figure 3.11. SANS plots for samples of EHAC/NaSal in deuterated solvents. Each plot shows the scattered intensity I vs. wave vector q. (a) Data for 60/30 and 60/60 mM EHAC/NaSal in glycerol at 25°C. (b) Data for 60/30 EHAC/NaSal in glycerol at 25°C and 65°C. (c) Data for 60/60 EHAC/NaSal in 90-10 Gly-EG at temperatures ranging from –20°C to 80 °C.

Next, the scattering from the 60/30 EHAC/NaSal sample in glycerol is studied at a higher temperature of 65°C. In this case (Figure 3.11b), I reaches a plateau at low q, which means that the micelles present are spherical. Note that the same sample at 25°C shows a much higher intensity at low q with a low-q slope of –0.3. The implication is that the relatively short cylinders present in this sample at 25°C shorten further and become nearly spherical at 65°C. Taken together, Figures 3.11a and 3.11b provide structural

evidence for the effects of composition and temperature on EHAC self-assembly in glycerol. The data confirm that: (a) micelles are present; (b) the micelles grow with addition of NaSal; (c) the micelles are likely to be long cylinders (WLMs) at an equimolar ratio of salt:surfactant at 25°C; and (d) increasing temperature shortens the micelles. We should emphasize that the above SANS data are very similar to those reported previously for aqueous WLMs, including those of EHAC/NaSal.[36,37,50]

We also conducted SANS studies using the 90-10 mixture of Gly-EG (both deuterated), corresponding to Figure 3.9. Data for a sample of 60/60 EHAC/NaSal in this solvent mixture are shown over a temperature range from –20°C to 80°C in Figure 3.11c. Over the entire range, the data overlap at high q, which suggest that micelles with comparable radii are present at all temperatures. At the lowest temperatures, there is increased scattering at low q and the slope of I at low q becomes approximately –0.4. This is again indicative of micellar growth into cylinders (WLMs). As temperature is increased, the intensity drops at low and intermediate q, implying a reduction in cylinder length. An unusual upturn in intensity is observed at low q in the 40°C and 80°C data. Such an upturn generally suggests that there are attractive interactions between the scattering objects,[65] although it is not clear why that should arise in this sample. The upturn is much more pronounced for the 90-10 Gly-EG sample in Figure 3.11c than for the glycerol sample in Figure 3.11b. If the upturn is ignored, the conclusion to be drawn from Figure 3.11c would be similar to the one from above: i.e., that the micelles shorten upon heating, or conversely lengthen (into WLMs) upon cooling.

SANS data can generally be fit to models, from which the sizes of scatterers can be extracted.[64,65] We have performed such model fitting, and the details are provided in the Figure 3.12. Excellent fits are obtained for a model that incorporates the form factor for cylinders of radius R and length L along with the structure factor for hard spheres.[64] The values of key parameters in the model are shown in Table 3.2. The micellar radius R is ~ 2.4 nm, and this is reliably obtained from the model fits. In fact, the same R can be calculated in a model-independent manner by plotting the scattering data in a cross-sectional Guinier plot, i.e., a plot of $\ln(Iq)$ vs. q^2.[65]

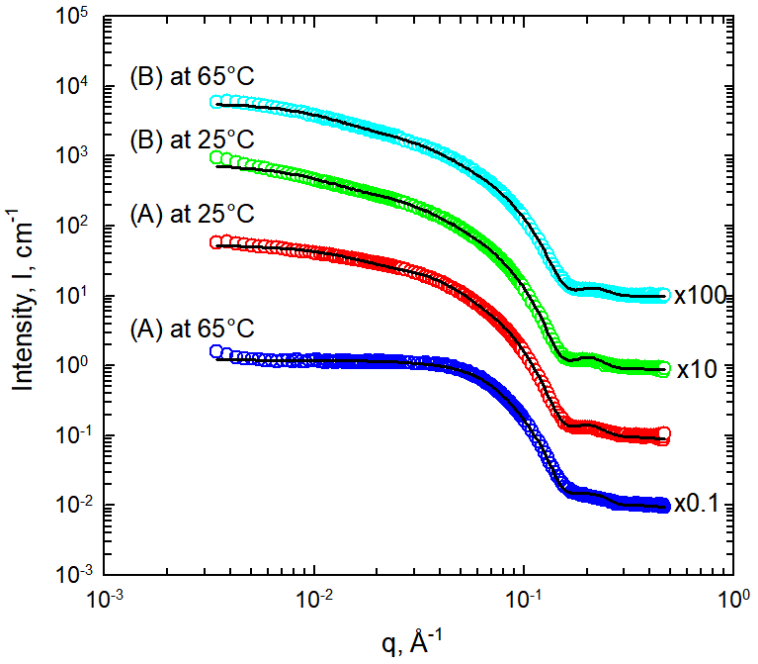

Figure 3.12. Model fits to SANS data shown in the paper. Plots of scattered intensity I vs. wave-vector q are shown for sample A (EHAC-NaSal 60-30 mM) and sample B (EHAC-NaSal 60-60 mM) at two different temperatures: 25 and 65°C. In each case, the data (open circles) are fit to a model, and the model fits are shown as continuous lines. The model is discussed in the previous section. Parameters corresponding to the fits are shown in the table 3.2.

Table 3.2. Fitting parameters for the data in Figure 3.12.

Sample EHAC-NaSal (mM)	Temp (°C)	Radius (Å)	Distribution of Radius	Length (Å)	Volume Fraction	Reduced χ^2
60-30	25	23.9	0.105	336	0.057	35.8
	65	23.5	0.088	93	0.076	33.5
60-60	25	24.0	0.096	473	0.036	33.2
	65	22.7	0.102	425	0.028	27.1

With regard to the model fits in Figure 3.12, we believe there is need for caution in interpreting some of the parameters obtained from the modeling. Specifically, the models are rather insensitive to the micellar contour length *L*, and hence *L* cannot be accurately obtained from these fits. The underlying reason is that WLMs are expected to have contour lengths *L* exceeding 100 nm. SANS, on the other hand, provides an accurate window primarily into structures between about 0.2 to 30 nm. In effect, when the WLM length exceeds this window, SANS only probes a portion of the entire WLM chain and is therefore insensitive to the contour length.[65] For example, the SANS data in Figure 3.11c for WLMs at temperatures of 0°C and –20°C are nearly identical; however, from the rheology data, we know that at the colder temperature, the WLMs must be much longer, which is why the sample is much more viscous. Despite these issues, it is clear that the SANS modeling supports the presence of surfactant-based WLMs in polar solvents.

Another model-independent approach to SANS analysis is by use of the Indirect Fourier Transform (IFT) method,[66,67] which permits the data to be analyzed without making *a priori* assumptions about the shapes or sizes of the scatterers. Figure 3.13

shows the pair distance distribution functions $p(r)$ obtained from IFT analysis of the SANS data from the 60/60 EHAC/NaSal sample at 25 and 65°C.

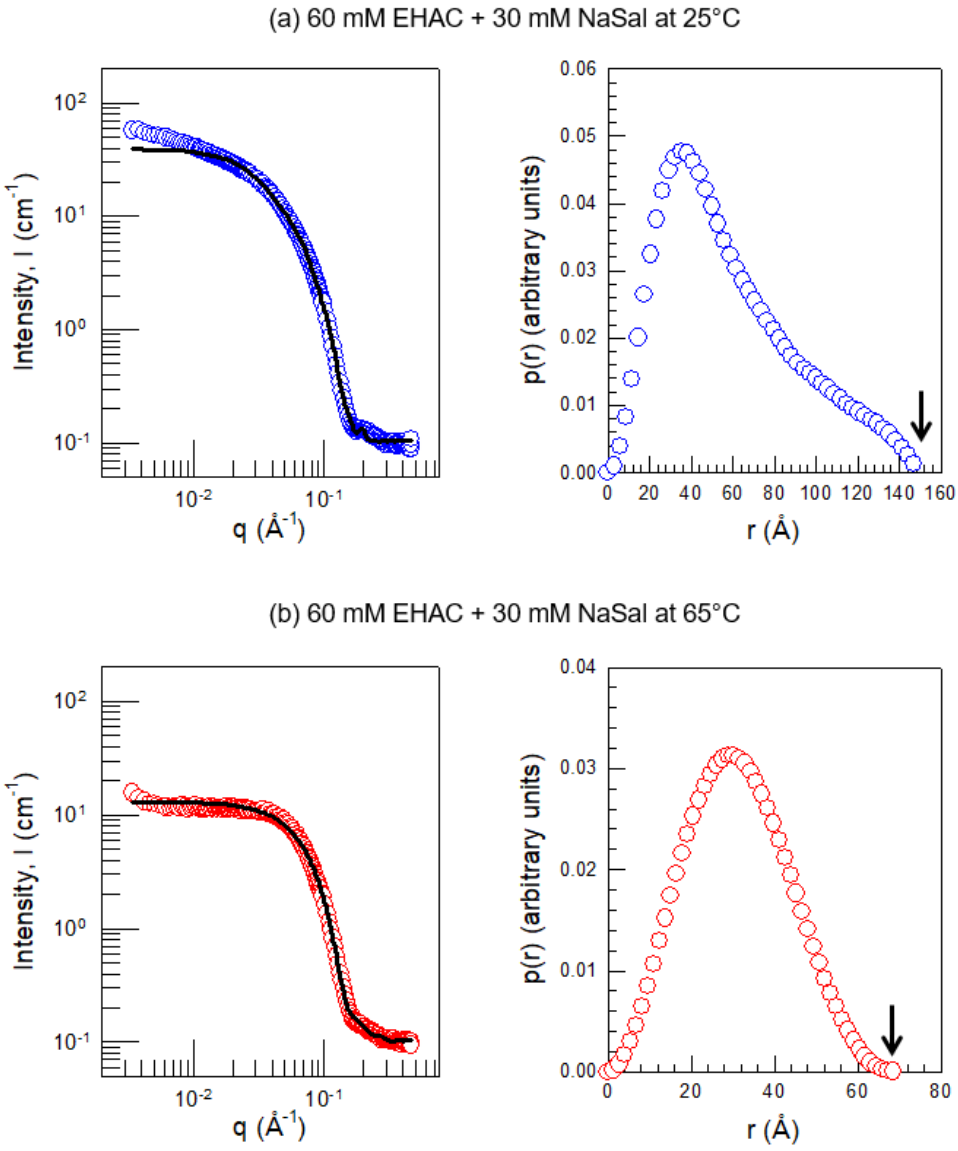

Figure 3.13. IFT analysis of SANS data on samples in glycerol. The data for the sample of EHAC-NaSal (60-30 mM) in glycerol at 25°C and 65°C are analyzed by IFT to obtain the corresponding pair distance distribution functions $p(r)$. (a) At 25°C, the $p(r)$ plot is asymmetrical and indicative of elongated micelles (WLMs). The point where $p(r)$ hits the x-axis (~ 150 Å), indicated by the arrow, is an estimate for the micellar length. (b) At 65°C, on the other hand, $p(r)$ is symmetrical, which is indicative of spherical micelles. The point where $p(r)$ hits the x-axis (~ 70 Å), indicated by the arrow, is an estimate for the micellar diameter.

The $p(r)$ at 25°C is asymmetrical and the curve hits the x-axis around 15 nm. This shape of $p(r)$ is known to be characteristic of cylindrical micelles,[66,67] with 15 nm being a lower estimate for their length. On the other hand, the $p(r)$ at 65°C is symmetrical and this shape is characteristic of spherical micelles.[66,67] In this case, the point where $p(r)$ hits the x-axis is about 7 nm, which corresponds to the diameter of the spheres. Thus, the IFT analysis also suggests that the micelles are larger and cylindrical (i.e., WLMs) at low temperatures and smaller and spherical at high temperatures, which is consistent with the discussion above.

3.4 Conclusions and Outlook

We have shown that it is possible for surfactants to self-assemble into large aggregates, specifically WLMs, in polar solvents like glycerol and formamide. This was achieved by combining a long-tailed (C_{22}) cationic surfactant (EHAC) with a 'binding' salt (NaSal or NaTos). Simple salts (NaCl or KCl) were unable to induce EHAC to form WLMs in polar solvents, although they are able to do so in water. Also, shorter-tailed (C_{16}) cationic surfactants did not assemble into WLMs in these solvents, whether they were combined with binding or simple salts. Thus, both the surfactant and the salt have to be chosen carefully to enable WLM formation in these non-aqueous systems. WLMs in polar solvents display viscoelastic and shear-thinning rheology, much like WLMs in water. However, the dynamic rheology of the former is quite unusual – the frequency spectra reveal multiple intersections of the elastic and viscous moduli (G' and G''). We have exploited the low Krafft point of EHAC and the low freezing points of Gly-EG mixtures to devise formulations in which WLMs persist down to sub-zero temperatures

(–20°C). SANS measurements confirm that WLMs are still present at these low temperatures. Thereby, we have been able to extend the range for WLM formation to much lower temperatures than in previous studies.

The ability to create non-aqueous viscoelastic fluids that withstand low temperatures is one notable point of this study. Because the fluids are formed by mixing commonly available precursors, they could be prepared in large quantities at low cost. Thereby, the fluids would be suitable for industrial applications that require cold temperatures, including as lubricants or as anti-freeze coatings on surfaces.[23] A simple experiment to illustrate the utility is shown in Figure 3.14. Here, aluminum-covered surfaces are placed at a near-vertical angle and a given amount of fluid is introduced onto it. As an example of a low-freezing liquid, we employ a 90-10 Gly-EG mixture (same as in Figure 3.9). If the liquid alone is introduced onto the surface, it flows down and dewets the surface in a short time, leaving it exposed (Figure 3.14a). However, if the same Gly-EG with WLMs of EHAC/NaSal is introduced, it too flows down, but still maintains a thin film over the entire surface (Figure 3.14b). Note that this is not just because the fluid has a higher viscosity, rather it reflects the *viscoelasticity* of the WLM solution. In fact, due to the shear-thinning nature of WLMs, the viscosity at high shear-rates (that are commonly encountered in spraying or blading operations) will be close to that of the solvent (see Figure 3.9). Thus, spraying such viscoelastic fluids onto a surface such as aircraft wings can be readily accomplished, and the fluids could be highly effective for de-icing or lubrication applications.

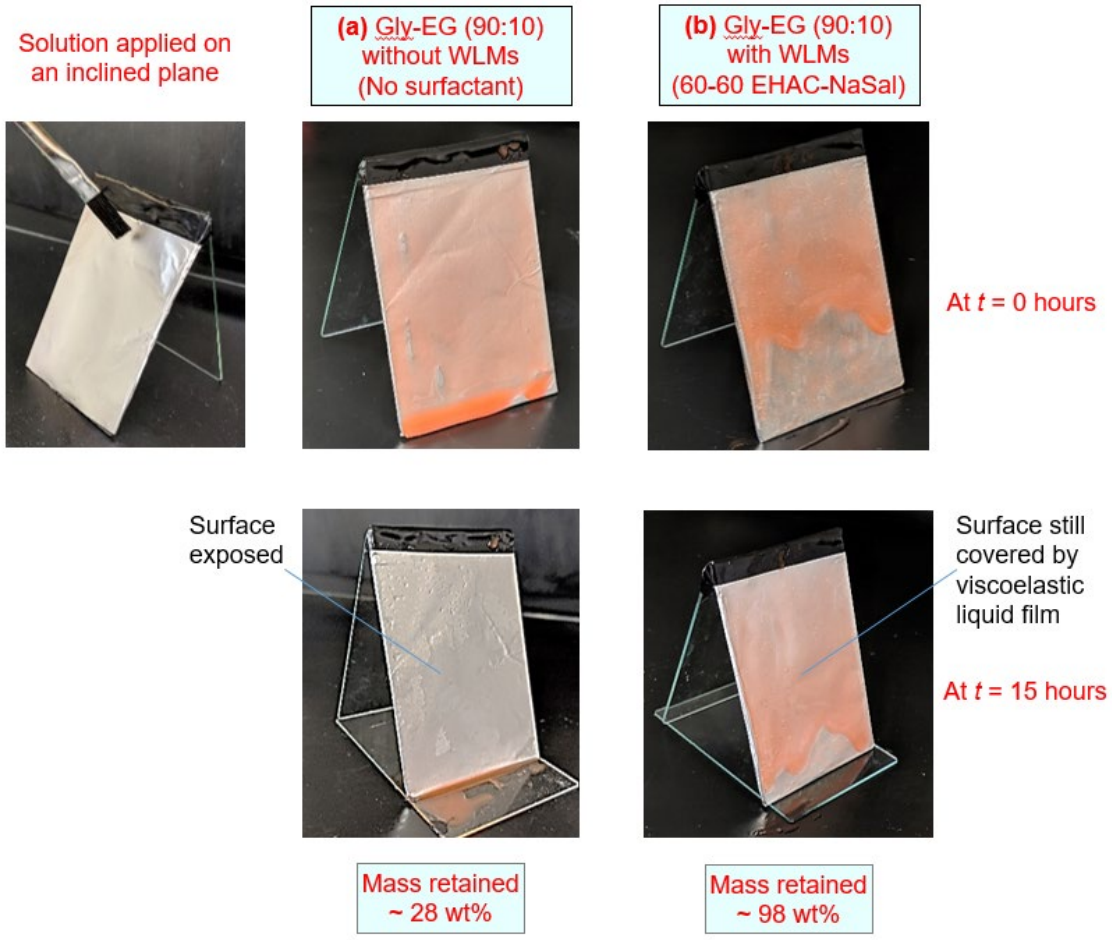

Figure 3.14. Experiment demonstrating the utility of viscoelastic WLMs in Gly-EG mixtures. A Gly-EG (90:10 v/v) mixture has a freezing point below –20°C. It can be rendered viscoelastic (due to the formation of WLMs) by adding EHAC-NaSal (60-60 mM). The bare solvent mixture and its viscoelastic counterpart are compared in a simple visual test. For this, inclined aluminum surfaces were created using glass slides covered with aluminum foil. Red iron oxide pigment (0.1 wt%) was added to the solutions for better visualization. Approximately 1 g of the respective samples were applied onto the surfaces using a paint brush (left top) at time $t = 0$, and the surfaces were then placed in the freezer ($T \sim -20$°C) for 15 hours. Due to the low freezing point of the solvent, neither sample froze into a solid. Results are shown in (a) for the Gly-EG solvent mixture and in (b) for the viscoelastic sample of WLMs in Gly-EG. In (a), the liquid initially coats the surface (top), but it quickly flows down the surface and collects in a pool below (bottom). The surface is thereby left exposed. Only 28% of the liquid mass was measured to remain on the surface. In (b), the viscoelastic sample coats the surface as a thin film (top), and this film persists even after 15 hours (bottom). 98% of the sample mass was found to remain on the surface.

Chapter 4

Rheology of Wormlike Micelles in Polar Solvents

4.1 Introduction

Wormlike micelles (WLMs) are long, flexible cylindrical chains formed by the self-assembly of surfactants.[4,5] They share many similarities with polymers in solution, including the ability to entangle and form transient networks, which makes the solution highly viscous and viscoelastic.[2,5,6,68,69] Most studies on WLMs have been conducted in water, and a typical formulation of aqueous WLMs consists of a cationic surfactant with a long tail (C_{16} or higher) combined with a salt.[6,18,31,34,37,40,48] WLMs in water tend to have diameters around 5 nm (the diameter is about twice the length of the surfactant tail) and contour (end-to-end) lengths L ranging from 100 to 5000 nm. This in turn implies aggregation numbers N_{agg} (*i.e.*, the number of molecules associated into a micelle) of a 1000 or higher.

In Chapter 3, we showed that WLMs could be formed in polar organic solvents such as glycerol and formamide. To our knowledge, this is the first report of WLMs in pure solvents of intermediate polarity. Previous studies in these solvents had only reported small micelles with N_{agg} of 100 or lower.[9-15,57] The system we studied contained a cationic surfactant with a long (C_{22}) tail, erucyl bis(hydroxyethyl)methyl ammonium chloride (EHAC) and an aromatic salt, sodium salicylate (NaSal). Equimolar mixtures of EHAC and NaSal gave rise to WLMs in glycerol, and the resulting samples were viscoelastic and flow-birefringent, as expected of WLMs. We also formed the WLMs in a

90-10 solvent mixture of glycerol and ethylene glycol, which had a freezing point well below 0°C. Thereby, we were able to confirm the existence of WLMs at sub-zero temperatures in these systems.

The focus of the current work is the rheology of WLMs in polar solvents like glycerol. In Chapter 3, we had briefly presented the dynamic rheology, i.e. plots of the elastic modulus (G') and viscous modulus (G'') against frequency ω, for one of those samples. The data exhibited several unusual features that made it distinct from the rheology of WLMs in water. From a rheological perspective, WLMs (in water) are considered a model viscoelastic fluid because their dynamic rheology closely follows the Maxwell model of viscoelasticity with a single relaxation time t_R.[6,20,31,34,68,70,71] In the case of a Maxwell fluid, G' and G'' show a single intersection at a crossover frequency ω_c, from which $t_R = 1/\omega_c$ can be estimated. In contrast, we find that WLMs in glycerol exhibit not one but two intersections of G' and G'' – at crossover frequencies of ω_{c1} and ω_{c2}. The entire dynamic frequency spectrum is thereby quite unique and can be demarcated into three regimes. The objective of this paper is to document the differences in rheology between WLMs in glycerol and water. We will then attempt to explain why the differences arise, i.e., to identify the unique attributes of WLMs in polar solvents.

4.2 Experimental Section

Materials: The surfactant erucyl bis(hydroxyethyl)methyl ammonium chloride (EHAC) was obtained from Akzo Nobel. EHAC was dried in a vacuum oven at room temperature before use. Sodium salicylate (NaSal) and glycerol (Gly) were obtained from Sigma Aldrich.

Sample Preparation. Stock solutions of EHAC and NaSal were prepared by adding weighed amounts of each into glycerol and heating to ~ 60°C on a hot plate under constant stirring for 4–5 h. After clear solutions were obtained, they were cooled and stored at room temperature. To prepare a sample with desired molar concentrations of surfactant and salt, the respective stock solutions were combined and diluted with the solvent. After vortex mixing, the sample was heated to 60°C for 10–15 min and then cooled to room temperature. Samples were left at room temperature for at least a day before any measurements.

Rheology. Rheological experiments were conducted on an AR2000 stress-controlled rheometer (TA Instruments). A cone-and-plate geometry (2° stainless steel cone) was used to perform the steady-shear and oscillatory-shear experiments. The temperature was controlled by a Peltier assembly on the rheometer, which employed a circulating fluid that was fed from a chiller. A 50-50 mixture of ethanol-water was used as the circulating fluid. Rheological experiments were conducted at temperatures ranging from 10 to 50°C. Dynamic frequency sweep experiments were conducted in the linear viscoelastic regime for each sample, which was determined from strain-sweep experiments.

4.3 Results and Discussion

4.3.1 Typical Rheology of WLMs in Water and Glycerol

WLMs in water are known to be single-t_R Maxwell fluids, even though the chains are highly polydisperse in their length.[31] The reason for this behavior was explained by Cates in 1987.[20] WLMs can release an applied stress in two ways. First, the chains can relax by reptation, much like polymers, and this is associated with a reptation time t_{rep}.[33] However, unlike polymers, WLM chains can also undergo reversible scission, i.e., they can break into segments, or broken segments can recombine into a whole. Micellar breaking provides a second mode for stress-relaxation in the case of WLMs that is absent for polymers, and this is associated with a breaking time t_{br}.[20] Cates predicted that, for the case of 'fast-breaking' WLMs with $t_{br} << t_{rep}$, the rheology would be that of a Maxwell fluid, and that the single relaxation time $t_R = \sqrt{t_{br} \cdot t_{rep}}$. Indeed, many WLM samples in water behave as Maxwell fluids and an example is shown in Figure 4.1a.[34] The sample consists of cationic surfactant cetyl pyridinium chloride (CPyCl, 100 mM) combined with 60 mM NaSal in water at 20 °C. The data, from a 1991 paper by Rehage and Hoffmann, were obtained using mechanical rheometry. Plots of G' and G'' vs. frequency ω are shown, and the lines through the data are fits to a single-t_R Maxwell model:[20]

$$G'(\omega) = \frac{G_p \omega^2 t_R^2}{1 + \omega^2 t_R^2};\ G''(\omega) = \frac{G_p \omega t_R}{1 + \omega^2 t_R^2} \tag{4.1}$$

where G_p is the plateau modulus, i.e., the value of G' at high ω. As expected, G' and G'' show a single intersection at a crossover frequency $\omega_c \sim 0.1$ rad/s, from which $t_R = 1/\omega_c$ can be estimated to be ~ 10 s.

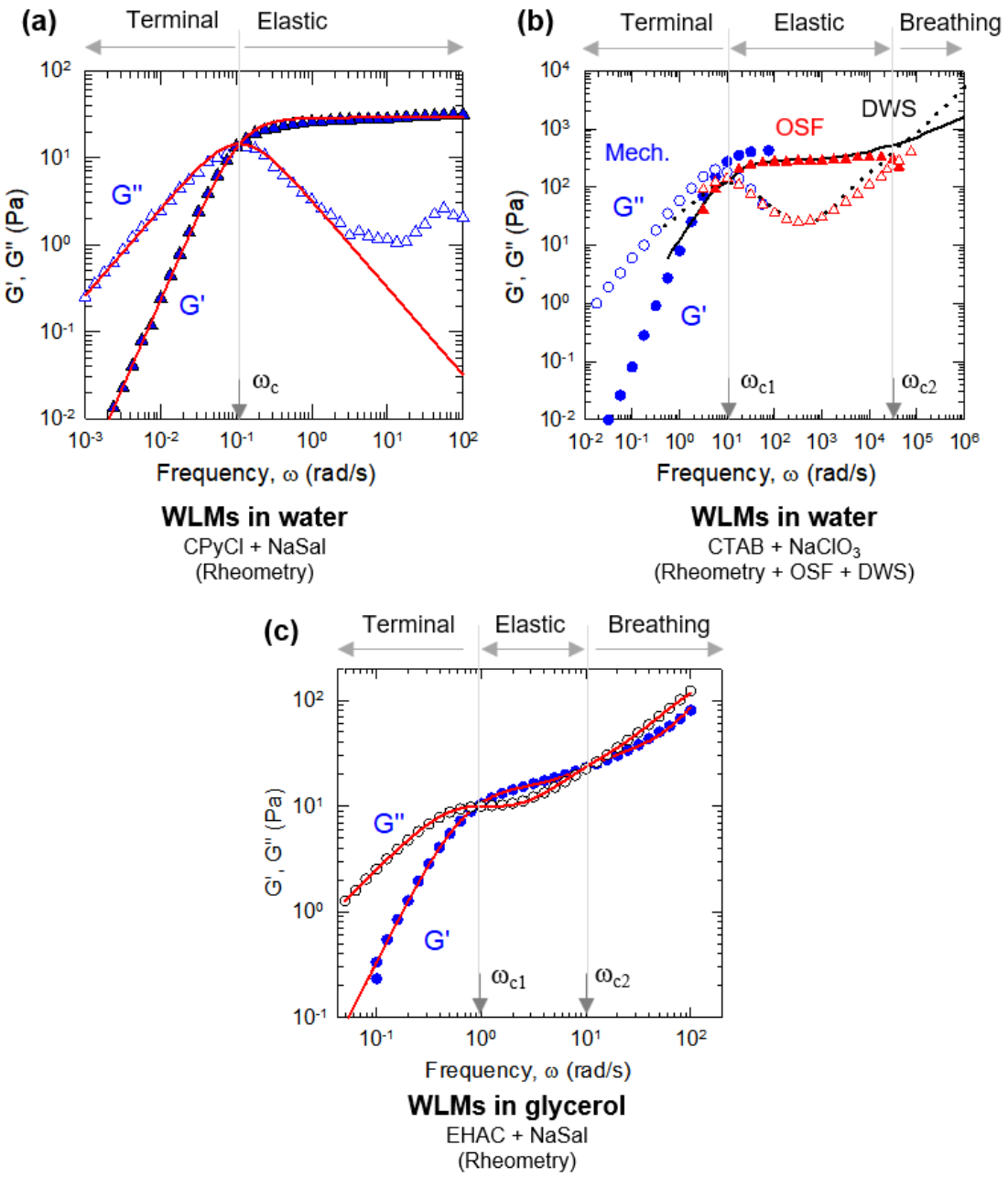

Figure 4.1. Comparing the dynamic rheology of WLMs in water and glycerol. In all cases, the elastic modulus G' and the viscous modulus G'' are plotted vs. frequency ω. (a) Typical WLMs in water (60 mM CPyCl + 60 mM NaSal) show the rheology of a single-t_R Maxwell fluid (lines are fits to this model).[34] The data are from rheometry. (b) Data for WLMs of 60 mM CTAB + 100 mM $NaClO_3$ in water are shown over a wide range of ω by combining measurements from rheometry, oscillatory squeeze flow (OSF) and diffusive wave spectroscopy (DWS).[19] In this case, G' and G'' cross twice, indicating three distinct regimes in the data. (c) Typical WLMs in glycerol (60 mM EHAC + 60 mM NaSal) show the same three regimes as in (b), but over a much narrower range of ω. The data are from rheometry. Lines are fits to a 4-mode Maxwell model.

The data in Figure 4.1a can be demarcated into two distinct regimes based on ω. For $\omega < \omega_c$, there is a 'terminal' regime where $G'' > G'$, indicating viscous behavior, with the slopes of the moduli being 1 and 2 on the log-log plot.[34,35] In this regime, the timescales are long enough for the WLMs to disengage from their transient network and relax slowly. At shorter timescales, i.e., for $\omega > \omega_c$, there is an 'elastic' regime, where G' reaches a plateau (G_p) and $G' > G''$. At these timescales, the rheology reflects the intact network of WLMs connected by entanglements. Midway through this elastic regime, G'' reaches a minimum and then begins an upturn at higher ω. However, in mechanical rheometry, the data are restricted to $\omega \sim 100$ rad/s and hence data for G' and G'' at higher ω cannot be obtained.[18,34]

WLM rheology at higher ω has been addressed in recent years,[19,72-74] and a typical dataset is shown in Figure 4.1b. The sample consists of the cationic surfactant cetyl trimethylammonium bromide (CTAB, 60 mM) combined with sodium chlorate ($NaClO_3$, 100 mM) in water. This data is from a 2010 paper by Oelschlaeger and were obtained by superposing measurements from three techniques: mechanical rheometry (at low ω), oscillatory squeeze flow (OSF, higher ω), and diffusive wave spectroscopy (DWS, highest ω).[19] We again note that there is a terminal regime at low ω (where $G'' > G'$), and then an elastic regime at medium ω, where $G' = G_p$ while G'' goes through a minimum and an upturn. There are two crossover frequencies at which G' and G'' intersect: the first occurs at $\omega_{c1} \sim 10$ rad/s and marks the end of the terminal regime, while the second

occurs at $\omega_{c2} \sim 10^5$ rad/s and marks the end of the elastic regime. We can conclude that, for WLMs in water, there will be two crossover frequencies that are widely separated by several decades.[19,35,75]

The third regime at $\omega > \omega_{c2}$ can be termed the 'breathing' regime.[33,35,71,73,76] At these very short timescales, the rheology reflects the dynamics of individual chain segments in an intact network. The chain segments will relax only via bending or 'breathing' motions (also termed 'Rouse-Zimm' modes). Note that in the breathing regime, both moduli are functions of ω, with $G'' > G'$, much like in the terminal regime. The breathing regime has been documented for entangled polymer solutions and melts.[33,77] For these systems, the technique of time-temperature superposition (TTS) is used to access a wide range of ω.[35,78] However, TTS cannot be used for WLMs because the WLM length changes with temperature. Thus, to cover all three regimes for WLMs, a wide range of ω must be accessed *at a single temperature*, and for this can be done only by resorting to advanced techniques like OSF and DWS, not by mechanical rheometry. For instance, the ω axis in Figure 4.1b spans from 10^{-2} to 10^6 rad/s, i.e., across eight decades.

In contrast, consider a typical plot of G' and G'' vs. ω for WLMs in glycerol, as shown in Figure 4.1c. The sample consists of EHAC (60 mM) combined with NaSal (60 mM), and the entire dataset is from mechanical rheometry. In this case, over a ω range of just three decades (10^{-1} to 10^2 rad/s) we find all the three regimes noted in Figure 4.1b: i.e., the terminal, elastic, and breathing regimes. There are two crossover

frequencies at which G' and G'' intersect: $\omega_{c1} \sim 1$ rad/s and $\omega_{c2} \sim 10$ rad/s. This means that the elastic regime spans only one decade in ω, and in fact G' keeps increasing in this regime instead of reaching a plateau. Also, the transition to the breathing regime occurs at a frequency that is 10^4 times lower than for the aqueous WLMs in Figure 4.1b, thereby allowing this regime to be accessed easily by rheometry. Clearly, the rheology of WLMs in glycerol is very different from that of aqueous WLMs. Incidentally, the lines through the data in Figure 4.1c are fits to a generalized Maxwell model that includes 4 modes, each with a different G_p and t_R.

4.3.2 Rheology of WLMs in Glycerol as a Function of Temperature

The data in Figure 4.1c are for a 60/60 EHAC/NaSal sample in glycerol at 25°C. It is useful to examine the dynamic rheological data for the above sample as a function of temperature (T). Data were collected on this sample from 10 to 50°C in increments of 1°C, and a subset of this data from 25 to 40°C are shown in a single plot in Figure 4.2a. As T increases, the contour length of the WLMs decreases exponentially, and hence, the WLMs relax exponentially faster (in turn, the zero-shear viscosity of the WLM solutions also plummets). This explains the broad trend in Figure 4.2a where both G' and G'' shift towards higher ω with increasing T. A second trend is that the terminal regime is more pronounced at higher T while the elastic and breathing regimes are more apparent at lower T. In the terminal regime, $G'' > G'$, with the slopes of G' and G'' being slopes close to 2 and 1 respectively, as expected for typical WLMs and polymeric fluids. After the moduli cross at ω_{c1}, G' overtakes G'' in the elastic regime. Thereafter, the moduli cross again at ω_{c2}, and $G'' > G'$ in the breathing regime. From the crossover frequencies at each

T, we can calculate $t_{R1} = 1/\omega_{c1}$, which is the 'long' relaxation time, and $t_{R2} = 1/\omega_{c2}$, which is the 'short' relaxation time.

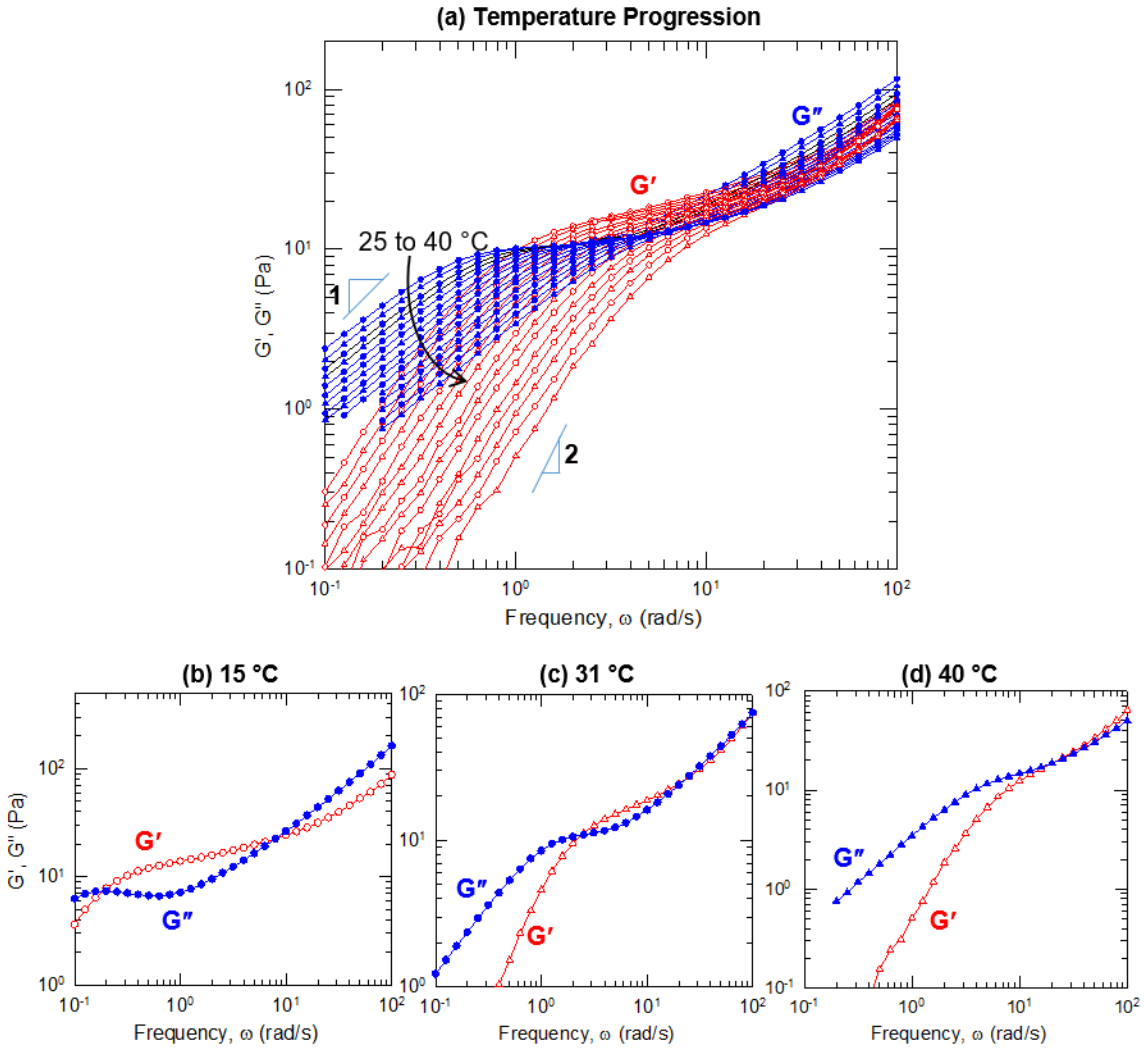

Figure 4.2. Dynamic rheology of WLMs in glycerol at various temperatures. In all cases, the elastic modulus G' and the viscous modulus G'' are plotted vs. frequency ω for a sample of 60 mM EHAC + 60 mM NaSal. (a) Data over a temperature range from 25 to 40°C in increments of 1°C. The moduli at specific temperatures are shown to indicate specific patterns in the data: (b) 15°C; (c) 31°C; and (d) 40°C.

Data at specific temperatures are highlighted in Figure 4.2b to 4.2d, and these reflect different prototypical shapes (or patterns) for the G' and G'' curves. At 15°C

(Figure 4.2b), G' and G'' cross twice, much like in the case of Figure 4.1c. This pattern persists between 15 and 30°C. Between the crossover points, the curves form a loop, and the width (i.e., range of ω) as well as the area of this loop decreases with increasing T. The curves at 31°C are particularly interesting (Figure 4.2c): in this case, the moduli cross *three times*, with two of these occurring in the breathing regime. This unusual pattern in the dynamic spectra is observed over a short range of temperatures: from 31 to 33°C. For $T \geq 34$°C, G' and G'' cross just once, as shown for the case of 40°C in Figure 4.2d. At this point, the loop between G' and G'' has vanished, and there appears to be a direct jump from the terminal to the breathing regime. The lack of an elastic regime at these higher T may imply that the WLMs are not long enough by this point to form an entangled network. Note that the moduli in the breathing regime are very close to each other (nearly overlap) over a range of ω.

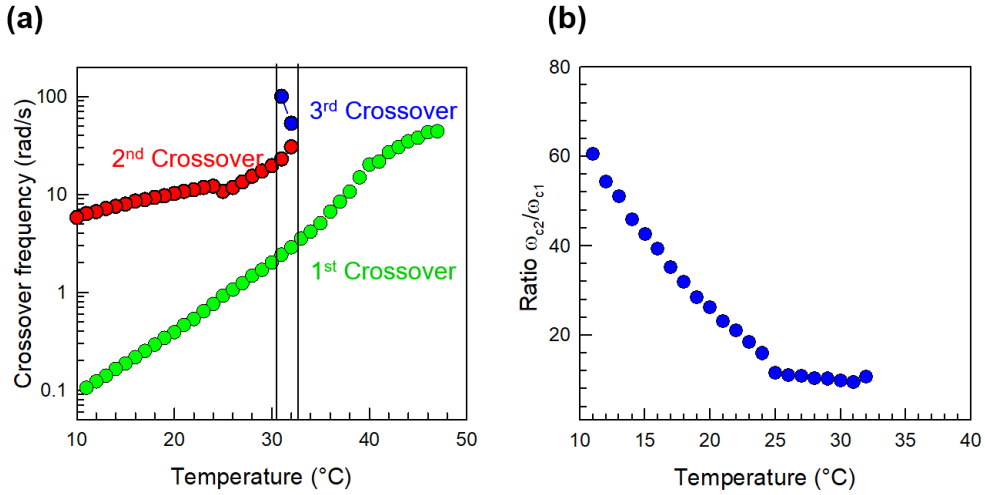

Figure 4.3. Parameters extracted from the temperature-dependent rheology of WLMs in glycerol. The parameters are from Figure 4.2, which shows data at various temperatures for a sample of 60 mM EHAC + 60 mM NaSal in glycerol. (a) Crossover frequencies ω_{c1}, ω_{c2}, and ω_{c3} as a function of temperature. (b) Ratio of ω_{c2}/ω_{c1} as a function of temperature.

Parameters extracted from the data in Figure 4.2 are shown in Figure 4.3. The crossover frequencies ω_{c1}, ω_{c2}, and ω_{c3} are plotted vs. T on a log-linear plot in Figure 4.3a. A linear relationship is found for both ω_{c1} and ω_{c2} over the range of T. This means that the corresponding relaxation times t_{R1} and t_{R2} decrease exponentially with T. ω_{c2} does not exist above 33°C and it is only in the vicinity of this temperature that ω_{c3} is measured. Another parameter of interest is the pseudo-plateau modulus G_p. Although G' does not reach a true plateau, G_p can be determined as the value of G' when the loss tangent $\tan\delta = G''/G'$ reaches a minimum.[77] We find that G_p is nearly constant (13-16 Pa) from 10 to 33°C (beyond this T, the elastic regime is absent and therefore G_p is undefined).

The implications of the above results are the following. It is known that G_p inversely correlates with the mesh size of the transient WLM network.[72,73] Thus, the constancy of G_p means that the network mesh size is constant from 10 to 33°C. Also, provided the WLMs are long enough to entangle, G_p will be independent of their contour length L. In other words, each WLM will be entangled many times with other WLMs. The distance along the micellar network between any two entanglement points is called the entanglement length L_e. A parameter that characterizes chain entanglement is the average number of entanglements per WLM chain, $Z = L/L_e$.[75] Recent studies have correlated Z with the ratio of ω_{c2}/ω_{c1}.[33] We have computed the above ratio of frequencies and plotted it against T in Figure 4.3b. The results reveal a steady, linear decrease in this ratio – from 60 at 10°C to 15 at 25°C – and thereafter the ratio remains constant until 33°C. This suggests that the WLMs are highly entangled (high Z, i.e., $L >> L_e$) at low T

when the WLMs are long. Increasing T decreases L and thus decreases Z. This analysis also reveals one important difference between WLMs in glycerol and those in water. For WLMs in glycerol, the highest ratio of ω_{c2}/ω_{c1} is about 60. For WLMs in water, the ratio of ω_{c2}/ω_{c1} can be 10^4 or higher, indicating a much higher number of entanglements per chain. From these results, we can infer that WLMs in glycerol are much shorter (and thus have far fewer entanglements per chain) compared to WLMs in water.

A common way to show the Maxwellian behavior of WLMs in water is by using the Cole-Cole plot, which is a linear plot of G'' vs. G'.[70,71] The Cole-Cole plot for a Maxwell fluid will be a perfect semicircle, with the diameter of the semicircle being the plateau modulus G_p. We had previously shown the Maxwellian rheology of WLMs in water in Figure 4.1a. The Cole-Cole plot of this data is shown in Figure 4.4a, and indeed it is close to a semicircle. For comparison, the data for WLMs in glycerol at 25°C (from Figure 4.1c) are shown on the same graph. In this case, the plot deviates from the semicircular shape and extends as a near-straight line. Data for the glycerol sample at various temperatures are plotted in the Cole-Cole format in Figure 4.4b. As T is increased, the plots initially follow semicircular arcs (see inset), with the diameter of the arc being higher at higher T. However, the plots then deviate from the arc and extend as straight lines. These lines fan out from the initial region, and the slopes of the lines decrease with increasing T.

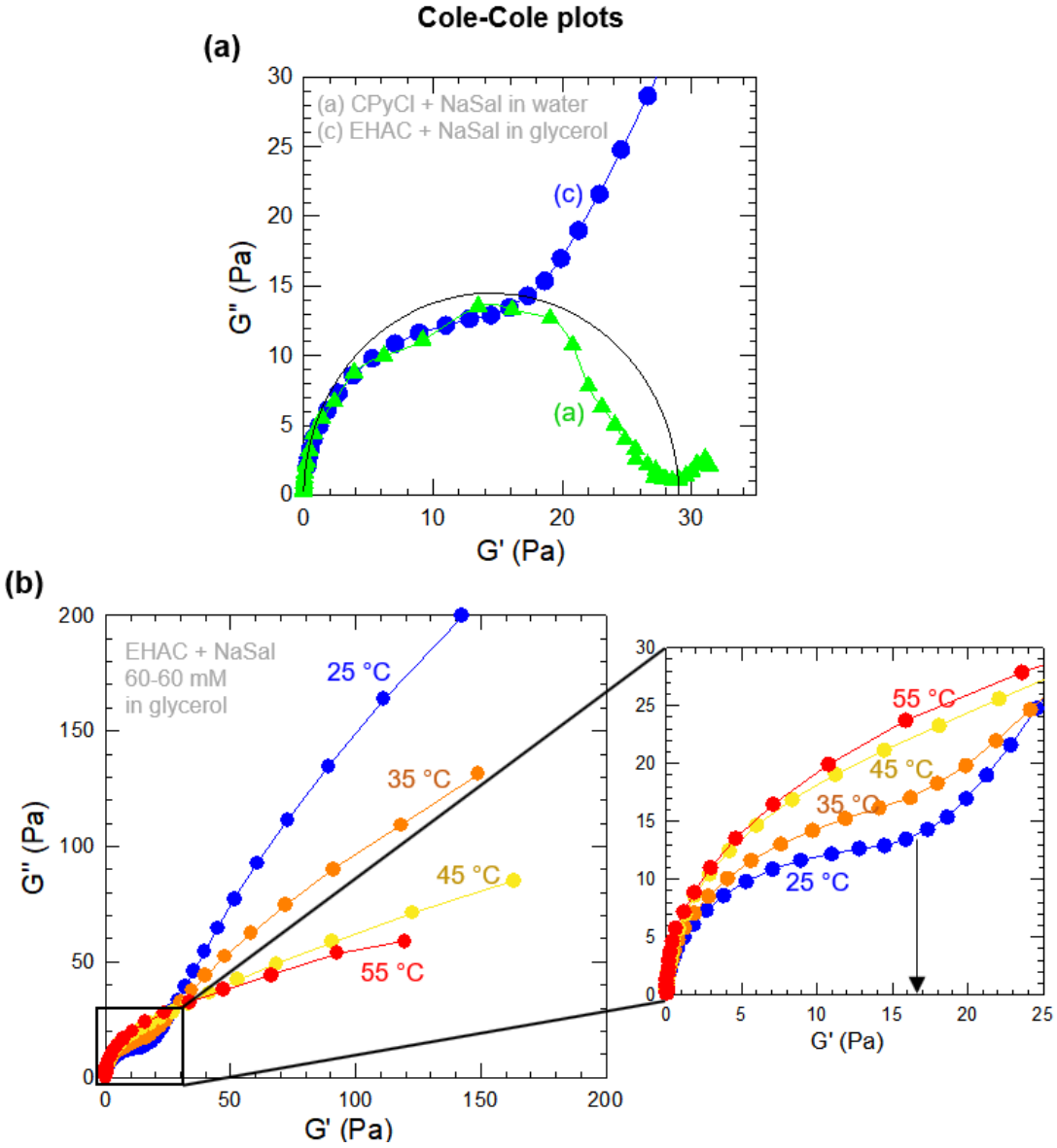

Figure 4.4. Cole-Cole plots for WLMs in water and glycerol. A Cole-Cole plot is one of *G″* vs. *G′*, with both axes on a linear scale. (a) Comparison via Cole-Cole plots at 25°C of WLMs in water (data from Figure 4.1a) and WLMs in glycerol (data from Figure 4.1c). The aqueous sample is a Maxwell fluid, which corresponds to a semicircle on the Cole-Cole plot. The glycerol sample deviates from the semicircular arc and extends as a straight line. (b) Cole-Cole plots for WLMs in glycerol at various temperatures (data from Figure 4.2a). The plots fan out in a series of straight lines at high moduli. The inset shows the initial portion of the graph, where the order of semicircular arcs is reversed.

4.3.3 Rheology of WLMs in Glycerol as a Function of Salt

In the previous section, we described the rheology of WLMs in glycerol as a function of temperature. Many other variables can be used to alter the rheology of such WLMs, including the concentration of the EHAC surfactant, the concentration of salt (NaSal), and the type of salt. Regardless of the variable studied, the unusual rheology with two crossovers of G' and G'' is seen for a range of samples. Here, we focus on the NaSal concentration and illustrate how it affects the rheology at a single temperature of 25°C (Figure 4.5). The EHAC concentration is fixed at 60 mM and only NaSal is varied. Until about 30 mM NaSal, the response is purely viscous (Figure 4.5a), with only the terminal region ($G'' > G'$ at all ω) being observed in the data. At 42 mM NaSal (Figure 4.5b), the response becomes viscoelastic, with G' and G'' overlapping over an intermediate range of ω. At 60 mM NaSal, the double-crossovers are observed, which is the pattern discussed in detail above. At this NaSal concentration, the salt and surfactant are at equimolar levels, and WLM formation in glycerol is maximized. This aspect has been discussed in detail in Chapter 3; note that the zero-shear viscosity η_0 reaches a maximum as a function of salt at this concentration. Accordingly, for NaSal > 60 mM, there is a reduction in viscoelasticity, i.e., the loop area between G' and G'' decreases and eventually drops to zero. An example is shown in Figure 4.5d for 78 mM NaSal: here, G' and G'' are separate curves that do not cross. Note the similarity between the curves in Figure 4.5d and those in Figure 4.2d for a lower NaSal but a higher temperature.

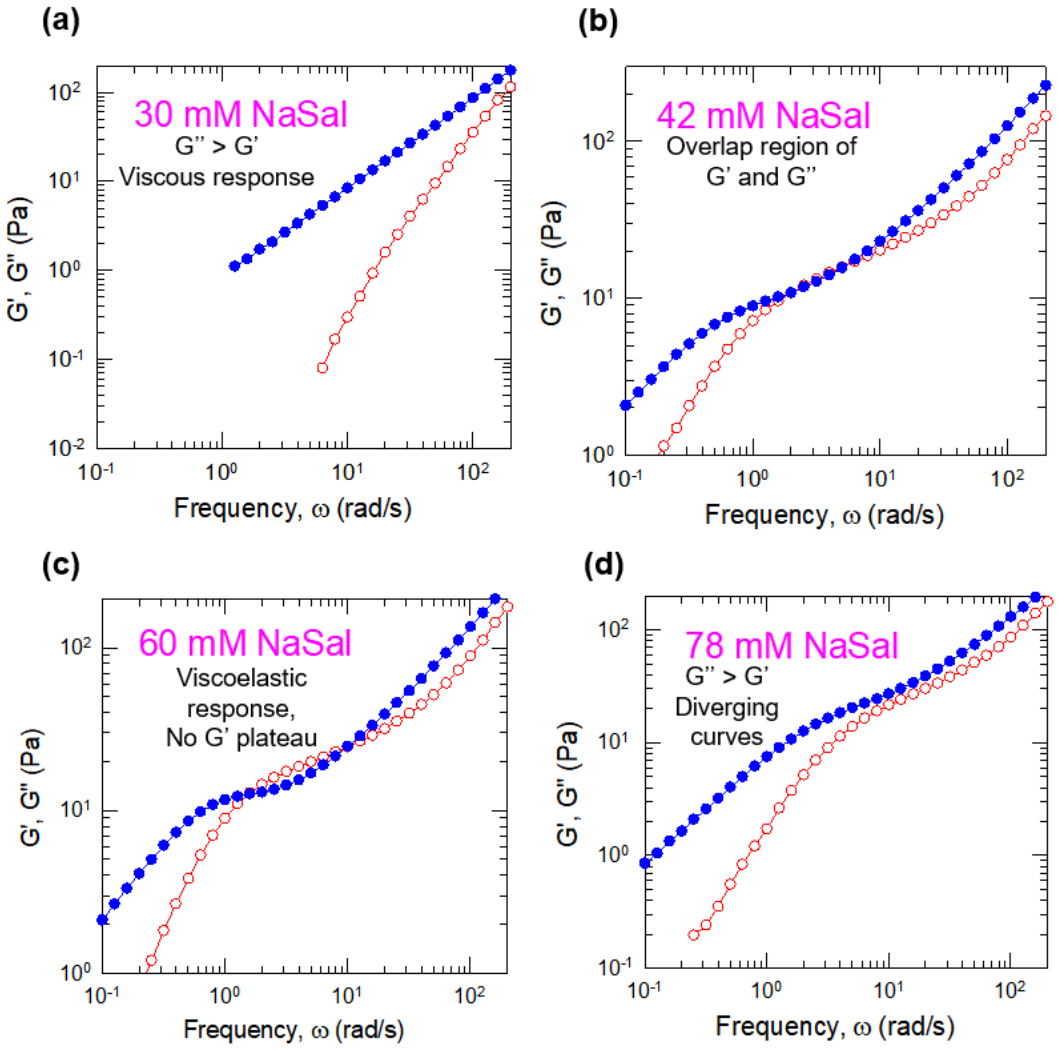

Figure 4.5. Dynamic rheology of WLMs in glycerol at various salt concentrations. In all cases, the elastic modulus G' and the viscous modulus G'' are plotted vs. frequency ω. All experiments were done at 25°C. The samples contain 60 mM EHAC and varying concentrations of salt (NaSal): (a) 30 mM; (b) 42 mM; (c) 60 mM; (d) 78 mM.

4.3.4 Differences Between WLMs in Glycerol and Water

We have demonstrated that WLMs in glycerol exhibit very different responses in dynamic rheology compared to WLMs in water. The differences can be summarized as follows:

(1) WLMs in water are Maxwell fluids with a single t_R, and this manifests as a semicircle on a Cole-Cole plot.[70] WLMs in glycerol are ***not*** **Maxwell fluids**; rather they exhibit a spectrum of relaxation times. Their response deviates sharply from a semicircle on a Cole-Cole plot.

(2) WLMs in water exhibit a single crossover of G' and G'' (at ω_{c1}) in the ω-range accessible by mechanical rheometry.[18,37] WLMs in glycerol exhibit **two crossovers** of G' and G'' (at ω_{c1} and ω_{c2}) in the ω-range accessible by mechanical rheometry.

(3) WLMs in water exhibit a second crossover of G' and G'' at $\omega_{c2} \sim 10^5$ rad/s, above which is the 'breathing regime', corresponding to segmental motion of the chains.[19,72,75] Data at such high ω can be recorded only by advanced techniques like OSF and DWS. The ratio of $\omega_{c2}/\omega_{c1}$is $\sim 10^4$ for these WLMs. In contrast, for WLMs in glycerol, ω_{c2} occurs around 10 rad/s, i.e., the breathing regime is reached at much lower ω, and the **ratio of ω_{c2}/ω_{c1} is ~ 10**.

Why do these differences arise, and what does it tell us about WLMs in glycerol? To understand the origin of these differences, we need to discuss how glycerol differs from water as a solvent. There are two factors in this regard: (a) glycerol is much more

viscous than water; and (b) the propensity of surfactants to self-assemble into micelles is much lower in glycerol than in water.[10,11] With regard to (b), self-assembly in water is driven by the hydrophobic effect, which is a strong interaction mainly due to the unique properties of water. In comparison, the driving force for self-assembly in glycerol is the 'solvophobic effect', which is much weaker.[12,28,29,58] This is why there are no examples of WLMs in glycerol apart from our own study in Chapter 3. Due to the weaker driving force, **WLMs in glycerol are likely to be shorter**, i.e., have lower contour lengths L compared to WLMs in water. The shorter WLMs will also have fewer entanglements per chain (lower $Z = L/L_e$), which explains why the ratio of $\omega_{c2}/\omega_{c1}$is much lower in glycerol than in water.

We also hypothesize a second difference: that the WLMs in glycerol are much less dynamic, i.e., they will break and recombine much less frequently compared to WLMs in water. In other words, the breaking time t_{br} for WLMs in glycerol will be much greater than the t_{br} for WLMs in water. The reason for this difference lies in the higher viscosity of glycerol, which is about 900 times that of water. For a WLM to break, surfactant unimers will have to diffuse out of a micelle in unison or in close succession. However, the timescale for such diffusion will be quite long because the solvent is so viscous. Thus, while individual surfactants may temporarily leave the WLM, the micelle will still not break, or its t_{br} will be very high. If our hypothesis is correct, WLMs in glycerol will never be in the fast breaking limit ($t_{br} << t_{rep}$) and this can explain why their rheology is never Maxwellian. The point then is that **WLMs in glycerol behave, not like micelles, but like polymers** – due to the 'unbreakable' nature of the chains.

The third key aspect is regarding the role of the viscous solvent towards the rheology of the WLMs in glycerol. As noted earlier, when the WLMs are in the breathing regime at high ω, the chains will undergo segmental motions.[19] Due to the viscous nature of glycerol, these segmental motions will be dissipative ($G'' > G'$), and moreover the **solvent will influence the rheology at these high ω.** We suggest that there are two factors that lead to the double-crossover of G' and G'' over a narrow range of ω. First, the WLMs are relatively short and weakly entangled – hence their terminal relaxation time is low (and in turn, ω_{c1} is quite high at ~ 1 rad/s). Second, the influence of the viscous solvent at high ω may push the second crossover within the ω-window of mechanical rheometry, i.e., ω_{c2} ~ 10 rad/s. In other words, if a sample only had short WLMs, but the solvent was of low-viscosity (like water), we may only observe a single crossover of the moduli. It is the glycerol that ensures the unusual double-crossover of G' and G'' within just a decade of ω.

4.4 Conclusions

We have demonstrated that the dynamic rheology of WLMs in glycerol is very different from that of WLMs in water. WLMs in glycerol are not Maxwell fluids; on the contrary, they exhibit a double-crossover of G' and G'' (at ω_{c1} and ω_{c2}), with the entire set of data falling within the ω-window accessible by rheometry (10^{-2} to 10^{2} rad/s). At frequencies above ω_{c2}, the rheology is dominated by the segmental motion of chains in the 'breathing regime' – this regime has been rarely studied for WLMs, although it is well-documented for polymer solutions and melts. We believe that glycerol, a solvent

that is much more viscous than water, exerts a key influence in pushing ω_{c2} to relatively low values around 10 rad/s; in comparison, ω_{c2} for WLMs in water is expected to fall around 10^5 rad/s. Our rheological studies also reveal key clues about the WLMs in glycerol. These WLMs are expected to be shorter and weakly entangled compared to WLMs in water. Moreover, in terms of their dynamics, WLMs in glycerol are expected to be similar to polymers – i.e., the chains will remain intact and not break and re-form frequently – which would explain why the samples do not behave like Maxwell fluids.

Chapter 5

Vesicles in Polar Organic Solvents

5.1 Introduction

In Chapters 3 and 4, we discussed the self-assembly of wormlike micelles (WLMs) in polar organic solvents. In this chapter, we turn our attention to the self-assembly of *vesicles* in the same solvents. Vesicles are spherical nanostructures formed by the self-assembly of amphiphiles that have a critical packing parameter CPP = 1 (Figure 5.1).[1] The CPP was defined in Chapter 2, and a CPP of 1 means that the amphiphiles have nearly equal cross-sectional areas of their head and tail regions, i.e., they are cylinder-shaped. This is achieved typically with lipids, which are biological amphiphiles with two tails (Figure 5.1). Lipids form the membranes of cells in our body, and each cell membrane is a *bilayer* of the lipids, where the lipids are arranged in a head-tail-tail-head fashion.[7] Vesicles formed from lipids (also called liposomes) have a similar bilayer-shell (thickness ~ 5 nm) that enclose a core of the solvent. The overall diameter of vesicles with a single bilayer (i.e., unilamellar vesicles) is ~ 100 nm.[1,3,79] Vesicles in water have been of great interest because their aqueous core can encapsulate drugs, which can be released through the shell. Thus, vesicles serve as nanocontainers for drug delivery.

Can vesicles be formed in polar organic solvents with high dielectric constants such as glycerol, formamide and ethylene glycol? These solvents can support self-

assembly due to solvophobic effects, and there is evidence for the formation of spherical surfactant micelles in the three solvents named above.[9-12,59] To our knowledge, however, there is no prior evidence for the formation of vesicles in these solvents. In fact, we have not found any reports on lipids at semidilute concentrations (< 10 wt%) in polar solvents.[80-83] We did find one study by Friberg *et. al.* from 1985 that focused on concentrated mixtures of lipids in glycerol (> 40 wt% lipid).[84] This study did not mention vesicles; instead it focused on the lyotropic liquid crystalline phases (lamellar, hexagonal and cubic) that arise at higher lipid concentrations. Recently, there have been a few studies done with surfactants in ionic liquids, and in one case, giant vesicles (> 10 μm) were reported.[16,17,85]

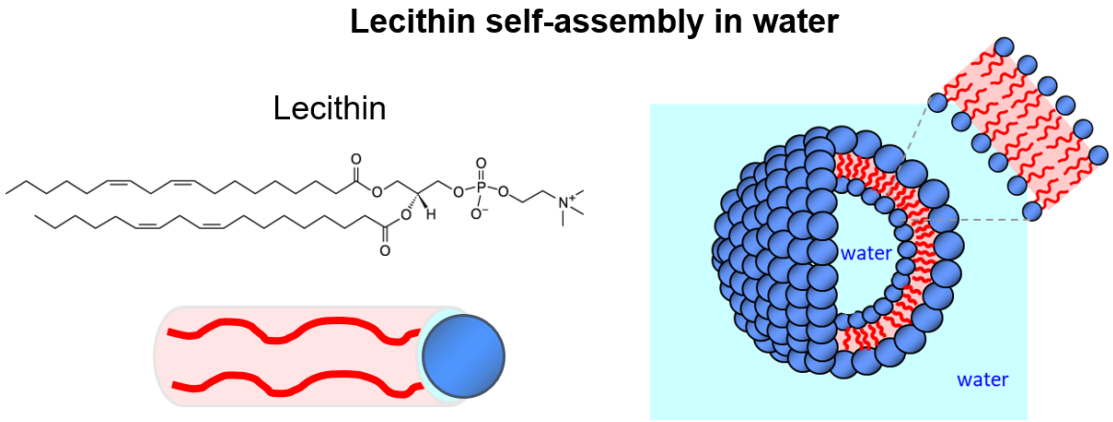

Figure 5.1. Lecithin self-assembly in water. Lecithin or L-α-phosphatidylcholine consists of two unsaturated non-polar tails (red) and a polar headgroup (blue). In water, lecithin self-assembles to form spherical vesicles with an aqueous core and lipid bilayer.

Here, we study the self-assembly of lecithin, a common phospholipid extracted from soybeans (Figure 5.1), in polar organic solvents such as glycerol, ethylene glycol and formamide. Lecithin has a zwitterionic phosphocholine head, and its self-assembly

into vesicles has been extensively studied in water, typically at concentrations ~ 1-2 wt%. In liquids like glycerol, we show that lecithin forms nanoscale vesicles over a wide range of concentrations (~ 2 to 15 wt%). At the higher end of this concentration range, the samples are gel-like and birefringent at rest. The birefringence is particularly interesting and unusual: it is not exhibited by vesicles in water, and it is associated with liquid crystalline phases. We will attempt to explain why these properties arise. While our study is focused on fundamental aspects, the systems described here could also be intriguing from a practical standpoint. For example, glycerol is widely used as a cryo-protectant in biological systems, i.e., to keep cells in a viable state at low temperatures.[86,87] Glycerol is also a hydrating agent for skin in cosmetics, while ethylene glycol is used in antifreeze formulations.[79] Thus, the ability to form vesicles and vesicle gels in these liquids could potentially be useful in pharmaceutics, cosmetics, and as lubricants or antifreeze agents for low temperatures.[21,22]

5.2 Experimental Section

Materials: Lecithin (soy-phosphatidylcholine (95% purity) was purchased from Avanti Polar Lipids. The solvents glycerol, ethylene glycol and formamide were obtained from Sigma Aldrich, while deuterated (d-8) glycerol ($C_3D_8O_3$) was from Cambridge Isotopes. Ultrapure deionized (DI) water from a Millipore filtration system was used to prepare aqueous samples.

Sample Preparation. Vesicles in water-solvent mixtures were prepared by a thin-film hydration method. Lecithin was dissolved in a 50-50 chloroform-methanol mixture, and

then the solvent was evaporated under nitrogen to yield a thin film of the lipid. The film was then dried in a lyophilizer for 8-10 h and then contacted with the water-solvent mixture. Finally, the solution was sonicated using a Branson tip sonicator for 3-4 min. Vesicles in pure solvents like glycerol were prepared by adding weighted amounts of lecithin and glycerol in a vial and heating to ~ 60°C on a hot plate under constant stirring for ~24 h. After clear solutions were obtained, they were cooled and stored at room temperature. Samples were left at room temperature for at least a day before any measurements.

Rheology. Rheological experiments were conducted on an AR2000 stress-controlled rheometer (TA Instruments). A cone-and-plate geometry (2° stainless steel cone) was used to perform the steady-shear and oscillatory-shear experiments. The temperature was controlled by a Peltier assembly on the rheometer, which employed a circulating fluid that was fed from a chiller. Rheological experiments were conducted at temperatures ranging from 25 to 65°C. Dynamic frequency sweep experiments were conducted in the linear viscoelastic regime for each sample, which was determined from strain-sweep experiments.

Cryogenic Scanning Electron Microscopy (Cryo-SEM). A Hitachi S-4800 field emission SEM with an operating voltage of 3 kV was used. Samples were placed into rivets mounted onto the cryo-SEM sample holder. This was then plunged into slushed liquid nitrogen for vitrification of the solvent. Samples were then fractured at −130°C using a flat-edge cold knife and the solvent was then sublimated at −95°C for 15 min.

The temperature was lowered back to −130°C, and the sample was then sputtered with a gold−palladium composite at 10 mA for 132 s before imaging.

Small Angle Neutron Scattering. SANS experiments were performed at the National Institute of Standards and Technology (NIST), Gaithersburg, MD on the NG-B (30 m) beamline. Neutrons with a wavelength λ of 6 Å were selected and the range of wave-vector q accessed was from 0.004 to 0.4 $Å^{-1}$. The sample holders were 1 mm titanium cells with quartz windows. The scattering data were reduced using IGOR-Pro software and were corrected to obtain an absolute scale of scattering intensity using NIST calibration standards. SANS fitting was done using the SasView software.

Small Angle X-ray Scattering. SAXS experiment was conducted on a Xenocs Xeuss 2.0 SAXS/WAXS machine with a Cu source (λ = 1.54 Å) for X-ray generation. A Pilatus 300K detector is used for 2D scattering pattern collection. The sample-to-detector distance (SDD) was adjusted to collect scattering data in a desired q-range.

Dynamic Light Scattering. The size of vesicles was determined using a Photocor-FC light scattering instrument used at 90°. This instrument was equipped with a 5 mW laser source at 633 nm and a logarithmic correlator was used.

UV-Vis Spectroscopy. A Varian Cary 50 UV-Vis spectrophotometer was used to monitor the absorbance of the vesicle solutions at 500 nm. The optical density is calculated from absorbance values and reported as OD500.

5.3 Results and Discussion

5.3.1 Lecithin in Water-Solvent Mixtures

First, we consider vesicle formation in water-solvent mixtures. Lipids like lecithin are known to form unilamellar vesicles in water.[79] What happens if water is gradually replaced by a polar solvent like glycerol? To study this, we prepared vesicles of 2% lecithin in water as well as in water/glycerol mixtures. The samples were first characterized by dynamic light scattering (DLS), which yields the hydrodynamic diameter (D_h) of the vesicles. The vesicles in water had a D_h of about 160 nm, which is consistent with previous studies from our lab. When water was replaced with water/glycerol mixtures, there were modest changes in the vesicle diameter. In the case of a 50/50 water/glycerol sample, a D_h of about 110 nm was measured by DLS.

Photos of sample vials containing 2% lecithin in water/glycerol weight ratios from 50/50 to 0/100 are shown in Figure 5.1a. In this range of solvent compositions, some differences between the samples are apparent from visual observations. It is well-known that vesicle solutions appear turbid (bluish or bluish-white in color) due to the scattering of light by the nanoscale vesicles. If the vesicles are smaller or are present at a lower concentration, the sample will appear less turbid. Here, we find that the turbidity decreases as the glycerol content increases. Samples at 20/80, 10/90 and 0/100 water/glycerol are almost perfectly clear, i.e., they scatter light to a much lower extent. This suggests that the vesicles get solubilized if glycerol is present at large amounts.

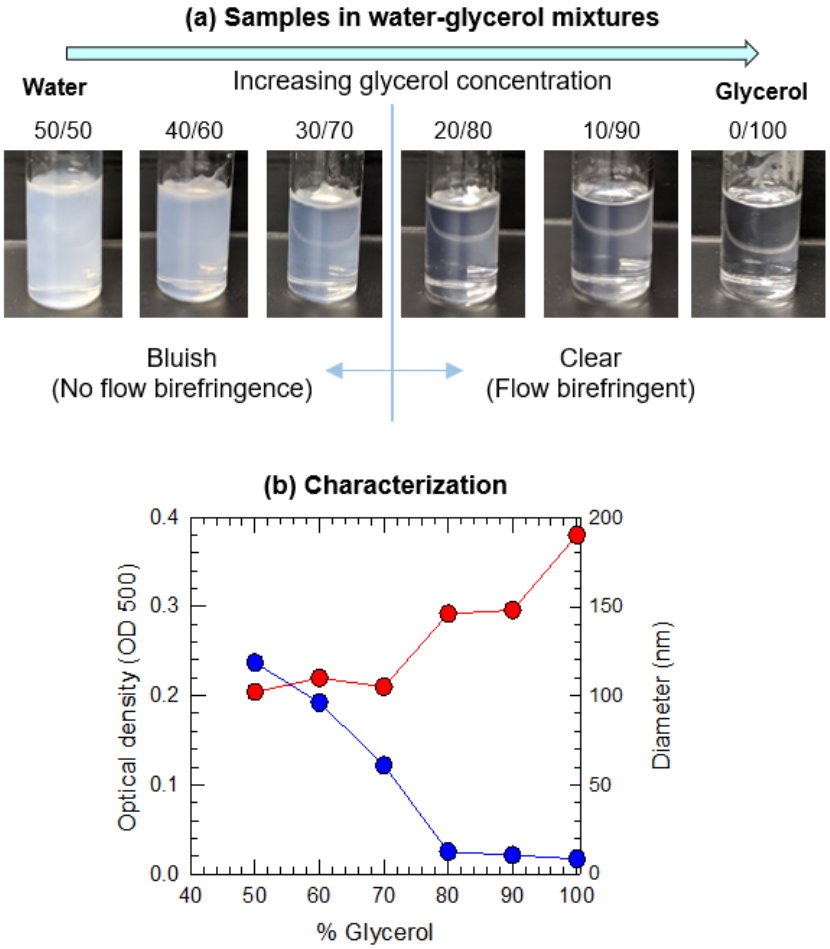

Figure 5.2. Lecithin self-assembly in water-solvent mixtures. (a) Sample images for lecithin vesicles (2 wt%) in water-glycerol mixtures are shown here. From left to right, the water-glycerol content changes from 50/50 to 0/100. Samples from 50/50 to 30/70 appear bluish and do not show flow birefringence, whereas samples from 20/80 to 0/100 appear clear and exhibit flow birefringence. (b) The optical density and diameter of the lecithin samples are shown here for increasing glycerol content.

An unusual observation about the 20/80, 10/90 and 0/100 samples is that they exhibit flow-birefringence. Birefringence implies that the sample has different refractive indices along perpendicular directions. To assess birefringence, samples are viewed under crossed polarizer plates. The above samples do not show birefringence at rest, but when the vials are shaken, streaks of light become visible in them, and this is called flow-birefringence. Vesicle samples are not expected to be flow-birefringent, and indeed it is

not seen for the samples from 50/50 to 20/80 water/glycerol. On the contrary, flow-birefringence is associated with wormlike micelles (WLMs) because flow causes alignment of WLMs, and aligned chains will interact differently with light along directions parallel and perpendicular to their axis of alignment.[18,50]

Figure 5.1b plots the optical density (OD), obtained by UV-Vis spectroscopy, for each of the samples in Figure 5.1a. The OD is a measure of sample turbidity. In addition, the hydrodynamic diameter (D_h) from DLS for the samples is also plotted. To obtain D_h, the calculation requires the viscosity of the solvent, which is a parameter in the Stokes-Einstein equation that relates the diffusivity measured by DLS to D_h. The data for OD confirm the visual observations and show that the samples become increasingly clear at higher glycerol content. The D_h from DLS is measured to be around 110 nm for samples with 50-70% glycerol, and around 150 nm for higher glycerol contents. Note that the lower turbidity from the 20/80, 10/90 and 0/100 samples meant that the scattered intensity (count rate) in DLS for these samples was also low. Hence, the D_h values for those samples must be viewed with some caution. Still, the fact that consistent diameters are obtained across the range of solvent compositions implies that vesicles are present in all the samples, including in pure glycerol.

5.3.2 Lecithin in Polar Solvents: Rheology

The previous results suggested that a sample of 2% lecithin in glycerol may contain vesicles. Next, we proceeded to study higher concentrations of lecithin in glycerol: from 2 to 15%. Typically, if such high lipid concentrations are added to water,

the vesicles would convert from unilamellar to multilamellar, and moreover, the samples would tend to be unstable and form two phases over time at room temperature. It should be noted that solid lecithin (powder) is insoluble in water – and so the lipid must be forced into water through the thin-film hydration method, followed by high shear (sonication or extrusion) to finally give rise to vesicles. In the case of glycerol, a solvent that is less polar than water, lecithin powder can be dissolved completely even at 15% without the need for high shear, and the resulting samples are clear and homogeneous.

We found, to our surprise, that most of these lecithin-glycerol samples were highly viscous or gel-like. This is shown by the steady-shear rheological data on the samples in Figure 5.3a, where the relative viscosity ($\eta/\eta_{solvent}$) is plotted as a function of shear-rate. For the 2 wt% sample, there is hardly any change in viscosity relative to the solvent, i.e., $\eta/\eta_{solvent}$ is 1.6, and the sample shows Newtonian behavior (viscosity independent of shear-rate). The 4 and 8% samples are moderately shear-thinning, with the viscosity being constant at low shear-rates (this value is called the zero-shear viscosity η_0) and then decreasing at higher shear-rates. The 15% sample is strongly shear-thinning and its $\eta_0/\eta_{solvent}$ is 1880. Visual observation shows that this sample is gel-like and is able to hold its weight in an inverted vial (Figure 5.3b). We had previously mentioned that the 2% lecithin sample (Figure 5.2a) was flow-birefringent. This is also the case for the 4 and 8% samples. The 15% sample is birefringent even at rest, as shown by the photo under crossed polarizers in Figure 5.3b. Static (at-rest) birefringence is generally indicative of a lyotropic liquid-crystalline phase.[84,88-90] In water, such phases

are formed by surfactants only above 20 wt%. So, what exactly is the nature of the 15% lecithin sample: does it contain vesicles, micelles, or something else?

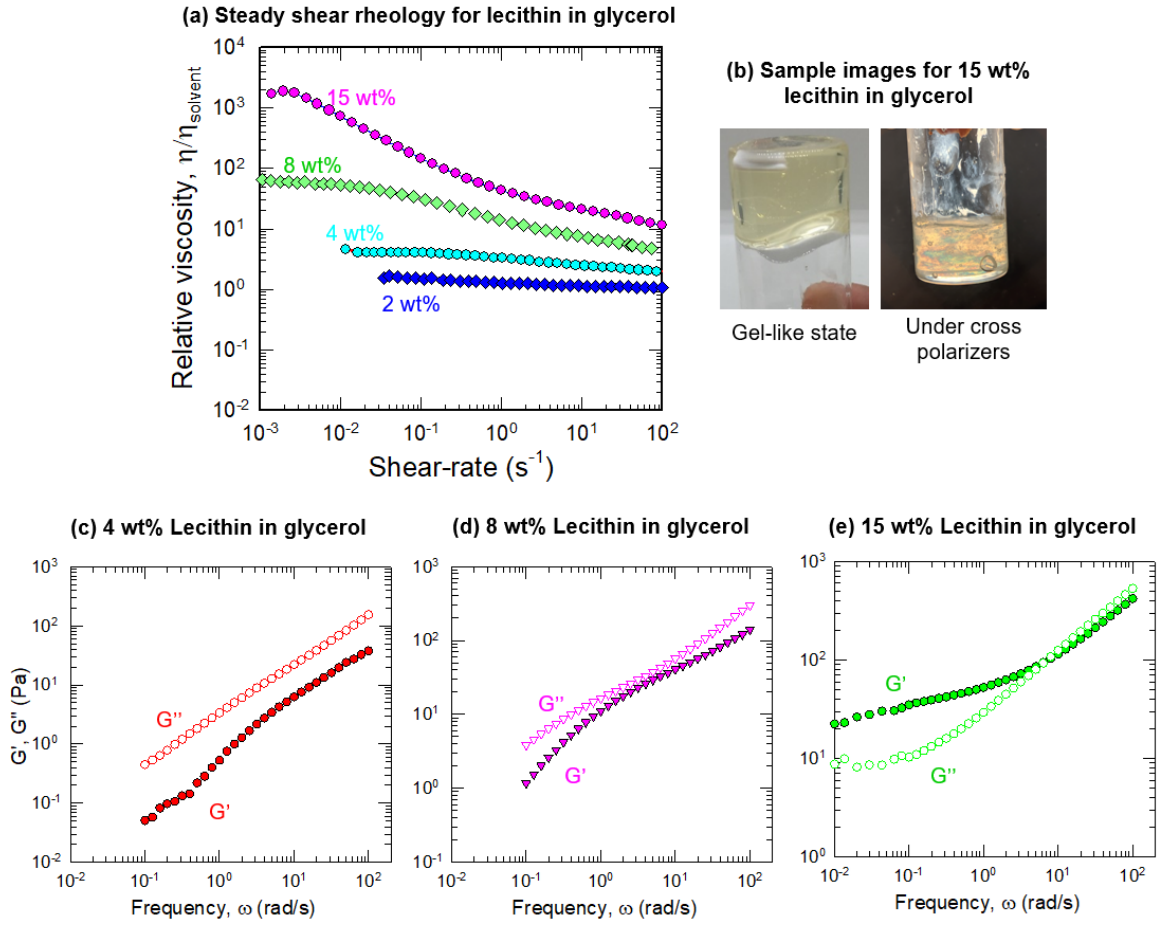

Figure 5.3. Steady-shear rheology for lecithin in glycerol solutions. (a) The steady-shear rheology (plots of the relative viscosity $\eta/\eta_{solvent}$ as a function of shear-rate) for lecithin concentrations 2, 4, 8 and 15 wt% in glycerol are shown. The 2 wt% lecithin sample shows Newtonian behavior, whereas 4, 8 and 15wt% lecithin samples are shear thinning. (b) The left image shows the vial inversion test for 15 wt% lecithin in glycerol, indicating that the sample can hold its weight and is gel-like. The right image is taken under cross polarizers and shows that the sample is birefringent at rest (bright streaks of light are visible). The dynamic rheology of (c) 4 wt%, (d) 8 wt% and (e) 15 wt% lecithin samples are shown. The 4 wt% and 8 wt% lecithin samples show viscous response, and 15 wt% lecithin sample is gel-like. In all cases, the elastic modulus G' and the viscous modulus G'' are plotted vs. frequency ω.

Dynamic rheological spectra for the samples in Figure 5.3a are shown in Figure 5.3 c, d and e. These are plots of the elastic modulus G' and the viscous modulus G'' as functions of the frequency ω. The 4% sample shows a viscous response, with $G'' > G'$ over the range of ω. The response of the 8% sample is similar, although G'' and G' are closer to each other. Conversely, the 15% sample shows rheology that is characteristic of a weak gel, consistent with the photo in Figure 5.3b. In this case, at low ω, $G' > G''$, with G' tending towards a plateau value around 20 Pa. This indicates elastic behavior at long timescales, i.e., the structure in the sample stores the energy of deformation without relaxing.

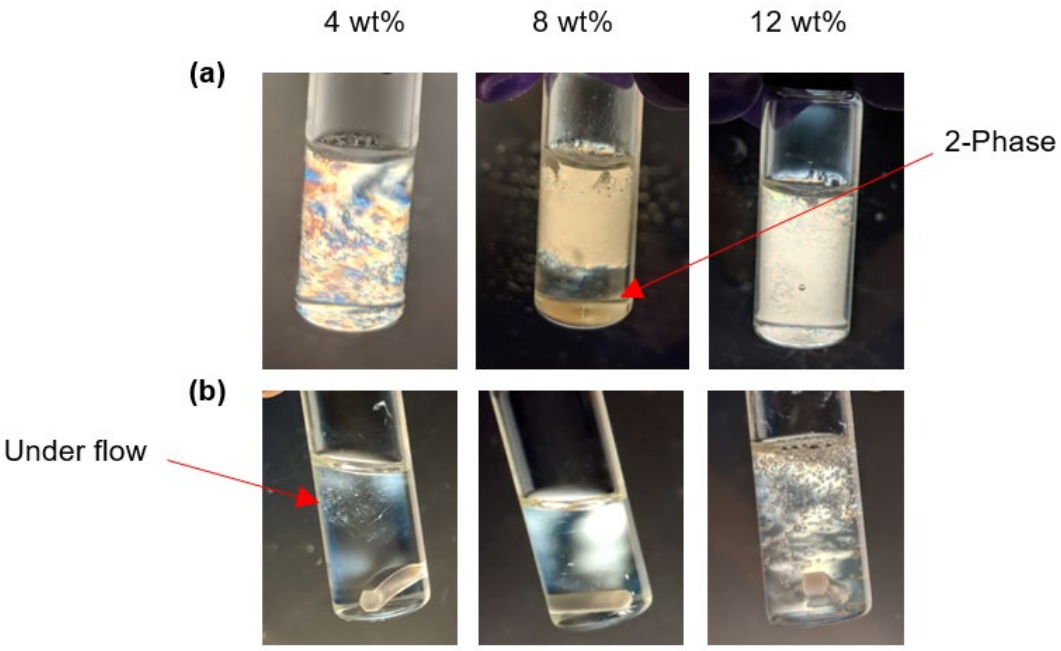

Figure 5.4. Birefringence of lecithin samples in ethylene glycol (EG) and formamide. All sample images are taken under cross polarizers. The samples of lecithin in (a) EG and (b) formamide containing 4, 8 and 12 wt% lecithin are shown. All samples are highly birefringent at rest, except for 4 wt% in formamide, which is flow birefringent. The 8 wt% lecithin in EG separates into two phases forming a lipid-rich phase (birefringent).

Solutions of lecithin were also prepared in two other polar solvents: ethylene glycol (EG) and formamide. The results were broadly similar to those in glycerol, with some differences. In EG, the 4, 8 and 12% lecithin solutions are viscous, but not gel-like as they flow in an inverted vial. Interestingly, even at 4%, the sample is highly birefringent at rest, as shown in Figure 5.4a. At 8% lecithin, a co-existence of two liquid phases is observed, with most of the lipids being confined to the upper phase, which is birefringent, whereas the lower phase is a thin EG solution. In formamide, the 4, 8 and 12% lecithin solutions are much more viscous than in EG, and the 12% sample is gel-like (Figure 5.4b). The 8 and 12% samples are birefringent at rest, while the 4% sample is flow-birefringent.

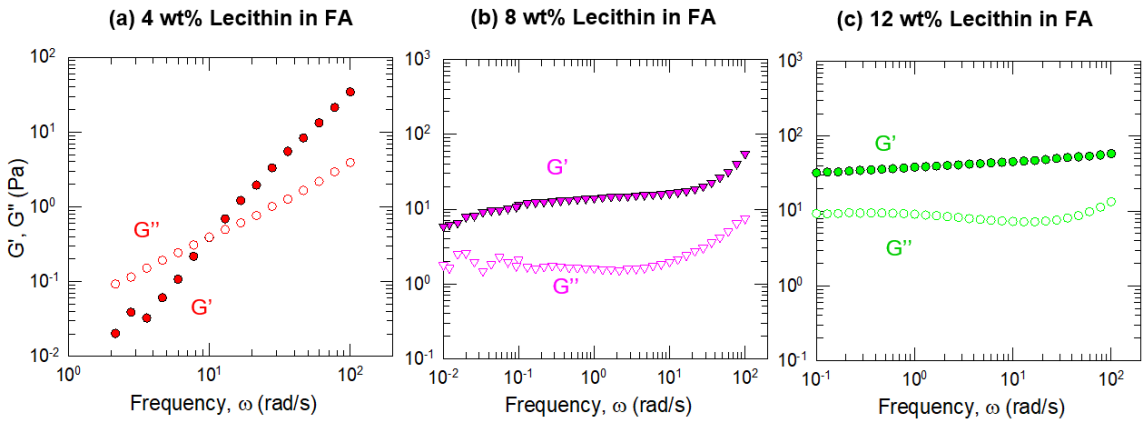

Figure 5.5. Dynamic rheology of lecithin in formamide. In all cases, the elastic modulus G' and the viscous modulus G'' are plotted vs. frequency ω. The samples contain lecithin in formamide at concentrations of (a) 4 wt%, (b) 8 wt% and (c) 15 wt%. The 4 wt% sample shows viscoelastic response, whereas 8 and 12 wt% samples show gel-like response.

The dynamic rheology of the formamide samples are shown in Figure 5.5. The 4% sample shows a viscoelastic response, with $G'' > G'$ at low ω and $G' > G''$ at high ω. In contrast, both the 8 and 12% samples show gel-like rheology, with $G' > G''$ at all ω.

The G' value in its plateau region is ~ 12 Pa for the 8% sample and 35 Pa for the 12% sample. We emphasize that the gel-like rheology for 15% lecithin in glycerol and 12% lecithin in formamide is very unusual. We had speculated if our samples contain WLMs, but if so, the rheology would have been viscoelastic (intersection of G' and G''), not gel-like. WLMs also would not show birefringence at rest.

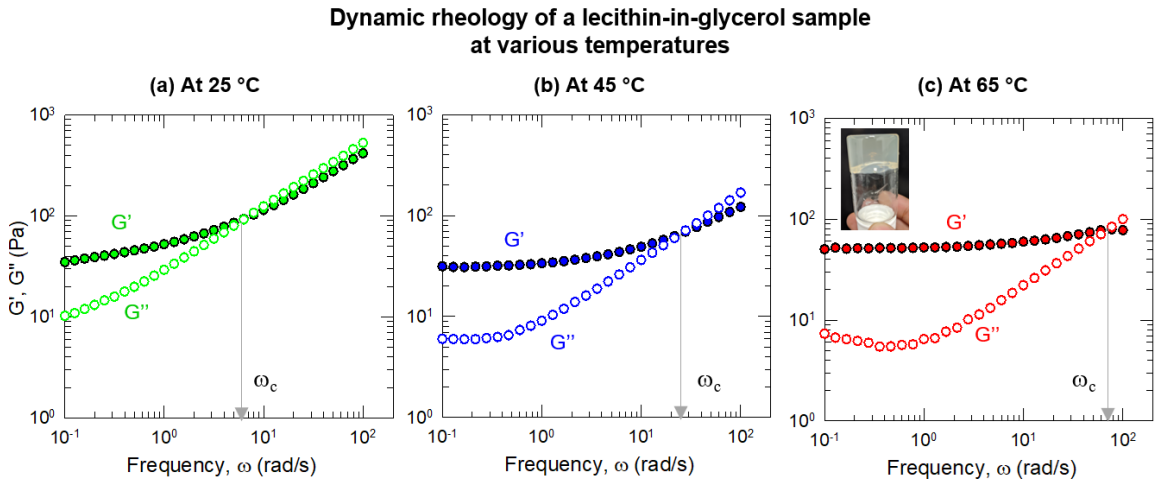

Figure 5.6. Temperature progression for a lecithin in glycerol sample. In all cases, the elastic modulus G' and the viscous modulus G'' are plotted vs. frequency ω. The 15 wt% lecithin in glycerol sample is studied at different temperatures (a) 25 °C, (b) 45°C and 65 °C. The sample remains gel-like at all temperatures. Inset: Vial photo of 15 wt% lecithin in glycerol at 65 °C.

The rheology of the gel-like samples was also investigated as a function of temperature (T), and this was done for the sample of 15% lecithin in glycerol. Plots of G' and G'' vs. ω at 25, 45 and 65°C are shown in Figure 5.6. From the data, it is clear that the sample remains gel-like over the entire range of T, and the plateau value of G' remains nearly constant with T. This is also consistent with visual observations, and a photo of the gel at 65°C is shown as an inset in Figure 5.6c. The only change with T is in

the crossover frequency ω_c at which the moduli intersect. For $\omega > \omega_c$, the viscous solvent (glycerol) influences the rheology. From the data, ω_c shifts to higher ω with increasing T, reflecting the reduction in viscosity of glycerol with T. The invariance in rheology with T is another indication that this sample does *not* contain WLMs. If the sample had WLMs, its viscosity would have significantly reduced upon heating because WLMs become exponentially shorter with increasing T.

5.3.3 Lecithin in Polar Solvents: Nanostructure

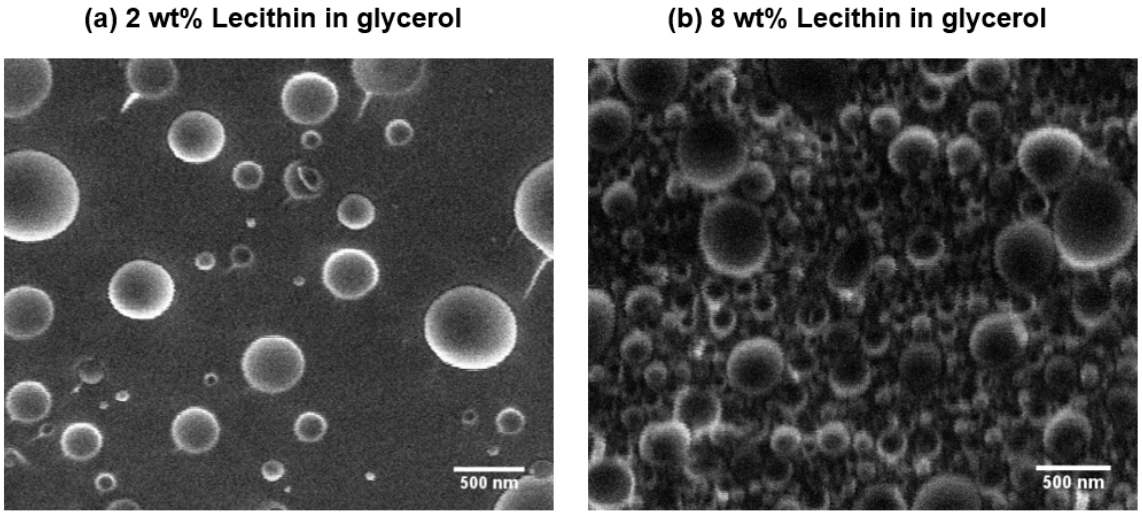

Figure 5.7. Cryo-SEM images of lecithin samples in glycerol. The electron micrographs for (a) 2 wt% and (b) 8 wt% lecithin in glycerol are shown. Both images show spherical structures ranging from 50 nm to 600 nm. The spheres are widely separated for 2 wt% sample but are very densely packed for the 8 wt% sample.

To make sense of the data shown up to this point, we need to elucidate the nanostructures present in the samples using microscopic or scattering techniques. With regard to microscopy, the technique of cryo-transmission electron microscopy (cryo-TEM) is the standard technique for visualizing the structure in aqueous solutions.[91,92]

However, cryo-TEM has not been used for solvents like glycerol, and moreover, the high viscosity of our samples complicates sample preparation for cryo-TEM. Therefore, we resorted to a related, but different technique, which is cryo-SEM. In this technique also, the sample is frozen rapidly so as to vitrify the solvent and thereby preserve the structure.

Representative images from cryo-SEM are shown in Figure 5.7 for samples of 2% and 8% lecithin in glycerol. Both samples contain spherical structures with diameters ranging from 50 to 600 nm. The spheres are well-separated in the 2% sample (Figure 5.7a). The smallest structures in this image appear to be in the background, and it is not clear if their actual sizes are larger. At the higher lipid concentration of 8% (Figure 5.7b), there are many more spheres in the field of view, and the spheres are close-packed so as to fill up the volume.

A logical inference from the images is that the structures are vesicles. They are too large to be spherical micelles (which are generally around 5 nm in diameter) and there is no evidence in the images for alternative possibilities such as cylindrical chains (WLMs) or lamellar sheets. The vesicles in these images are comparable in size with the average D_h measured by DLS, which was 110 nm (Figure 5.2). The sizes seen here are also comparable with the sizes of liposomes formed by lecithin in water, which generally fall in the 100–200 nm range. Note that a 50 nm vesicle in the images is likely to be unilamellar, i.e., have a shell of ~ 5 nm thickness formed by a single bilayer. On the other hand, a 600 nm vesicle is likely to be multilamellar, i.e., it will be an onion-like structure with multiple concentric bilayers in its shell. From these images, we cannot distinguish

conclusively between unilamellar and multilamellar vesicles. However, a majority of the vesicles being multilamellar could account for the birefringence (see below).[93,94]

One key insight from the images of the 8% sample in Figure 5.7b is that close-packing of vesicles could account for gel formation in these systems. Our rheological data indicated that the 8% sample was viscous, but not a gel (Figure 5.3). If the lecithin concentration was increased to 15%, the vesicle volume fraction would further increase and the vesicles would be even more densely packed, which could result in the gel-like rheology for this sample.

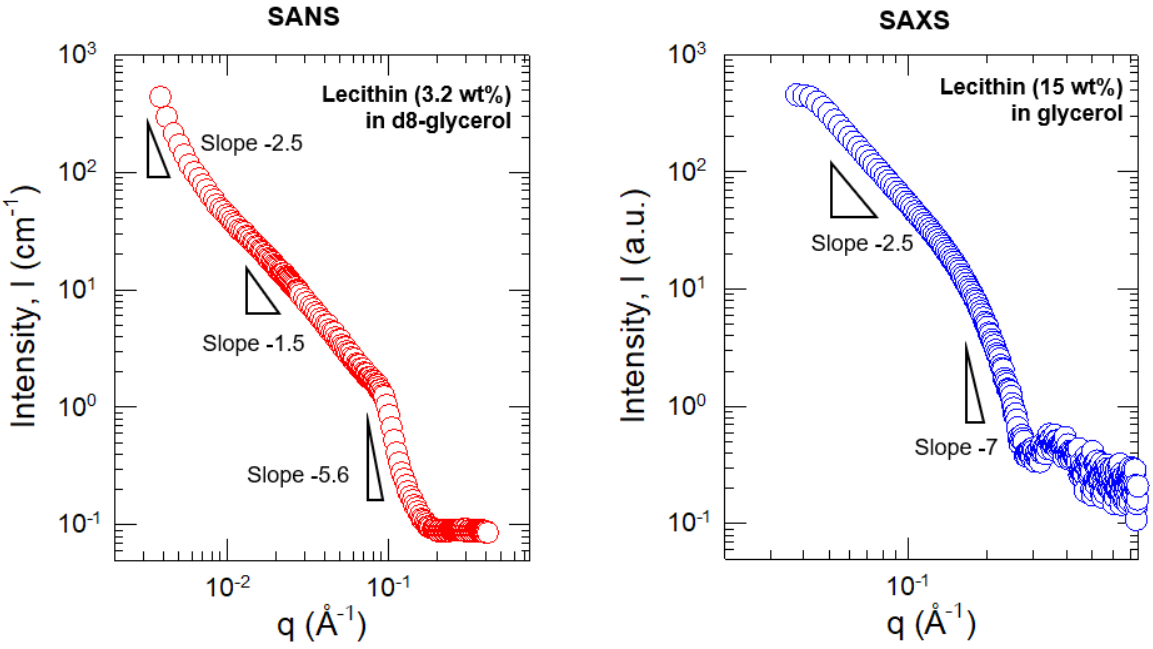

Figure 5.8. SANS and SAXS for lecithin in glycerol. Each plot shows the scattered intensity *I* vs. wave vector *q*. (a) SANS data for of 3.2 wt% lecithin in deuterated (d-8) glycerol. (b) SAXS data for 15 wt% lecithin in glycerol. Slope values at different *q*-regions are included.

We also used scattering techniques (SANS and SAXS) to probe the nanostructure in lecithin-glycerol samples. SANS data are shown in Figure 5.8a as a plot of the scattering intensity I vs. wave vector q for a sample of 3.2 wt% lecithin in deuterated glycerol. The deuterated solvent was used to ensure sufficient contrast between the scattering objects and the liquid. The SANS data reveal a complex pattern that is rather different from that of vesicles in water, which show a characteristic slope of –2 at low and intermediate q. Here, a slope of –1.5 is found at intermediate q. At higher q, an inflection is seen in the SANS data at $q^* = 0.092$ Å^{-1}. From Bragg's law, this corresponds to a length scale of $2\pi/q^* = 6.8$ nm. It is not clear if this length scale has a particular significance. One possibility is that it represents the spacing between adjacent bilayers in a multilamellar vesicle.

SAXS data are shown in Figure 5.8b, again as an I vs. q plot, with I on an arbitrary scale. This data was acquired on a concentrated (15%) lecithin sample in glycerol, which is gel-like and birefringent at rest (Figure 5.3). The SAXS data show a slope of –2.5 at low q, and the shape of this plot is again different from that of vesicles in water. Despite the birefringence, there is no evidence of peaks corresponding to a liquid-crystalline phase for this sample.

Based on all the results, what can we conclude regarding the nature of lecithin solutions in polar liquids? Considering that lecithin forms vesicles in water, we expected that it would form vesicles in polar liquids as well. However, some of our findings conflicted with this view, including (a) the clarity of the samples, and thereby the weak

intensity of light scattering; (b) the static birefringence; and (c) the gel-like rheology. Nevertheless, we believe the cryo-SEM images conclusively prove that vesicles are indeed present in these samples, and we can explain how the above findings are consistent with this picture.

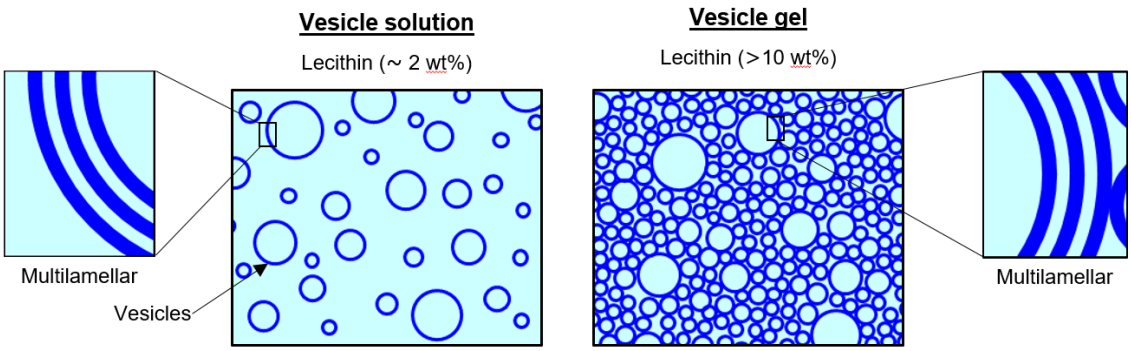

Figure 5.9. Schematic of vesicle self-assembly in polar solvents. Vesicle solutions, obtained at low lecithin concentrations (~ 2wt%), are represented by widely separated multilamellar or "onion" vesicles in the left image. The multilamellar structures are represented as concentric vesicles. The vesicle gels are comprised of densely packed multilamellar vesicles which are obtained at high lecithin concentrations (> 10wt%).

Schematics of the nanostructure in the samples at low and high lecithin concentrations are shown in Figure 5.9. In both cases, we suggest that the vesicles are multilamellar vesicles (MLVs), which are also termed 'onions' in the literature.[91,93-96] At low lecithin concentrations, the MLVs are spaced well-apart and hence do not interact with each other (Figure 5.9a). The sample is then like a suspension of spherical particles occupying a volume fraction ϕ_{MLV} of ~ 40%, and its viscosity is low. As the lecithin concentration increases, ϕ_{MLV} increases to more than 60%, and the vesicles become close-packed, i.e., they fill up the entire volume. At this point, the sample starts to show gel-like rheology. That is, when a stress is applied on the sample, the stress is transmitted

throughout the sample because each MLV is in contact with its neighbors. Thus, the close-packed MLVs act like a connected structure, similar to a network of chains, and the structure does not relax, which is why G' shows a plateau at low ω.[97]

The above results are consistent with previous studies on stable MLVs (onions) in water at high packing densities.[88,89,92-96] Such systems with MLVs did not use lipids, but instead were typically mixtures of a surfactant, a co-surfactant (like an alcohol), and salt. In several cases, close-packed MLVs exhibiting gel-like rheology have been reported.[88-90] Moreover, many such systems are reported to be birefringent at rest when ϕ_{MLV} is high and flow-birefringent at lower ϕ_{MLV}, which is exactly what we observe.[98] The gel modulus of these MLV systems has been shown to increase with ϕ_{MLV}, and it also increases as the MLV size decreases.[91,98] The term 'vesicle gel' has been used to describe these systems.

Finally, we should mention some of the unique aspects about our 'vesicle gels' made with polar liquids in contrast to the aqueous vesicle gels. In aqueous systems, the sizes of MLVs are typically a function of the shear applied on the sample during sample preparation. This is because the MLVs are usually not an equilibrium state; instead, they are formed by shearing lamellar sheets. The higher the shear, the smaller the MLVs. In contrast, our vesicle gels of lecithin in glycerol do not show any shear-dependence, and this may be because the lipid is completely soluble in glycerol. Also, all samples of lecithin in glycerol are highly stable and can be stored at room temperature for several months without any change in sample rheology.

With regard to the clarity of lecithin-based samples in glycerol, we believe the reason may lie in the refractive indices (n) of the lipid (lecithin) versus those of the solvent. Although a precise value of n for lecithin is not available, we can estimate the n to be similar to those of long alkanes or alkenes, since the lipid has long alkyl tails. For example, the n for hexadecane is 1.43. In the case of the solvents, n for water is 1.33 and n for glycerol is 1.47. This suggests that the n for the lipid may be much closer to that for glycerol, which means that the optical contrast between the vesicle bilayer and the solvent will be low. This could explain why the vesicle solutions and gels in glycerol do not scatter light as strongly, i.e., they are much more clear (less bluish or turbid) than vesicles in water.

5.4 Conclusions

This study has demonstrated that vesicles can be self-assembled in a variety of polar organic solvents including glycerol, formamide and ethylene glycol. The amphiphilic molecule used to create these vesicles is the simple phospholipid, lecithin or soy-phosphatidylcholine. Lecithin is insoluble in water, but dissolves readily in polar solvents at concentrations up to 15%, with the resulting fluids being clear and colorless. At low concentrations (~ 2 to 4%), the fluids are viscous and flow-birefringent. At higher concentrations (> 10 wt%), the fluids are gel-like and strongly birefringent at rest. Dynamic rheology of the latter reveals an elastic, gel-like response, with $G' > G''$ and G' being frequency-independent at low frequencies. Images from cryo-scanning electron microscopy (cryo-SEM) indicate that the concentrated samples are ‘vesicle gels’, where

MLVs (onions), with sizes between 50 to 600 nm, are close-packed across the entire sample volume. This structure explains both the rheology and the birefringence. To our knowledge, this is the first report of such a ‘vesicle-gel’ phase in polar solvents. Our study significantly expands the possibilities for self-assembly in polar solvents, and our new formulations may open new avenues for applications in cosmetics, pharmaceutics, and as lubricants or antifreeze agents.

Chapter 6
Conclusions and Recommendations

6.1 Conclusions

In this dissertation, we have presented the self-assembly of surfactants and lipid in polar organic solvents, forming different types of macromolecular structures. Specifically, we have focused on the self-assembly of wormlike micelles (WLMs) and vesicles in non-aqueous polar solvents including glycerol, ethylene glycol and formamide. Our studies contribute towards the fundamental understanding of self-assembly in polar solvents, as well as has technological significance by finding applications in pharmaceuticals, cosmetics, lubricants and anti-freezing agents.

In chapter 3, we have shown that wormlike can be formed in polar organic solvents including glycerol and formamide. We have formed long, flexible WLMs by employing a system of long tailed (C_{22}) cationic surfactant, erucyl bis(2-hydroxyethyl)methyl ammonium chloride (EHAC) and binding salt, sodium salicylate (NaSal) in glycerol. This forms a highly viscous and viscoelastic solution, and a unique dynamic rheology is obtained with two crossovers between viscous and elastic moduli (G' and G''). We found that simple salts such as sodium chloride (NaCl) or potassium chloride (KCl) were unable to induce WLMs in glycerol, whereas they do so in water. Additionally, we have reported that WLMs can be formed at low and sub-zero conditions

in non-aqueous polar solvents by exploiting the low Krafft temperature of the surfactant and the low freezing points of glycerol and ethylene glycol mixtures. This study may have potential applications in forming lubricants and anti-freezing coating for airplanes and turbines at very low temperatures.

In chapter 4, we have further investigated the dynamic rheology of wormlike micelles formed in glycerol as compared to that in water. In particular, the dynamic rheology exhibits multiple crossovers between viscous and elastic moduli (G' and G'') in the frequency range of mechanical rheometer (10^{-2} to 10^{2} rad/s). This can be achieved in water at very high frequencies by using advanced techniques such as diffusive wave spectroscopy (DWS). For WLMs in glycerol, the second crossover is observed at a frequency around 10 rad/s, whereas it is found at ~10^{5} rad/s for WLMs in water or polymer solutions. This occurs due to high viscosity of the solvent which affects the segmental motions of chains at high frequencies. Furthermore, the low diffusivity of the WLMs in glycerol prevents the chains from undergoing stress relaxation by breaking and recombination method, and they behave similar to polymer solutions. We found that the wormlike micelles in glycerol are shorter, weakly entangled and less dynamic that those in water.

In chapter 5, we have shifted our attention to the self-assembly of vesicles in polar organic solvents such as glycerol, formamide and ethylene glycol (EG). We have used lecithin, or soy-phosphatidylcholine, which is one of the most commonly used phospholipids to form vesicles. At dilute and semi-dilute concentrations, we find that

lecithin forms multilamellar vesicles in solutions of glycerol, formamide and EG. For high concentrations of lecithin (~15 wt%) in glycerol, a gel-like sample is obtained which can hold its weight in an inverted vial, and shows a gel-like response in dynamic rheology. In addition, the lecithin samples in glycerol, formamide and EG are either highly birefringent at rest or flow birefringent when observed under cross-polarizers. Further investigations from electron microscopy reveals that low lecithin concentrations (~2 wt%) have widely separated vesicles, whereas a close packing of multilamellar vesicles (onions) is observed at high lecithin concentrations (>8 wt%). Thus, we show that a densely packed system of vesicles, known as 'vesicle gels', are formed in glycerol at high lecithin concentrations.

6.2 Recommendations for Future Work

We suggest two main projects for future work, which would extend the studies conducted in this dissertation as well as explore new concepts and applications.

6.2.1 Wormlike Micelles Dynamics using Molecular Simulations

In the recent years, computer simulations techniques have been applied to study the dynamics of surfactant aggregation by using molecular dynamics or coarse-grained techniques. Molecular dynamics simulation (MD) is an important tool to explore the dynamics of wormlike micelles. We have discussed the formation of wormlike micelles (WLMs) in polar organic solvents such as glycerol and formamide in chapters 3 and 4. We have also studied the dynamic rheology of these solutions which shows that the WLMs in glycerol are less likely to undergo stress relaxation using breaking and recombination mechanism, but rather reptation and breathing modes are observed. A study focusing on the dynamic interactions of wormlike micelles and stress relaxation methods can provide invaluable addition to the experimental results shown here. The comparison with water also indicated that WLMs in glycerol are formed using EHAC and binding salts such as NaSal, but simple salts such as NaCl are unable to induce WLMs in glycerol. Typically, WLMs are induced due to reduction in electrostatic repulsions between surfactants by adding salt counterions. This leads to conversion of spherical to cylindrical micelles. The counterions generated by binding salts are embedded in the micellar layer and are more effective in forming wormlike micelles. This difference in interaction of salts with micelles in glycerol can be explored using MD simulations by studying the equilibrium structure of the wormlike micelles.

6.2.2 Self-Assembly in Water-Solvent mixtures

We have shown that wormlike micelles (WLMs) and vesicles can be formed in pure polar organic solvents including glycerol, formamide and ethylene glycol (EG). Future studies can be based on bridging the gap between pure water and pure solvent by extending the studies to water-solvent mixtures. We have performed preliminary experiments for forming WLMs in water-EG mixtures using the same system of surfactant and salt (EHAC-NaSal).

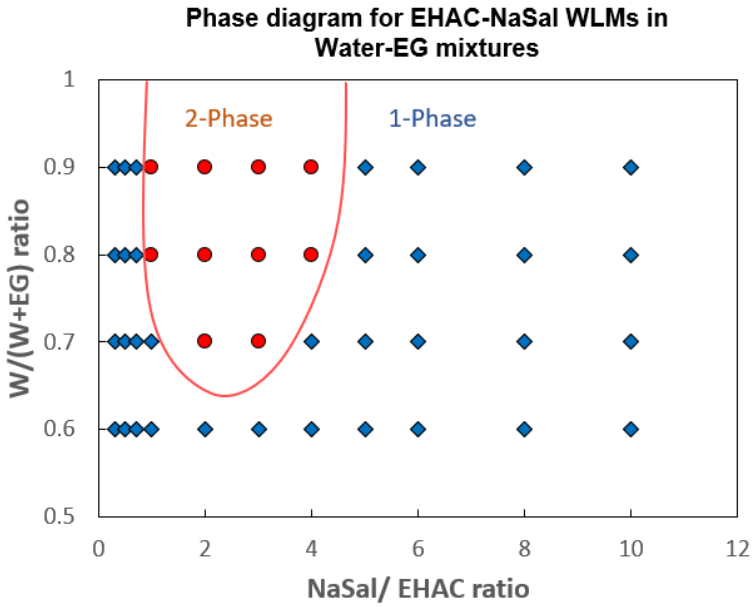

Figure 6.1 Phase behavior of WLMs in water-EG mixtures. WLMs were studied for increasing NaSal/EHAC molar ratio at different concentrations of water-EG mixtures ranging from 60/40 to 100/0 water-EG. The EHAC concentration is 60 mM. The blue and red data indicate the single phase (isotropic) and 2-phases (coacervate) of WLMs solutions respectively.

For EHAC-NaSal WLMs in water, an unusual phase behavior has previously been reported such that a coacervate phase is obtained below a characteristic temperature known as cloud point (T_c). It has been shown that many samples that are isotropic (or 1-

phase) at room temperature undergo phase separation upon heating, and this is known as 'cloud' phenomenon. At 25 °C, it has been observed that the liquid-liquid coacervate phase is obtained for an intermediate range of salt/surfactant ratios resulting in surfactant-rich and surfactant-poor phases.

Here, figure 6.1 shows the phase behavior of wormlike micelles in water-EG solvent mixtures formed by gradually replacing water with EG from 100/0 to 60/40. For 60 mM EHAC solution in water, increasing the NaSal/EHAC molar ratio from 0.1 to 10 shows a 2-phase region for salt/surfactant ratio from 1 to 5. When EG is added to the solution to form 90/10 and 80-20 W-EG samples, we observe that the 2-phase region shrinks to between 1 and 4. Further increasing the concentration of EG to 70/30 shrinks the coacervate phase region more to only samples exhibiting coacervate phases between surfactant/salt ratio of 2 and 3. Interestingly, the 2-phase region is not observed at all for 60/40 W-EG samples, and all the samples are isotropic in nature. This shows that introducing EG in WLMs in water can change the phase behavior of the WLM solutions. This reveals a systematic trend in the phase behavior of W-EG WLMs. For future studies, we recommend a systematic study of how the phenomenon of 'coacervation' and 'cloud points' are affected when the solvent is changed from pure water to a mixture of water and a polar liquid like EG. Similar studies performed for water-glycerol solvent mixtures would also be interesting in understanding the effect of different solvents on the self-assembly of WLMs.

References

[1] Israelachvili, J. N. *Intermolecular and Surface Forces, 3rd ed.*; Academic Press: San Diego, 2011.

[2] Jonsson, B.; Lindman, B.; Holmberg, K.; Kronberg, B. *Surfactants and Polymers in Aqueous Solutions*; Wiley: New York, 1998.

[3] Evans, D. F.; Wennerstrom, H. *The Colloidal Domain: Where Physics, Chemistry, Biology, and Technology Meet*; Wiley-VCH: New York, 2001.

[4] *Giant Micelles: Properties and Applications*; Zana, R.; Kaler, E. W., Eds.; CRC Press: Boca Raton, 2007.

[5] *Wormlike Micelles: Advances in Systems, Characterisation and Applications*; Dreiss, C. A.; Feng, Y. J., Eds.; RSC: Cambridge, 2017.

[6] Cates, M. E.; Candau, S. J. "Statics and dynamics of worm-like surfactant micelles." *Journal of Physics-Condensed Matter* **1990**, *2*, 6869-6892.

[7] Israelachvili, J. N.; Mitchell, D. J.; Ninham, B. W. "Theory of self-assembly of hydrocarbon amphiphiles into micelles and bilayers." *Journal of the Chemical Society-Faraday Transactions Ii* **1976**, *72*, 1525-1568.

[8] Tung, S. H.; Huang, Y. E.; Raghavan, S. R. "A new reverse wormlike micellar system: Mixtures of bile salt and lecithin in organic liquids." *Journal of the American Chemical Society* **2006**, *128*, 5751-5756.

[9] Ray, A. "Micelle formation in pure ethylene glycol." *Journal of the American Chemical Society* **1969**, *91*, 6511-6512.

[10] Wijaya, E. C.; Greaves, T. L.; Drummond, C. J. "Linking molecular/ion structure, solvent mesostructure, the solvophobic effect and the ability of amphiphiles to self-assemble in non-aqueous liquids." *Faraday Discussions* **2013**, *167*, 191-215.

[11] Warnheim, T. "Aggregation of surfactants in nonaqueous, polar solvents." *Current Opinion in Colloid & Interface Science* **1997**, *2*, 472-477.

[12] Greaves, T. L.; Weerawardena, A.; Drummond, C. J. "Nanostructure and amphiphile self-assembly in polar molecular solvents: amides and the "solvophobic effect"." *Physical Chemistry Chemical Physics* **2011**, *13*, 9180-9186.

[13] Ruiz, C. C.; Diaz-Lopez, L.; Aguiar, J. "Self-assembly of tetradecyltrimethylammonium bromide in glycerol aqueous mixtures: A thermodynamic and structural study." *Journal of Colloid and Interface Science* **2007**, *305*, 293-300.

[14] Evans, D. F.; Yamauchi, A.; Roman, R.; Casassa, E. Z. "Micelle formation in ethylammonium nitrate, a low-melting fused salt." *Journal of Colloid and Interface Science* **1982**, *88*, 89-96.

[15] Akhter, M. S.; Alawi, S. M. "A comparison of micelle formation of ionic surfactants in formamide, in N-methylformamide and in N,N-dimethylformamide." *Colloids and Surfaces a-Physicochemical and Engineering Aspects* **2003**, *219*, 281-290.

[16] Lopez-Barron, C. R.; Wagner, N. J. "Structural transitions of ctab micelles in a protic ionic liquid." *Langmuir* **2012**, *28*, 12722-12730.

[17] Gayet, F.; Marty, J. D.; Brulet, A.; Lauth-de Viguerie, N. "Vesicles in Ionic Liquids." *Langmuir* **2011**, *27*, 9706-9710.

[18] Raghavan, S. R.; Kaler, E. W. "Highly viscoelastic wormlike micellar solutions formed by cationic surfactants with long unsaturated tails." *Langmuir* **2001**, *17*, 300-306.

[19] Oelschlaeger, C.; Suwita, P.; Willenbacher, N. "Effect of Counterion Binding Efficiency on Structure and Dynamics of Wormlike Micelles." *Langmuir* **2010**, *26*, 7045-7053.

[20] Cates, M. E. "Reptation of living polymers - dynamics of entangled polymers in the presence of reversible chain-scission reactions." *Macromolecules* **1987**, *20*, 2289-2296.

[21] Fuller, S.; Li, Y.; Tiddy, G. J. T.; Wynjones, E.; Arnell, R. D. "Formulation of lyotropic lamellar phases of surfactants as novel lubricants." *Langmuir* **1995**, *11*, 1980-1983.

[22] Zheng, D.; Wang, X.; Zhang, M.; Liu, Z.; Ju, C. "Anticorrosion and lubricating properties of a fully green lubricant." *Tribology International* **2019**, *130*, 324-333.

[23] Yin, H. Y.; Feng, Y. J.; Li, P. X.; Doutch, J.; Han, Y. X.; Mei, Y. J. "Cryogenic wormlike micelles." *Soft Matter* **2019**, *15*, 2511-2516.

[24] Davey, T. W.; Ducker, W. A.; Hayman, A. R.; Simpson, J. "Krafft Temperature Depression in Quaternary Ammonium Bromide Surfactants." *Langmuir* **1998**, *14*, 3210-3213.

[25] Scartazzini, R.; Luisi, P. L. "Organogels from lecithins." *Journal of Physical Chemistry* **1988**, *92*, 829-833.

[26] Shchipunov, Y. A. "Lecithin organogel - A micellar system with unique properties." *Colloids and Surfaces a-Physicochemical and Engineering Aspects* **2001**, *183*, 541-554.

[27] Auvray, X.; Petipas, C.; Anthore, R.; Rico, I.; Lattes, A. "X-ray diffraction study of mesophases of cetyltrimethylammonium bromide in water, formamide, and glycerol." *The Journal of Physical Chemistry* **1989**, *93*, 7458-7464.

[28] Ray, A. "Solvophobic interactions and micelle formation in structure forming nonaqueous solvents." *Nature* **1971**, *231*, 313-315.

[29] Moya, M. L.; Rodriguez, A.; Graciani, M. D.; Fernandez, G. "Role of the solvophobic effect on micellization." *Journal of Colloid and Interface Science* **2007**, *316*, 787-795.

[30] Sedov, I. A.; Stolov, M. A.; Solomonov, B. N. "Thermodynamics of solvation and solvophobic effect in formamide." *Journal of Chemical Thermodynamics* **2013**, *64*, 120-125.

[31] Dreiss, C. A. "Wormlike micelles: where do we stand? Recent developments, linear rheology and scattering techniques." *Soft Matter* **2007**, *3*, 956-970.

[32] Ezrahi, S.; Tuval, E.; Aserin, A. "Properties, main applications and perspectives of worm micelles." *Advances in Colloid and Interface Science* **2006**, *128*, 77-102.

[33] Rubinstein, M.; Colby, R. H.‡Polymer Physics.† **2003**.

[34] Rehage, H.; Hoffmann, H. "Viscoelastic surfactant solutions - Model systems for rheological research." *Molecular Physics* **1991**, *74*, 933-973.

[35] Larson, R. G. *The Structure and Rheology of Complex Fluids*; Oxford University Press: New York, 1999.

[36] Raghavan, S. R.; Edlund, H.; Kaler, E. W. "Cloud-point phenomena in wormlike micellar systems containing cationic surfactant and salt." *Langmuir* **2002**, *18*, 1056-1064.

[37] Kalur, G. C.; Frounfelker, B. D.; Cipriano, B. H.; Norman, A. I.; Raghavan, S. R. "Viscosity increase with temperature in cationic surfactant solutions due to the growth of wormlike micelles." *Langmuir* **2005**, *21*, 10998-11004.

[38] Shikata, T.; Hirata, H.; Kotaka, T. "Micelle formation of detergent molecules in aqueous media: viscoelastic properties of aqueous cetyltrimethylammonium bromide solutions." *Langmuir* **1987**, *3*, 1081-1086.

[39] Shikata, T.; Hirata, H.; Kotaka, T. "Micelle formation of detergent molecules in aqueous-media .3. Viscoelastic properties of aqueous cetyltrimethylammonium bromide salicylic-acid solutions." *Langmuir* **1989**, *5*, 398-405.

[40] Croce, V.; Cosgrove, T.; Maitland, G.; Hughes, T.; Karlsson, G. "Rheology, cryogenic transmission electron spectroscopy, and small-angle neutron scattering of highly viscoelastic wormlike micellar solutions." *Langmuir* **2003**, *19*, 8536-8541.

[41] Shikata, T.; Hirata, H.; Kotaka, T. "Micelle formation of detergent molecules in aqueous-media .2. Role of free salicylate ions on viscoelastic properties of aqueous cetyltrimethylammonium bromide sodium-salicylate solutions." *Langmuir* **1988**, *4*, 354-359.

[42] Macosko, C. W. *Rheology: Principles, Measurements, and Applications*; Wiley-VCH: New York, 1994.

[43] Morrison, F. A. *Understanding rheology*; Oxford University Press: New York, 2001.

[44] Lindner, P.; Zemb, T. *Neutron, x-ray and light scattering : introduction to an investigative tool for colloidal and polymeric systems : proceedings of the European Workshop on Neutron, X-Ray and Light Scattering as an Investigative Tool for Colloidal and Polymeric Systems, Bombannes, France, 27 May-2 June, 1990*; North-Holland
Sole distributors for the U.S.A. and Canada, Elsevier Science Pub. Co.: Amsterdam ; New York, 1991.

[45] Guinier, A.; Fournet, G. r. *Small-angle scattering of X-rays*; Wiley: New York, 1955.

[46] Yang, J. "Viscoelastic wormlike micelles and their applications." *Current Opinion in Colloid & Interface Science* **2002**, *7*, 276-281.

[47] Sullivan, P.; Nelson, E. B.; Anderson, V.; Hughes, T. Oilfield applications of giant micelles. In *Giant Micelles: Properties and Applications*; Zana, R., Kaler, E. W., Eds.; CRC Press: Boca Raton, 2007; pp 453-472.

[48] Couillet, I.; Hughes, T.; Maitland, G.; Candau, F.; Candau, S. J. "Growth and scission energy of wormlike micelles formed by a cationic surfactant with long unsaturated tails." *Langmuir* **2004**, *20*, 9541-9550.

[49] Kalur, G. C.; Raghavan, S. R. "Anionic wormlike micellar fluids that display cloud points: Rheology and phase behavior." *Journal of Physical Chemistry B* **2005**, *109*, 8599-8604.

[50] Kumar, R.; Kalur, G. C.; Ziserman, L.; Danino, D.; Raghavan, S. R. "Wormlike micelles of a C22-tailed zwitterionic betaine surfactant: From viscoelastic solutions to elastic gels." *Langmuir* **2007**, *23*, 12849-12856.

[51] Wang, Y. J.; Zhang, Y. M.; Liu, X. L.; Wang, J. Y.; Wei, L. M.; Feng, Y. J. "Effect of a Hydrophilic Head Group on Krafft Temperature, Surface Activities and Rheological Behaviors of Erucyl Amidobetaines." *Journal of Surfactants and Detergents* **2014**, *17*, 295-301.

[52] Kelleppan, V. T.; Moore, J. E.; McCoy, T. M.; Sokolova, A. V.; de Campo, L.; Wilkinson, B. L.; Tabor, R. F. "Self-assembly of long-chain betaine surfactants: Effect of tailgroup structure on wormlike micelle formation." *Langmuir* **2018**, *34*, 970-977.

[53] Liu, H. B.; Wang, W.; Yin, H. Y.; Feng, Y. J. "Solvent-Driven Formation of Worm-Like Micelles Assembled from a CO2-Responsive Triblock Copolymer." *Langmuir* **2015**, *31*, 8756-8763.

[54] Wei, Y. Q.; Han, Y. X.; Zhou, H.; Wang, H.; Mei, Y. J. "Rheological Investigation of Wormlike Micelles Based on Gemini Surfactant in EG-Water Solution." *Journal of Surfactants and Detergents* **2016**, *19*, 925-932.

[55] Zhou, H.; Han, Y. X.; Wei, Y. Q.; Wang, H.; Mei, Y. J. "Effect of EG and low temperature on solution behaviors of wormlike micelles." *Journal of Molecular Liquids* **2016**, *221*, 603-607.

[56] Yin, H.; Feng, Y.; Li, P.; Doutch, J.; Han, Y.; Mei, Y. "Cryogenic viscoelastic surfactant fluids: Fabrication and application in a subzero environment." *Journal of Colloid and Interface Science* **2019**, *551*, 89-100.

[57] Aramaki, K.; Olsson, U.; Yamaguchi, Y.; Kunieda, H. "Effect of water-soluble alcohols on surfactant aggregation in the C12CO8 system." *Langmuir* **1999**, *15*, 6226-6232.

[58] Ronis, D.; Martina, E.; Deutch, J. M. "The solvophobic effect in simple fluid mixtures." *Chemical Physics Letters* **1977**, *46*, 53-55.

[59] Stuart, M. C. A.; Van de Pas, J. C.; Engberts, J. "Phase behavior of laundry surfactants in polar solvents." *Journal of Surfactants and Detergents* **2006**, *9*, 153-160.

[60] Kratky, O.; Porod, G. "Diffuse small-angle scattering of x-rays in colloid systems." *Journal of Colloid Science* **1949**, *4*, 35-70.

[61] Koehler, R. D.; Raghavan, S. R.; Kaler, E. W. "Microstructure and dynamics of wormlike micellar solutions formed by mixing cationic and anionic surfactants." *Journal of Physical Chemistry B* **2000**, *104*, 11035-11044.

[62] Bijma, K.; Engberts, J. "Effect of counterions on properties of micelles formed by alkylpyridinium surfactants .1. Conductometry and H-1-NMR chemical shifts." *Langmuir* **1997**, *13*, 4843-4849.

[63] Lane, L. B. "Freezing Points of Glycerol and Its Aqueous Solutions." *Industrial & Engineering Chemistry* **1925**, *17*, 924-924.

[64] Pedersen, J. S.; Schurtenberger, P. "Scattering functions of semiflexible polymers with and without excluded volume effects." *Macromolecules* **1996**, *29*, 7602-7612.

[65] Pedersen, J. S. "Analysis of small-angle scattering data from colloids and polymer solutions: modeling and least-squares fitting." *Advances in Colloid and Interface Science* **1997**, *70*, 171-210.

[66] Glatter, O. "NEW METHOD FOR EVALUATION OF SMALL-ANGLE SCATTERING DATA." *Journal of Applied Crystallography* **1977**, *10*, 415-421.

[67] Ogunsola, O. A.; Kraeling, M. E.; Zhong, S.; Pochan, D. J.; Bronaugh, R. L.; Raghavan, S. R. "Structural analysis of "flexible" liposome formulations: new insights into the skin-penetrating ability of soft nanostructures." *Soft Matter* **2012**, *8*, 10226-10232.

[68] Rehage, H.; Hoffmann, H. "Rheological properties of viscoelastic surfactant systems." *Journal of Physical Chemistry* **1988**, *92*, 4712-4719.

[69] Wang, J.; Feng, Y.; Agrawal, N. R.; Raghavan, S. R. "Wormlike micelles versus water-soluble polymers as rheology-modifiers: similarities and differences." *Physical Chemistry Chemical Physics* **2017**, *19*, 24458-24466.

[70] Turner, M. S.; Cates, M. E. "Linear viscoelasticity of living polymers - a quantitative probe of chemical relaxation-times." *Langmuir* **1991**, *7*, 1590-1594.

[71] Granek, R.; Cates, M. E. "Stress-relaxation in living polymers - results from a poisson renewal model." *Journal of Chemical Physics* **1992**, *96*, 4758-4767.

[72] Oelschlaeger, C.; Schopferer, A.; Scheffold, F.; Willenbacher, N. "Linear-to-Branched Micelles Transition: A Rheometry and Diffusing Wave Spectroscopy (DWS) Study." *Langmuir* **2009**, *25*, 716-723.

[73] Zou, W. Z.; Tang, X. M.; Weaver, M.; Koenig, P.; Larson, R. G. "Determination of characteristic lengths and times for wormlike micelle solutions from rheology using a mesoscopic simulation method." *Journal of Rheology* **2015**, *59*, 903-934.

[74] Morishima, K.; Inoue, T. "High frequency viscoelastic measurements using optical tweezers on wormlike micelles of nonionic and cationic surfactants in aqueous solutions." *Journal of Rheology* **2016**, *60*, 1055-1067.

[75] Zou, W. Z.; Tan, G.; Jiang, H. Q.; Vogtt, K.; Weaver, M.; Koenig, P.; Beaucage, G.; Larson, R. G. "From well-entangled to partially-entangled wormlike micelles." *Soft Matter* **2019**, *15*, 642-655.

[76] Nakaya-Yaegashi, K.; Ramos, L.; Tabuteau, H.; Ligoure, C. "Linear viscoelasticity of entangled wormlike micelles bridged by telechelic polymers: An experimental model for a double transient network." *Journal of Rheology* **2008**, *52*, 359-377.

[77] Liu, C. Y.; He, J. S.; van Ruymbeke, E.; Keunings, R.; Bailly, C. "Evaluation of different methods for the determination of the plateau modulus and the entanglement molecular weight." *Polymer* **2006**, *47*, 4461-4479.

[78] Ferry, J. D. *Viscoelastic properties of polymers*, 3d ed. ed.; Wiley: New York, 1980.

[79] Lasic, D. D. *Liposomes : from physics to applications*; Elsevier: Amsterdam ;, 1993.

[80] Bleasdale, T. A.; Tiddy, G. J. T.; Wynjones, E. "Cubic phase formation in polar nonaqueous solvents." *Journal of Physical Chemistry* **1991**, *95*, 5385-5386.

[81] Dorfler, H. D.; Senst, A. "Influence of glycerol on the formation of lyotropic mesophases - microscopic texture observations for determining preliminary phase-diagrams of binary k-soap glycerol systems." *Colloid and Polymer Science* **1993**, *271*, 173-189.

[82] Elnokaly, M. A.; Ford, L. D.; Friberg, S. E.; Larsen, D. W. "The structure of lamellar lyotropic liquid-crystals from lecithin and alkanediols." *Journal of Colloid and Interface Science* **1981**, *84*, 228-234.

[83] McDaniel, R. V.; McIntosh, T. J.; Simon, S. A. "Non-electrolyte substitution for water in phosphatidylcholine bilayers." *Biochimica Et Biophysica Acta* **1983**, *731*, 97-108.

[84] Friberg, S. E.; Wohn, C. S. "A system with non-aqueous birefringent microemulsions." *Colloid and Polymer Science* **1985**, *263*, 156-159.

[85] Lopez-Barron, C. R.; Li, D. C.; DeRita, L.; Basavaraj, M. G.; Wagner, N. J. "Spontaneous Thermoreversible Formation of Cationic Vesicles in a Protic Ionic Liquid." *Journal of the American Chemical Society* **2012**, *134*, 20728-20732.

[86] Dashnau, J. L.; Nucci, N. V.; Sharp, K. A.; Vanderkooi, J. M. "Hydrogen Bonding and the Cryoprotective Properties of Glycerol/Water Mixtures." *The Journal of Physical Chemistry B* **2006**, *110*, 13670-13677.

[87] Schrader, A. M.; Cheng, C. Y.; Israelachvili, J. N.; Han, S. G. "Communication: contrasting effects of glycerol and dmso on lipid membrane surface hydration dynamics and forces." *Journal of Chemical Physics* **2016**, *145*.

[88] Hoffman, C.; Thunig, C.; Schmiedel, P.; Munkert, U. "Surfactant systems with charged multilamellar vesicles and their rheological properties." *Abstracts of Papers of the American Chemical Society* **1994**, *208*, 227-COLL.

[89] Hoffmann, H.; Horbaschek, K.; Witte, F. "Vesicle phases with semipolar additives." *Journal of Colloid and Interface Science* **2001**, *235*, 33-45.

[90] Horbaschek, K.; Hoffmann, H.; Thunig, C. "Formation and properties of lamellar phases in systems of cationic surfactants and hydroxy-naphthoate." *Journal of Colloid and Interface Science* **1998**, *206*, 439-456.

[91] Gradzielski, M. "Vesicles and vesicle gels - structure and dynamics of formation." *Journal of Physics-Condensed Matter* **2003**, *15*, R655-R697.

[92] Gradzielski, M.; Muller, M.; Bergmeier, M.; Hoffmann, H.; Hoinkis, E. "Structural and macroscopic characterization of a gel phase of densely packed monodisperse, unilamellar vesicles." *Journal of Physical Chemistry B* **1999**, *103*, 1416-1424.

[93] vanderLinden, E.; Buytenhek, C. J. "Spontaneous formation of onion phases in a single surfactant system and their salt-induced transformation towards ordinary lamellar phases." *Physica A* **1997**, *245*, 1-10.

[94] Versluis, P.; van de Pas, J. C.; Mellema, J. "Influence of salt concentration and surfactant concentration on the microstructure and rheology of lamellar liquid crystalline phases." *Langmuir* **2001**, *17*, 4825-4835.

[95] Panizza, P.; Roux, D.; Vuillaume, V.; Lu, C. Y. D.; Cates, M. E. "Viscoelasticity of the onion phase." *Langmuir* **1996**, *12*, 248-252.

[96] Sein, A.; Engberts, J.; Vanderlinden, E.; Vandepas, J. C. "Salt-induced transition from a micellar to a lamellar liquid-crystalline phase in dilute mixtures of anionic and nonionic surfactants in aqueous-solution." *Langmuir* **1993**, *9*, 1714-1720.

[97] Mezzenga, R.; Meyer, C.; Servais, C.; Romoscanu, A. I.; Sagalowicz, L.; Hayward, R. C. "Shear rheology of lyotropic liquid crystals: A case study." *Langmuir* **2005**, *21*, 3322-3333.

[98] Fernandez, P.; Willenbacher, N.; Frechen, T.; Kuhnle, A. "Vesicles as rheology modifier." *Colloids and Surfaces a-Physicochemical and Engineering Aspects* **2005**, *262*, 204-210.

List of Publications

Publications:

1. Agrawal, N.R.; Yue, X.; Feng, Y.; Raghavan, S.R., Wormlike micelles of a cationic surfactant in polar organic solvents: Extending surfactant self-assembly to sub-zero temperatures. *Langmuir* 2019, 35, 39, 12782-12791.

2. Torres-Luna, C.; Koolivand, A.; Fan, X.; Agrawal, N.R.; Hu, N.; Zhu, Y.; Domszy, R.; Briber, R.M.; Wang, N.S.; Yang, A., Formation of drug-participating catanionic aggregates for extended delivery of non-steroidal anti-inflammatory drugs from contact lenses. *Biomolecules* 2019, 9(10), 593.

3. Fernandes, J.C.; Agrawal, N.R; Bothun, G.D.; McCormick, A.V.; John V.T.; Raghavan, S.R., Does the solvent in a dispersant impact the efficiency of crude-oil dispersion? Langmuir 2019, Accepted.

4. Wang, H.; Shen, J.; Kline, D.J.; Eckman, N.; Agrawal, N.R.; Wu, T.; Wang, P.; Zachariah, M.R., Direct Writing of a 90 wt% Particle Loading Nanothermite. *Advanced Materials* 2019, 31, 23, 1806575.

5. Wang, J.; Feng, Y. J.; Agrawal, N. R.; Raghavan, S. R., Wormlike micelles versus water-soluble polymers as rheology-modifiers: similarities and differences. *Physical Chemistry Chemical Physics* 2017, 19 (36), 24458-24466.

Manuscripts in Preparation:

1. Agrawal, N.R.; Raghavan, S.R., A simple class of responsive liposomes that transform into micelles upon heating. Manuscript in preparation (2020)

2. Agrawal, N.R.; Rubinstein, M; Raghavan, S.R., Dynamic rheology of wormlike micelles in polar organic solvents. Manuscript in preparation (2020)

3. Agrawal, N.R.; Omarova, M; John, V.T.; Raghavan, S.R., Vesicle-gels in polar organic solvents. Manuscript in preparation (2020)

List of Conference Presentations

1. Agrawal, N.R., Yue, X. & Raghavan, S.R. (2019) Wormlike micelles in cold and sub-zero conditions: New insights into the self-assembly of ionic surfactants in polar organic solvents. Society of Rheology 91st Annual Meeting, Raleigh NC.

2. Agrawal, N. R. & Raghavan, S. R., (2019) A Simple Class of Responsive Liposomes that Transform into Micelles Upon Heating. Mid-Atlantic Soft Matter (MASM) Conference, Baltimore, MD.

3. Agrawal, N. R., Yue, X., Feng, Y, & Raghavan, S. R., (2019) Can Self-Assembly into Wormlike Micelles Occur in Polar Solvents at Sub-Zero Temperatures? ACS National Meeting & Expo, Orlando, FL.

4. Agrawal, N. R., Raghavan, S. R., (2019) A Simple Class of Responsive Liposomes that Transform into Micelles Upon Heating, ACS National Meeting & Expo, Orlando, FL.

5. Agrawal, N. R., Raghavan, S. R., (2019) Self-Assembly of Wormlike Micelles in Polar Organic Solvents, Mid-Atlantic Soft Matter (MASM) Conference, Rockville, MD.

6. Agrawal, N. R., Yue, X., Feng, Y, & Raghavan, S. R. (2018). Can Wormlike Micelles be Formed in Polar Organic Solvents? Insights into Self-Assembly at Low and Sub-Zero Temperatures, 9th American Conference on Neutron Scattering, ACNS, College Park, MD.

7. Agrawal, N. R., Fernandes, J. C., Omarova, M., John, V. T., & Raghavan, S. R. (2018). The impact of the solvent base for a dispersant on the efficiency of crude-oil dispersion, Gulf of Mexico Oil Spill & Ecosystem Science Conference. New Orleans, LA.

8. Agrawal, N. R., & Raghavan, S. R. (2017). Food-grade dispersants for remediation of oil spills: Insights from colloid science, 254th ACS National Meeting & Exposition. Washington, DC.